NOTICE

The quality of this microform is heavily dependent upon the quality of the original thesis submitted for microfilming. Every effort has been made to ensure the highest quality of reproduction possible.

If pages are missing, contact the university which granted the degree.

Some pages may have indistinct print especially if the original pages were typed with a poor typewriter ribbon or if the university sent us an inferior photocopy.

Reproduction in full or in part of this microform is governed by the Canadian Copyright Act, R.S.C. 1970, c. C-30, and subsequent amendments.

AVIS

La qualité de cette microforme dépend grandement de la qualité de la thèse soumise au microfilmage. Nous avons tout fait pour assurer une qualité supérieure de reproduction.

S'il manque des pages, veuillez communiquer avec l'université qui a conféré le grade.

La qualité d'impression de certaines pages peut laisser à désirer, surtout si les pages originales ont été dactylographiées à l'aide d'un ruban usé ou si l'université nous a fait parvenir une photocopie de qualité inférieure.

La reproduction, même partielle, de cette microforme est soumise à la Loi canadienne sur le droit d'auteur, SRC 1970, c. C-30, et ses amendements subséquents.

Canada

Clay Dispersion: Implications to Clay Barriers' Long-Term Performance

Mohammad Ali Ijhaish

A Thesis

in

The Department

of

Civil Engineering

Presented in Partial Fulfillment of the Requirements

for the Degree of Master of Applied Science at

Concordia University

Montreal, Quebec, Canada

December 1993

ISBN 0-315-90898-X

Canada

ABSTRACT

Clay Dispersion: Implications to Clay Barriers' Long-Term Performance

Mohammad Ali Ijhaish

The long-term performance of clay barriers is of great importance in geo-environmental projects dealing with the disposal of high-level radioactive waste. The main objective of this thesis is to address the long-term performance of clay barrier proposed for use in the Canadian Nuclear Fuel Waste Management Program. To achieve this objective, it is necessary to accomplish two primary objectives. In addition, concepts in clay colloid chemistry of relevance to this study are reviewed.

The first primary objective is to study the effect of pore water chemistry on the flocculation/deflocculation of clay particles at clay water interface. This is accomplished experimentally by comparing the results of critical coagulation concentrations and sediment volumes of a 2% bentonite clay suspension in NaCl & $CaCl_2$ and synthetic solutions used in the sedimentation tests.

The second primary objective is to study the rate of release of clay particles from the expanding clay in various solutions. This is accomplished by measuring the concentration profiles as a function of time from the expanding clay in various solutions.

Results obtained from the above two achieved objectives suggest that the bentonite gel is flocculated and the amount of particles released is insignificant. The unexpected result of no particle release from the gel in the distilled water is attributed to the presence of residual salt in the clay.

The results also support the long-term performance of the bentonite clay barrier proposed for use in the Canadian Nuclear Fuel Waste Management Program.

ACKNOWLEDGMENTS

The author wishes to express his gratitude to his thesis supervisor, Dr Steven Cheung, for his guidance, for the great amount of time he gave, and for his constructive suggestions throughout the course of this research. His supply of diffusion data is highly appreciated as well.

The author is in debt for his family for their constant moral support and continuos encouragement. Without their backing, the completion of this work would have been impossible.

The financial support of NSERC operating fund, RA-20-N396 is highly appreciated.

TABLE OF CONTENTS

LIST OF SYMBOLS

C	Contaminant Concentration
C_0	Electrolyte Concentration in the Free solution
C_c	Electrolyte Concentration at the Midway between two parallel particles
D *	Diffusion Coefficient
e	Elementary Charge
G_c	Specific Gravity of Clay
K	Boltzmann Constant
M	Molar Concentration
N_0	Concentration of Ions in the Free Solution
N_i	Concentration of Ions of species i
P	Osmotic Pressure
P_c	Osmotic Pressure Midway between two Parallel Particles.
W_i	Work done in bringing an ion to point where the potential is ψ_i
R	Gas Constant
X	Distance from Particle Surface
X_d	Half Distance between two Parallel particles
Z	Valence of Exchangeable Cations
Z_i	Ionic Valence
ψ	Electric Potential
ψ_0	Surface Potential
κ	Reciprocal Thickness of the Diffuse Ion Layer

ψ_c	Electric Potential Midway between Parallel Interacting Particles
W	Water Content in wt. %
S	Surface Area of Clay per Unit Mass
T	Temperature
t	Time
σ	Surface Charge Density

LIST OF NOTATIONS

A°	Angstrom (10^{-10}m)
AH	Hamaker Constant
CCC	Critical Coagulation Concentration
CEC	Cation Exchange Capacity
EDL	Electrical Double Layer
DL	Diffuse Ion Layer
DDW	Deionized Distilled Water
ESP	Exchangeable Sodium Percentage
EE	Edge to Edge particle association
EF	Edge to Face particle association
FF	Face to Face particle association
NSLI	Normalized Scattered Light Intensity
SAR	Sodium Absorption Ratio
SCSSS	Standard Canadian Shield Saline Solution
V_T	Net Interaction Energy between clay particles
V_R	Repulsive Interaction Energy between clay particles
V_A	Attractive Interaction Energy between clay particles
Wt%	Weight Percentage
WN-1	Whiteshell Nuclear groundwater.

LIST OF FIGURES

LIST OF TABLES

CHAPTER 1

INTRODUCTION

1.1. STATEMENT OF THE PROBLEM

Clay is used increasingly in many engineering applications. For example, clay is used as core material in dams to serve as hydraulic flow barrier because of its low permeability. Clay is also used as liner to act as contaminant barrier in landfills in geo-environmental engineering due to its low permeability and high sorption capacity.

It is well known that permeability depends on clay type, clay density and other environmental factors such as pore water chemistry and temperature (Mouradian 1993; Yong and Warkentin 1975). Generally, a decrease in clay density will increase the permeability and decrease the shear strength.

Bentonite clay possesses many properties desirable for the barrier such as low permeability, low diffusivity, high sorption capacity and self healing (Cheung and Gray 1990). However, bentonite is characterized by its high swelling potential when it is in contact with water. One problem associated with this swelling, is a possible dispersion of clay particles from the clay mass during the swelling process. The dispersion of particles from the clay mass and their subsequent transport away from the swelling bentonite surface will cause a

decrease in the density of the clay barrier. The decrease of the density will increase the permeability and impair the performance of the barrier.

Generally, dispersion of particles from the bentonite clay mass, in contact with water, depends on water flow conditions as well as on the clay particle arrangement at clay-water interface. The particles' arrangement dictated by the interparticle forces (repulsive and attractive forces) leads to either flocculated structure or dispersed structure (figure 1.3) depending on the resultant of these forces. Groundwater act as the carrier of dispersed particles from the clay mass by advection and/or diffusion under mass concentration gradient (Freeze and Cherry 1979).

While past studies have concentrated on clay dispersion under the effect of high seepage velocities (Sherard 1976 and Sherard et al. 1976), little attention has been given to studying clay dispersion and the subsequent transport under stagnant water condition. Thus the consequences of particles' dispersion and subsequent transport on the performance of the barrier under stagnant water conditions are not yet clear and need to be investigated.

Stagnant water conditions exist in many geo-environmental projects. For example in lagoons, stagnant water is contained within the clay barrier. Another example is in the proposed disposal vault of the Canadian Nuclear Fuel Waste Management Program, where stagnant ground water is outside the barrier in the rock fissures (figures 1.1; 1.2).

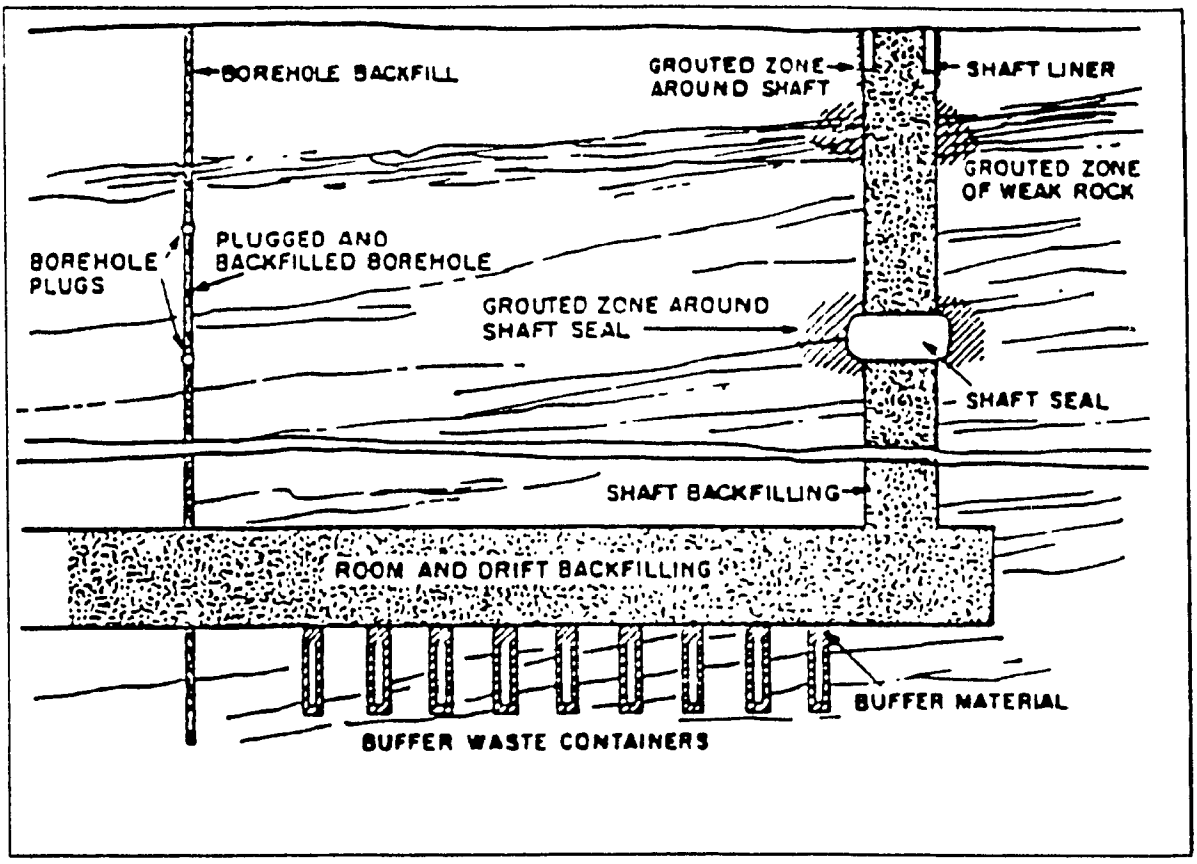

Figure 1 1. Schematic diagram of proposed disposal vault in the Canadian Nuclear Fuel Waste Management Program (after Hancox 1986)

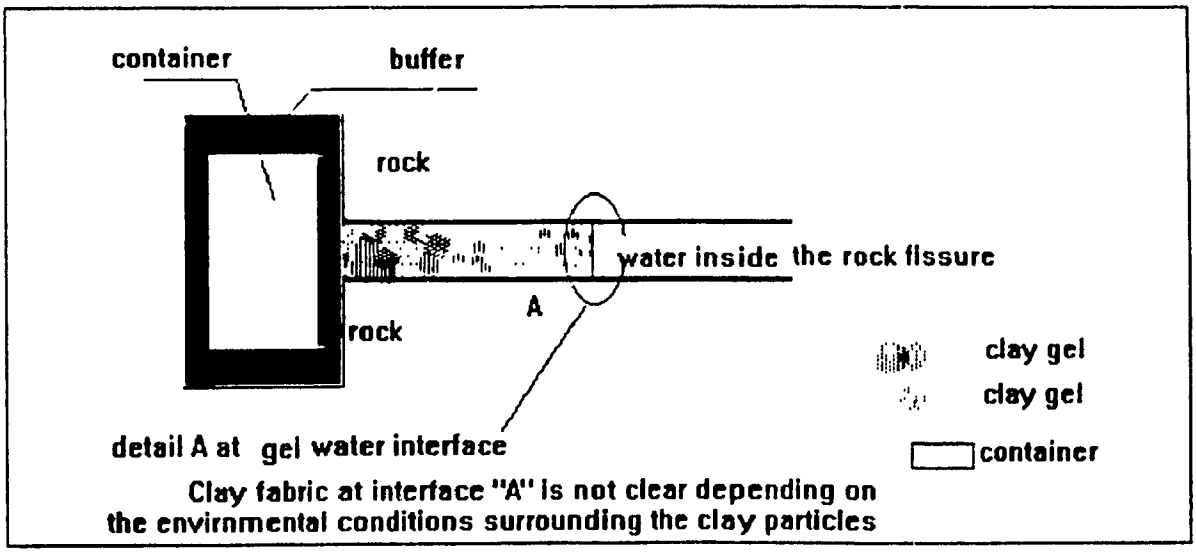

Figure 1.2.Schematic diagram of clay gel Penetration from the buffer into a rock fissure (figure 1.1).

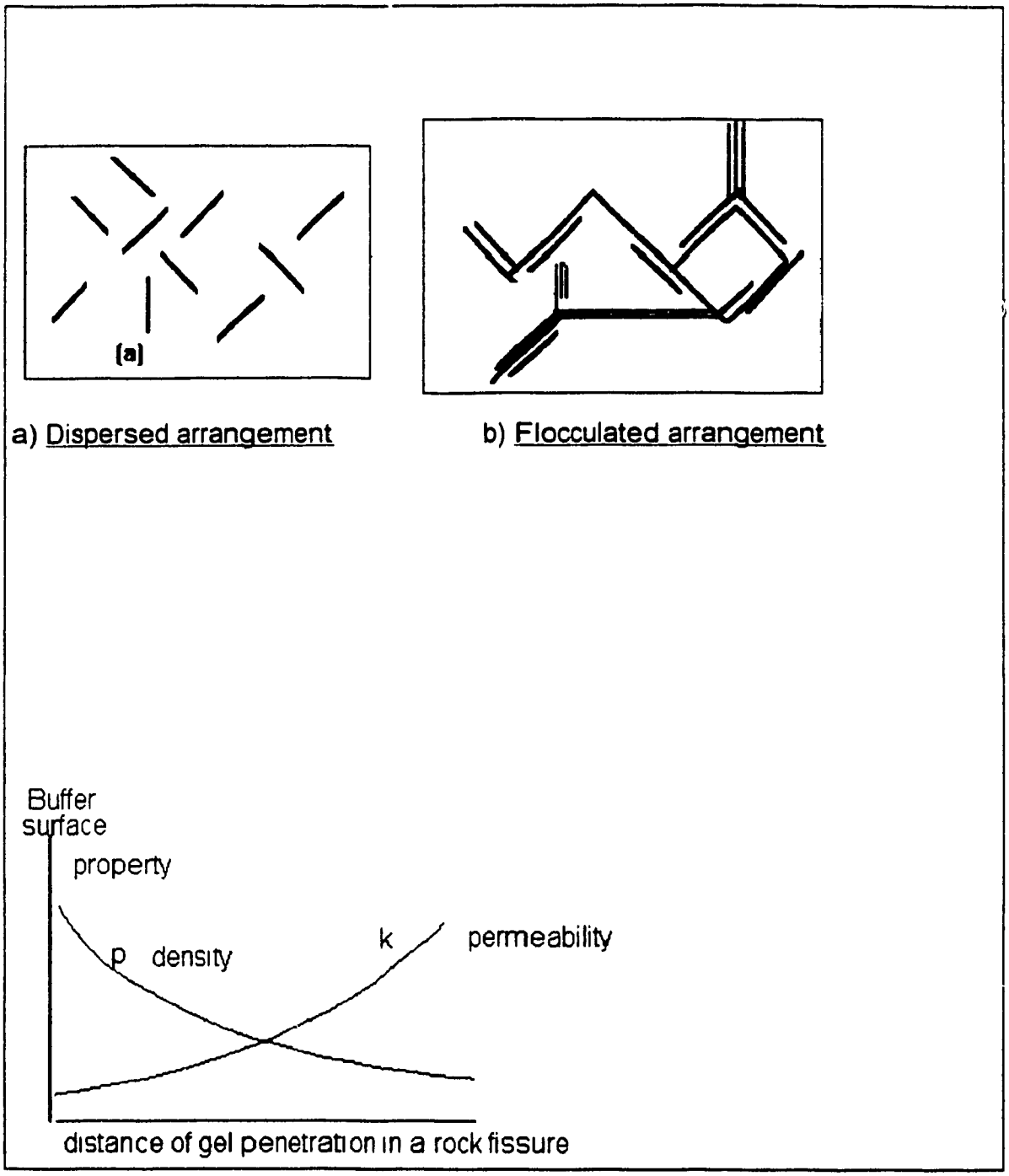

Figure 1.3. Schematic diagram showing the clay fabric at detail A, and the relation between permeability, density, and the extent of gel penetration into the rock fissure (figure 1.2).

The significance of studying the long-term performance in bentonite barrier in stagnant water will be demonstrated in the Canadian Nuclear Fuel

Waste Management Program, where the waste to be isolated is a high-level radioactive waste containing radionuclides having half- lives of many thousands of years. It is also important to note that the results obtained from this study on bentonite barrier in the Canadian Nuclear Fuel Waste disposal vault can be generalized for use to similar clay liners under stagnant water condition in other engineering applications (e.g. landfills and lagoons) by considering the groundwater salinity.

Accordingly, this thesis addresses the long-term performance of the clay barrier (proposed for use in the disposal vault in the Canadian Nuclear Fuel Waste Management Program) through studying the dispersion of particles from the clay mass and their subsequent transport under stagnant water, as will be discussed below.

In the Canadian Nuclear Fuel Waste Management Program, the used fuel waste has been proposed to be buried deep in the stable rock of the Canadian shield (Hancox 1986). In addition to the massive natural rock barrier, artificial barriers are proposed to minimize the movement of the radionuclides from the waste to the surrounding environment. Clay barrier is one of the artificial barriers surrounding the container in the borehole as illustrated in figure 1.1.The main function of the clay barrier is to inhibit the transport of radionuclides from the failed container to the surrounding groundwater. To meet this requirement, the barrier should possess properties such as: (1) very low permeability, (2) low diffusivity, (3) good self-sealing ability, (4) high sorption capacity, (5) high thermal conductivity, and (6) sufficient strength and good deformation properties to support the container. A compacted mixture of sand and bentonite has been found to possess the above properties and proposed for use as barrier in the borehole.

In the Canadian Nuclear Fuel Waste Management Program, the problem under investigation is: in post-closure period of the disposal vault it is expected that the groundwater will slowly restore its original level, then the bentonite will absorb water and, due to its high swelling potential, it swells and penetrates as a gel into the fissures of the surrounding rock. At the furthest point of penetration into the rock, possible release of bentonite particles from the expanded gel into the adjacent groundwater is expected. This results in a gradual decrease in the density of the clay gel. As the gel density continues to decrease, additional material from the buffer mass would swell into the rock. The removal of significant amounts of fine particles into groundwater would thus eventually result in a decrease in the buffer density and consequently an increase in its hydraulic conductivity (figure1.3). In addition, the bearing capacity of the bufferwould decrease and the waste container would consequently experience a downward shift.

From the above study, it can be realised that dispersion of bentonite particles from the clay barrier into groundwater and their subsequent transport has important implications to its long-term performance.

In order to study the dispersion of particles from the clay mass, it is important to study the particles arrangement (fabric) at the clay water interface and whether this arrangement is flocculated or dispersed. As will be seen in the following chapter (literature review), the arrangement of particles (fabric) depends on the interactions between the particles, which in turn depend on the pore water chemistry. Hence, the effect of pore water chemistry on the flocculation in bentonite buffer mass should be examined. The concentration of groundwater often varies and the main cations commonly found in the field are Na, Ca, and Mg (Freeze and Cherry 1979). Therefore, NaCl and CaCl2 solutions

will be used in bentonite clay suspensions to study the effect of Na and Ca cations on the flocculation of particles. With this knowledge, the effect of a given groundwater composition on particles arrangement can be assessed.

1.2. OBJECTIVES

The main objectives of this thesis are:

1. To study the fabric (flocculated or dispersed) of the penetrating clay gel. This is accomplished by measuring the Critical Coagulation Concentrations (CCC) and sediment volumes of bentonite suspensions using solutions of NaCl and $CaCl_2$ and simulated groundwater.

2. To study the particles release from the expanding bentonite gel. This is accomplished by measuring the time-dependent concentration profiles of bentonite particles from the gel surface using various solutions.

From the above studies, one can assess the long-term performance of a clay barrier in a given groundwater environment.

To accomplish this study, the thesis is organized as illustrated in figure 1.4

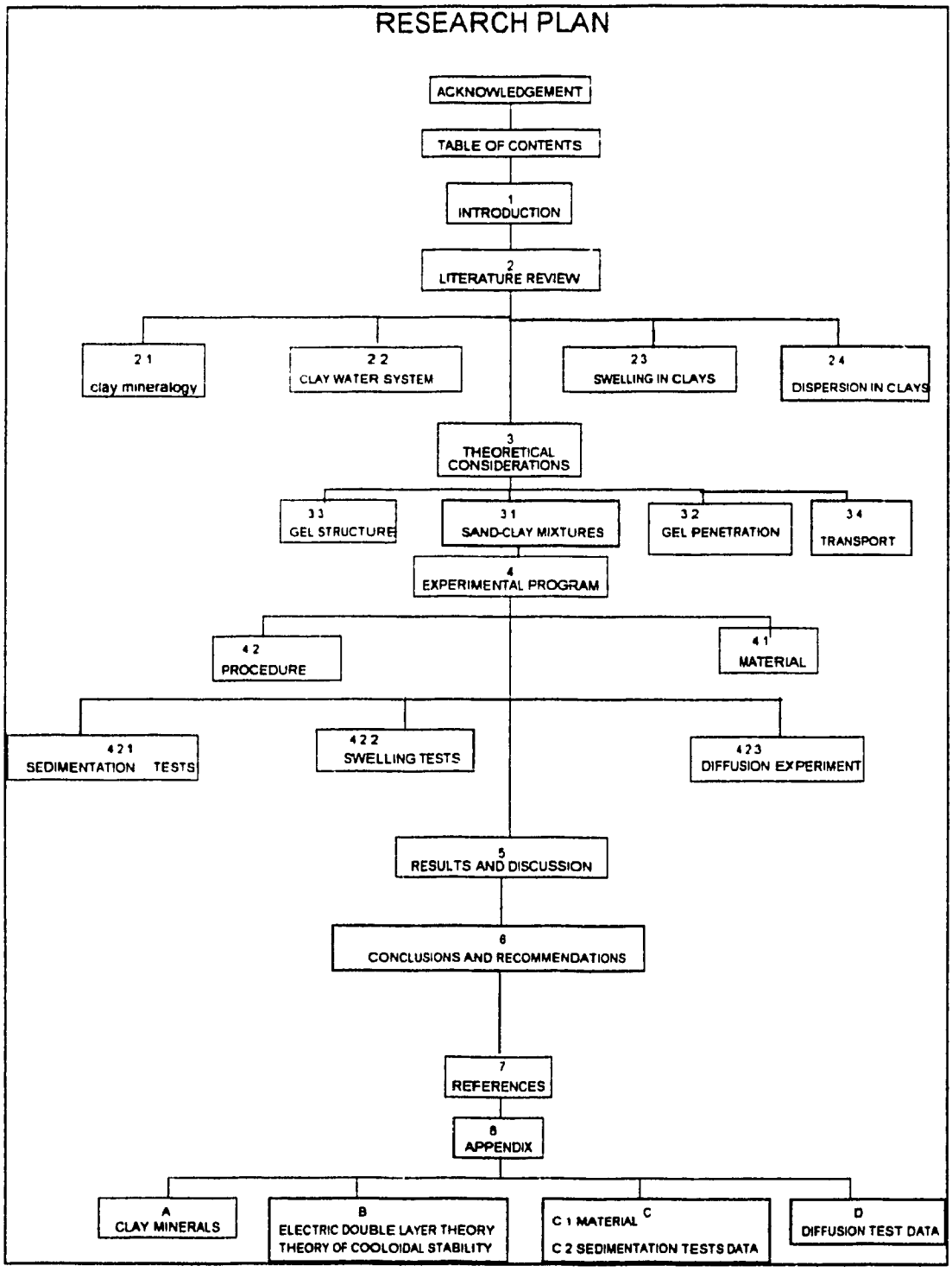

Figure 1.4. Flow chart showing the organization of the thesis.

CHAPTER 2

LITERATURE REVIEW

This chapter reviews the mineralogy of clay in order to understand the properties possessed by bentonite as mentioned in chapter 1 As bentonite behaves as colloidal particles, a review on the clay colloid chemistry is needed to explain the physical properties of the bentonite clay such as the low permeability, the high sorption capacity, the high swelling potential of bentonite clay, and the flocculation / deflocculation phenomena in bentonite suspensions.

2.1. CLAY MINERALOGY

Soil particles range in size from gravel, sand, silt, to clay in terms of the size. Generally, sand and silt particles are approximately equidimensional, but clay particles are mainly plate-shaped. Clays are consisted of small crystalline particles containing mainly hydrous aluminum silicates, where all or part of the aluminum in the crystal would be replaced by magnesium or iron (Grim 1968). The clay may exert an influence on physical properties far exceeding its actual ratio in the soil.

BASIC STRUCTURAL UNITS

There are two basic structural units of clay minerals which are Silica tetrahedron and Alumina octahedron. Silicate tetrahedrons (Si and 4 O) are combined in a way to form silica sheets of thickness of 4.93A^0 in the clay mineral. Alumina octahedrons (Al and 6 OH) are combined together to form Alumina sheets of thickness 5.05A^0 in the clay mineral, generally known as gibbsite. If magnesium, Mg, replaced the aluminum in the Alumina octahedron, the sheet is called brucite (figure 2.1). The combination of the basic units into certain patterns results in different clay minerals (figure 2.2), (Yong and Warkentin 1975).

Since bentonite is a montmorillonite mineral rich clay, The montmorillonite clay mineral will be reviewed here. Other clay minerals are discussed in appendix A

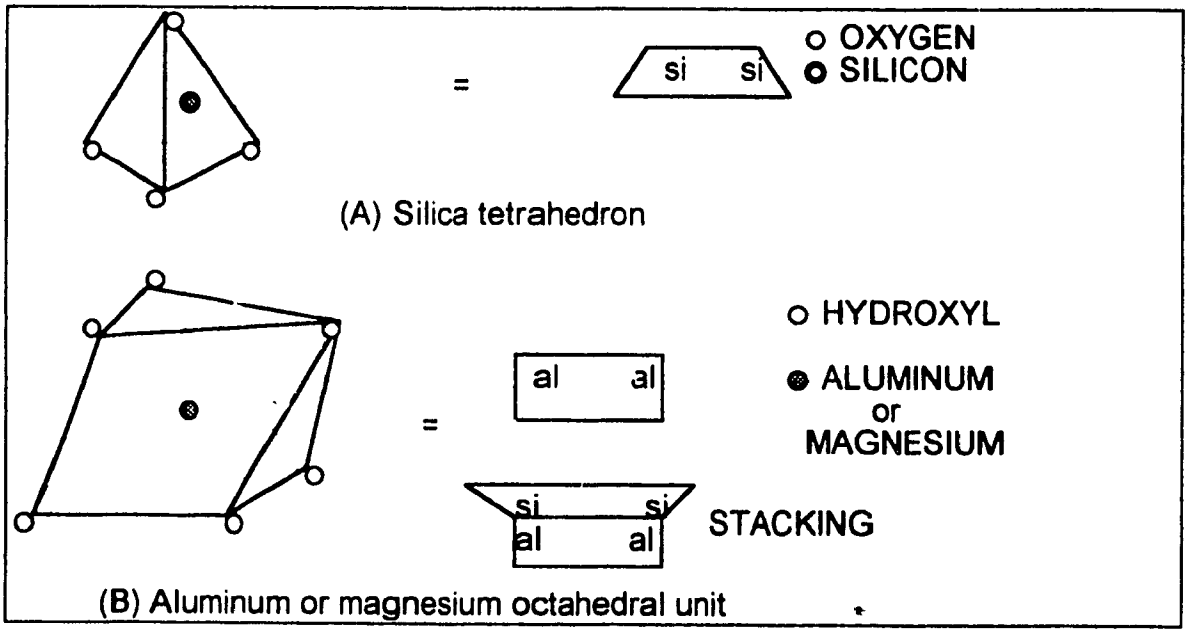

Figure 2.1. Schematic representation of silica tetrahedron and alumina octahedron (Yong and Warkentin 1975).

2.1.1. MONTMORILLONITE CLAY MINERALS:

Montmorillonite consists of repetitive stacks of layers consisting of an Alumina sheet sandwiched between two silica sheets (figure 2.2). The negative charge on montmorillonite surfaces is due to the occasional isomorphous substitution that occurs mainly in the alumina sheet with magnesium or iron substituting the aluminum in the dioctahedral minerals. In montmorillonite, there are no ions to bond the layers together and therefore water can enter between the layers as illustrated in figure 2.2. Montmorillonite minerals are distinguished by their high specific surface area and high liquid limit.

Chemical analysis of montmorillonite shows that there are sufficient substitutions to account for the observed cation exchange capacity due to cation adsorption needed to compensate the negative charge on clay particles. Values of 80-100 meq / 100g of montmorillonite clay for the cation exchange capacity were reported (van Olphen 1963; Grim 1968). Broken bonds at the edges of the silica-alumina layers would also give rise to unbalanced charges; however there is an evidence that clay particles carry a positive charge at the edges in acid or neutral media (van Olphen 1964).

One characteristic of the montmorillonite is that it swells to several times its dry volume when placed in contact with water. The swelling is due to water adsorbed between the layers thus pushing the layers apart. The layers become separated by several water layers, often $9A^0$. A group of such layers is called a tactoid, with distance between tactoids being several tens of angstroms. The tactoids of sodium-saturated montmorillonite can be dispersed into individual layers by water. One such dispersed layer is only of $10A^0$ thickness

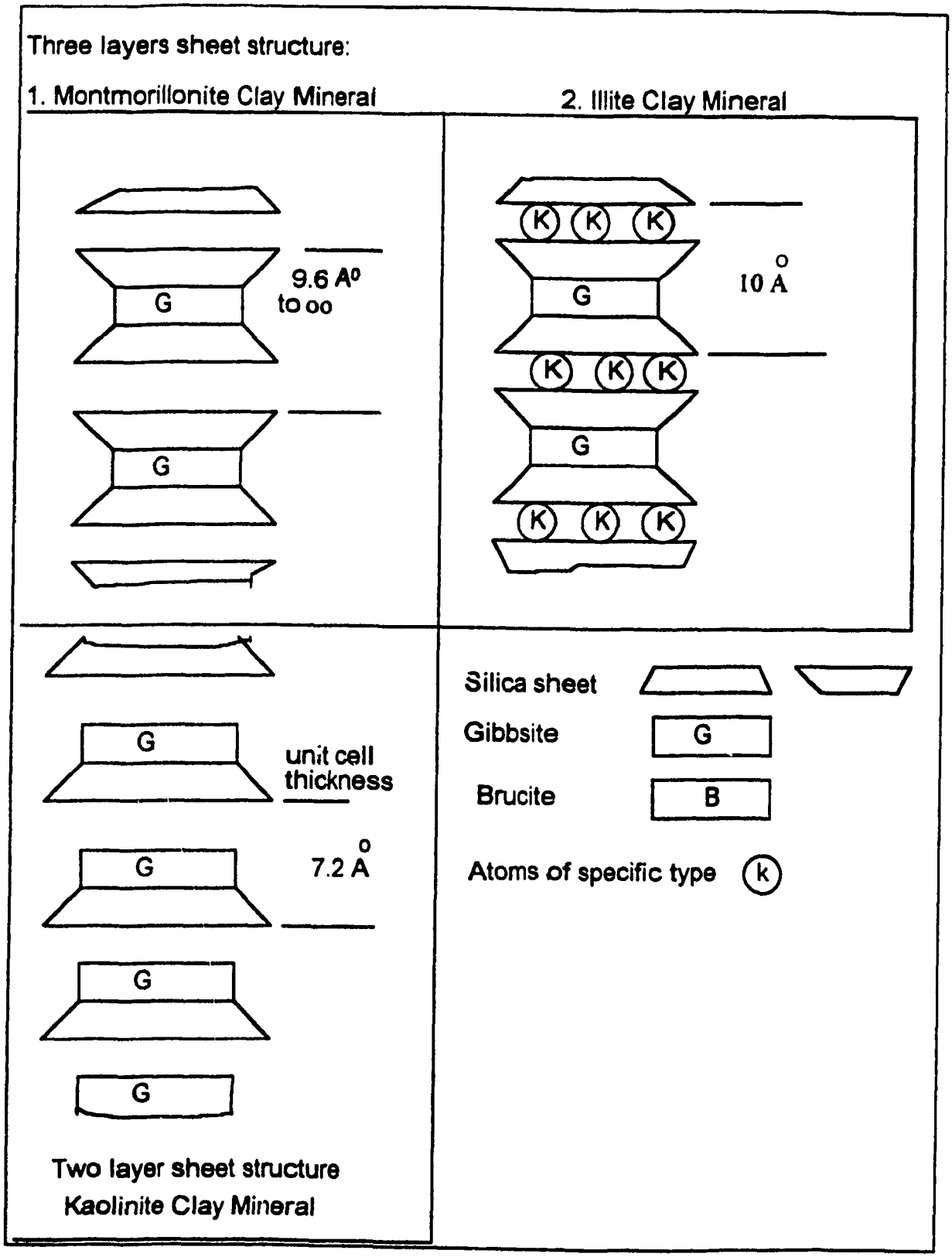

Figure 2.2. Schematic representation of different clay minerals structure (Yong and Warkentin 1975).

2.2. CLAY-WATER SYSTEM

In this section, the distribution of ions adjacent to clay surfaces (in water suspensions), which carry negative charges, and the attractions of ions to the clay surfaces are considered. The consequences in terms of clay particle interactions in suspensions are reviewed. Clay-water system is considered to be a two-phase system with a large interfacial area. The behavior of the system is dominated by interparticle forces and the particles can flocculate in the presence of a small amount of salt. The critical coagulation concentration for clay suspensions in different electrolytes is discussed in terms of cations valence and salt concentration. The different arrangements of particles predicted are reviewed.

2.2.1. ELECTRIC DOUBLE LAYER

The negative charge of the colloidal clay particles is considered to be distributed evenly over the surface. Because of this negative charge, the clay surface can attract cations. However, these cations are not distributed uniformly throughout the dispersion medium. Some of the cations are held on or near the clay surface. Other cations can diffuse from the surface due to their thermal motion. Water is also hydrated to the cations located on the clay particle surface. The exchangeable cation becomes much larger once hydrated Na hydrated cation diameter is 15.6A^0 while the unhydrated one is 1.96A^0 The hydrated sodium ions are too large to fit onto the surface of the clay mineral, and are forced to move away to points of equilibrium (Lambe and Whitman 1979).

The negative charge on the clay surface and the cations diffusing under the influence of the negative charge constitute the electric double layer as illustrated in figure 2.3. The latter is defined as the diffuse ion layer by Gouy (1910) and by Chapman (1913). Quantitative description of the Gouy-Chapman model of the diffuse ion layer is in appendix B.

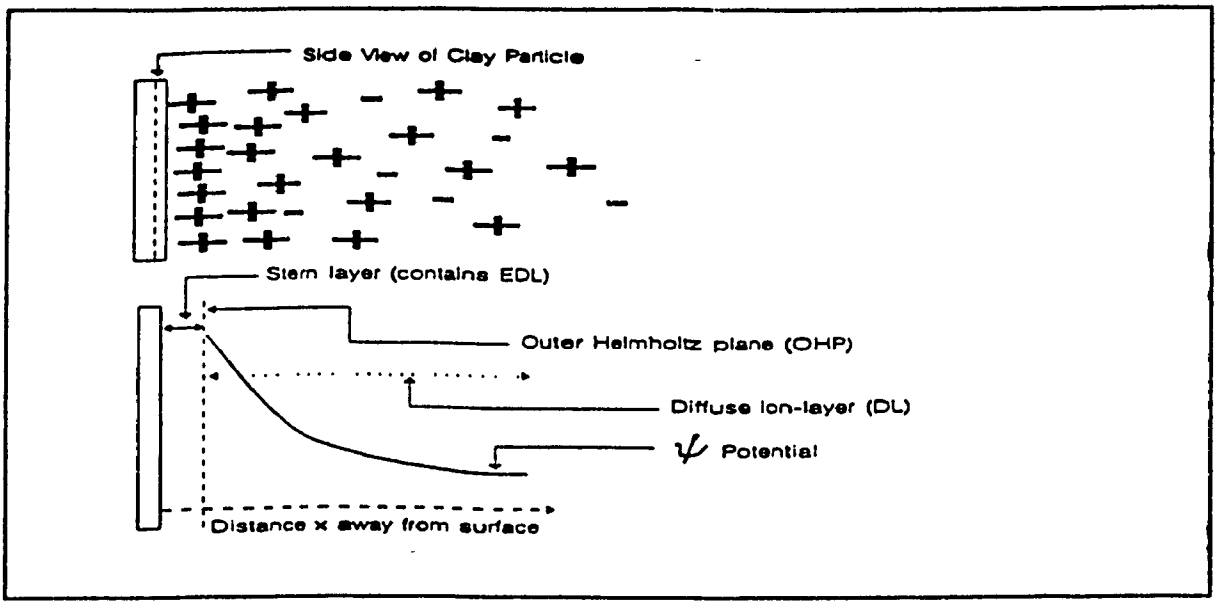

Figure 2.3. Diagram showing interaction of ions with charged clay particle, the diffuse ion-layer and the variation of the average electrical potential as a function of distance away from clay particle surface (Yong et al. 1992).

A correction to the Gouy-Chapman model was proposed by Stern (1924) to account for the thickness of cations (ionic dimension) attracting to the clay surface because the Gouy-Chapman model deals with point charges; whereas, ions are of finite size. The Stern layer shown in figure 2.3 is assumed to consist of counterions with associated water molecules in a closely packed layer close and tightly bound to the clay surface with an adjacent diffuse layer extending into solution. The Stern water layer is estimated to be 0.4nm for montmorillonite clay.

2.2.1.1. EFFECT OF ELECTROLYTE ON THE THICKNESS OF DIFFUSE ION LAYER

The calculations of the effect of electrolytes on the distribution of the electric potential (van Olphen 1977, Yong and Warkentin 1975) show that an increase in valence of the counter-ions and electrolyte concentration decreases the thickness of the diffuse ion layer and the potential at the same distance from the particle surface (figure 2.4, 2.5 and table 2.1). However, the corresponding effect of the similarly charged ions is comparatively small, i.e. the anions effect can be neglected.

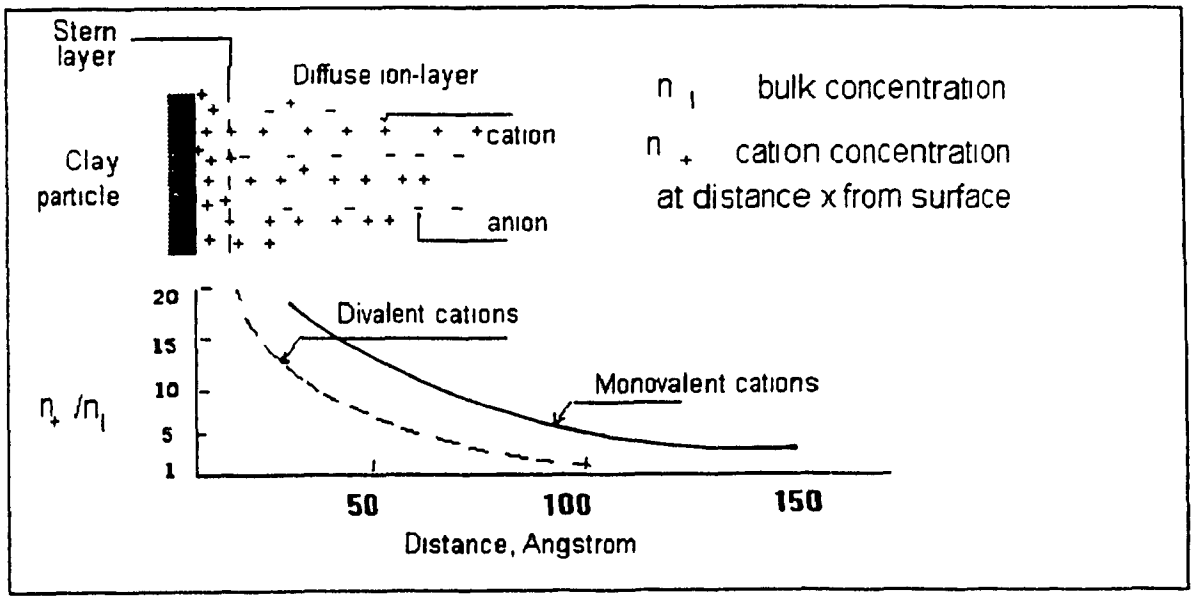

Figure 2.4. Theoretical distribution of ions adjacent to a charged surface showing influence of valence on thickness of diffuse ion-layer (Yong et al. 1992).

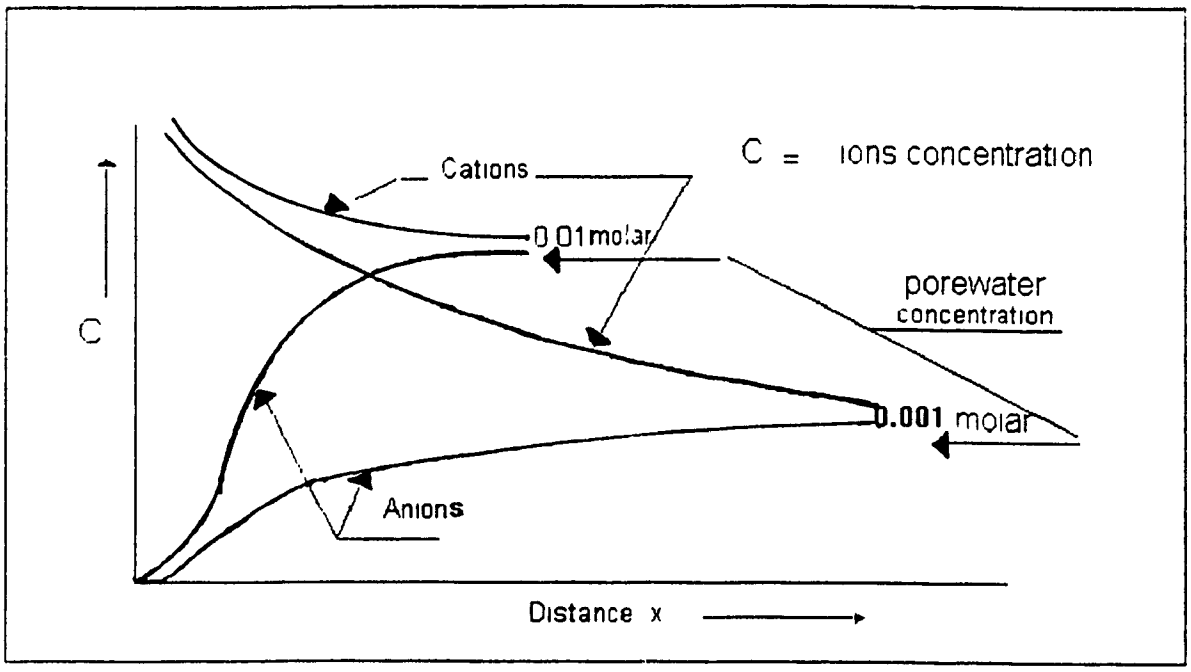

Figure 2.5. Theoretical distribution of ions adjacent to a charged surface showing influence of molar concentration of electrolyte on cation and anion distribution (Yong et al. 1975).

Table 2.1. Approximate Thickness of the Diffuse Ion Layer as a function of salt concentration.

Salt Concentration	"Thickness" of the diffuse ion layer, A°	
mmol/dm³	Monovalent ions	Divalent ions
0.01	1000	500
1.0	100	50
100	10	5

The following gives the equations derived to show the factors affecting the cation concentration and potential in the diffuse ion layer, and also the thickness of the diffuse ion layer.

Cation Concentration:

The theoretical distribution of the cations at a negatively charged surface has been expressed by the following equation (Yong and Warkentin 1975):

$$N_+ = N_0(\coth 0.16Z\sqrt{C_0}x)^2$$

N_+ = number of cations per unit volume at any distance x from the surface

N_0 = number of cations per unit volume in the pore water away from the influence of the surface

Z = valence of cations

C_0 = concentration of cations in moles / liter away from the influence of the surface

x = distance from surface in angstrom

As an example:

For 0.001 M salt (NaCl), the value of N_+ = 0.016M at x = 50 A°

For 0.001M salt ($CaCl_2$), the value of N_+ = 0.004M at x = 50 A°

Potential equation

For small potentials in dilute electrolytes (ψ < 25mV), the potential within the diffuse ion layer has been expressed as follows (van Olphen 1977):

$$\psi = \psi_o \quad e^{-\kappa \quad x} \qquad [2.2]$$

Ψ = electric potential at distance x from particle surface.

Ψ_o = electric potential at particle surface assumed to be equal to Stern potential.

κ = constant depending on electrolyte concentration and cation valency and is considered as the reciprocal length of the diffuse ion layer (figure 2.3).

x = distance from particle surface for potential ψ .

The thickness of the diffuse ion layer

The thickness of the diffuse ion layer ($1/\kappa$) is usually referred to as the distance between the Stern layer and where the center of gravity of the space charge coincides with the plane $\kappa x = 1$ or $x = 1/\kappa$ (van Olphen 1977),
The thickness of the diffuse ion layer is expressed as follows:

$$\frac{1}{\kappa} = \left(\frac{\varepsilon K T}{8 \pi N_o e^2 Z^2}\right)^{1/2} \quad \text{cm} \qquad [2.3]$$

where

$1/\kappa$ = the thickness of the diffuse ion layer in cm.

Z = valence of the counter ions.

e = elementary charge (4.77×10^{-10} esu).

N_o = Concentration of electrolyte

= (molarity $\times 10^{-3} \times 6.02 \times 10^{23}$) ions/cm^3

ε = Dielectric constant of the solvent.

K = The Boltzmann constant

T = Temperature

$KT = 0.4 \times 10^{-13}$ ergs at room temperature

The implication of this equation is that the diffuse layer is of importance only in dilute electrolyte solutions (< 0.1 mol . dm-3), (Le Bell 1978; van Olphen 1977).

Clay Particles Interaction:

When two particles approach one another, their diffuse ion layers overlap over a certain distance and the mid-plane potential will increase (figure 2.6) This results in a higher cation concentration in the mid plane than that in the bulk water solution. Water flows from the bulk water through the clay due to the net effect of the chemical osmosis. If the particles are confined, a pressure (osmotic pressure) is generated which can be calculated as described in appendix B. In case the particles are free to move, the distance between the particles increases to an extent such that the pressures are in equilibrium. This distance depends on the thickness of each diffuse ion layer. Since the thickness of diffuse ion layer is dependent on the concentration of the electrolyte and valency of the exchangeable cations, the repulsive forces and the consequent swelling between the clay particles are also dependent on the valency and concentration of electrolyte. The increase in electrolyte concentration will decrease the mid-plane potential and decrease the repulsive forces as well as the swelling (figure 2.7).

The Gouy-Chapman theory deals mainly with counter-ion distribution and the interaction between negatively charged particle surfaces and counter-ions It does not take into consideration the London-Van der Waals' attraction that

exists between two parallel clay particles which will be discussed in the colloidal stability theory in next section.

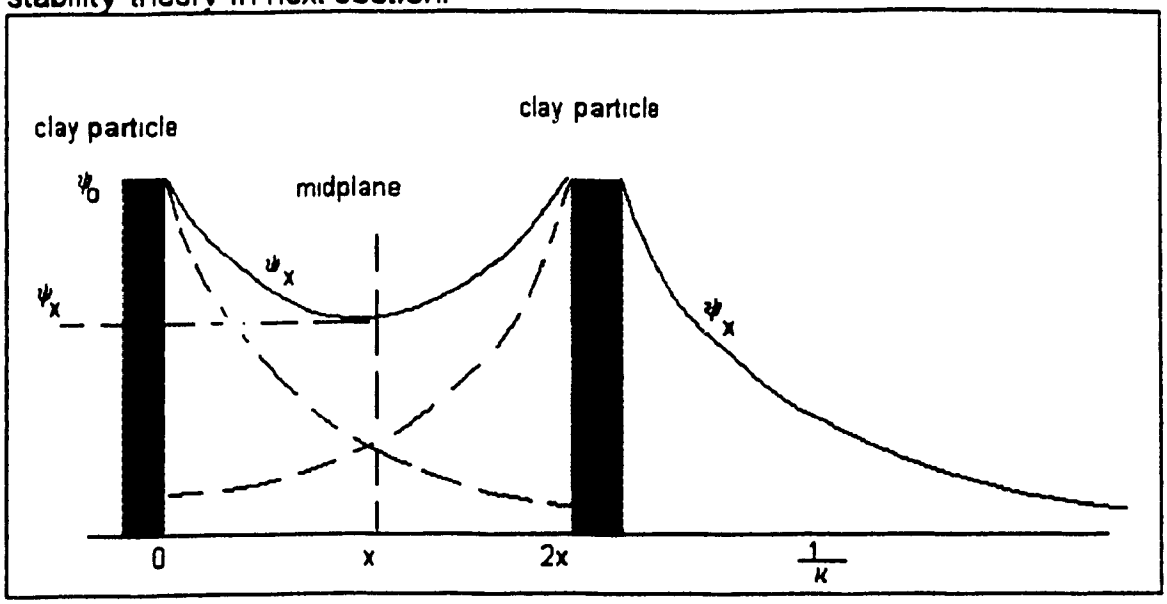

Figure 2.6. Schematic representation of the electric potential between two plates in comparison with that for a single double layer (Shaw 1966).

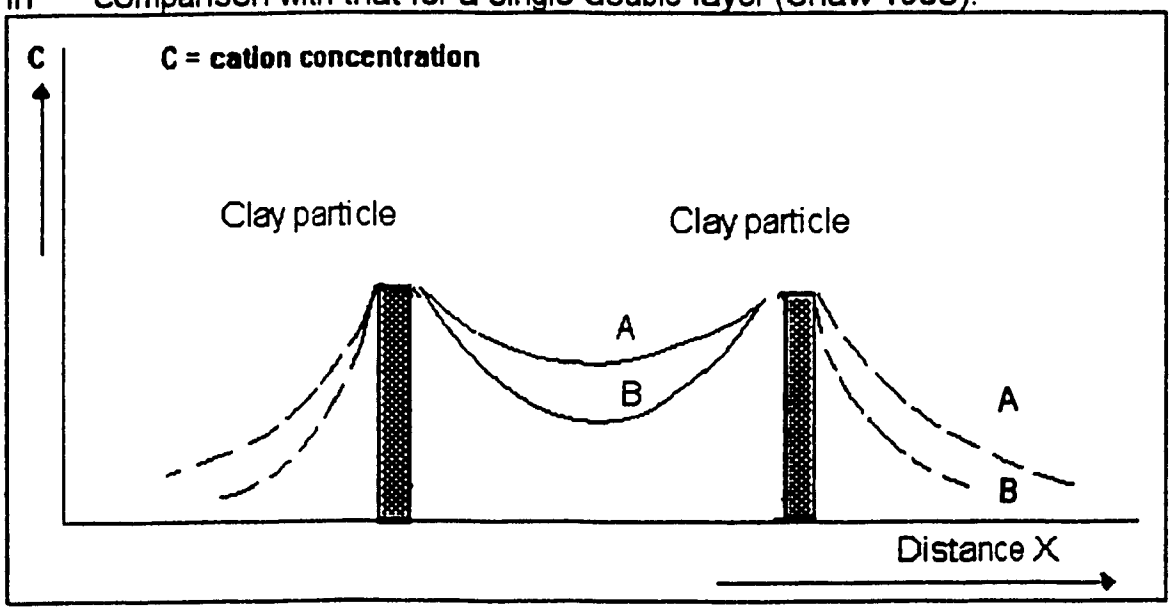

Figure 2.7. Interaction of diffuse ion-layers. Curve A = interaction in fresh water or solution with low salt concentration; Curve B = interaction in solution with high salt concentration (Yong and Warkentin 1975).

2.2.2. THEORY OF COLLOIDAL STABILITY (DLVO THEORY)

The theory of colloidal stability was developed by Verwey and Overbeek and by Derjaguin and Landau, and has been named the DLVO theory.

According to the DLVO theory, colloidal particles would spontaneously flocculate when the Van der Waals' attractive force overcomes the repulsive force generated by the electrical double layers of particles approaching each other.

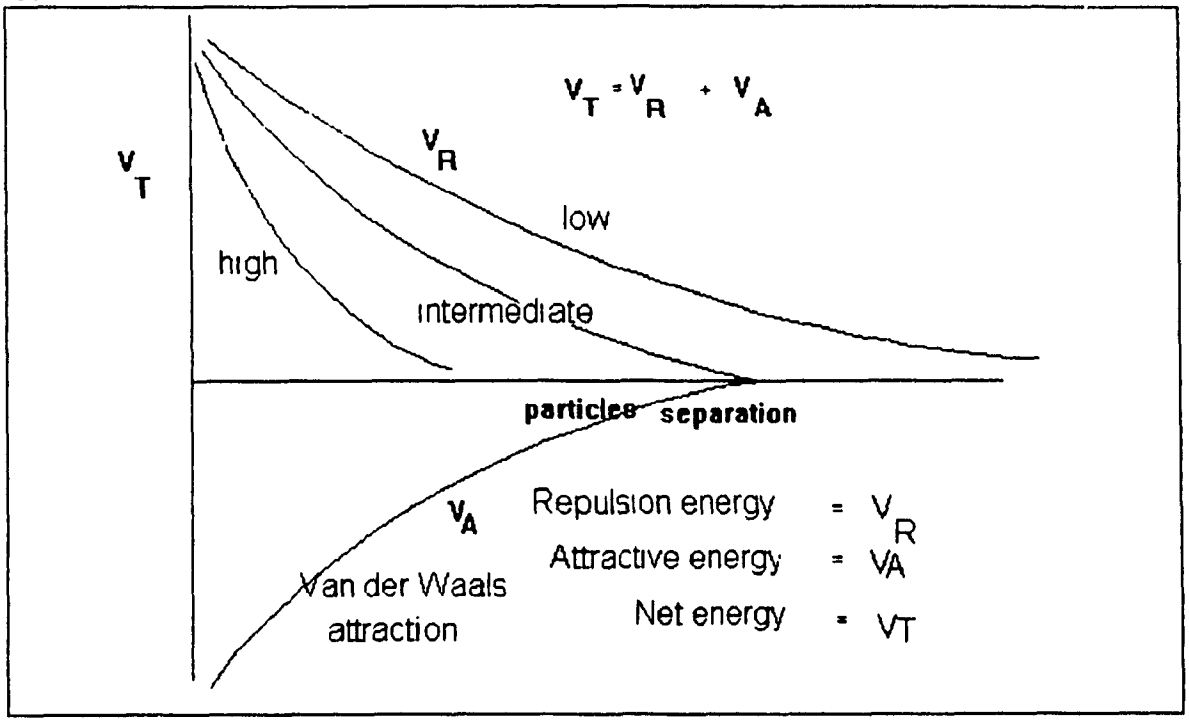

Figure 2.8. Repulsion and Attractive energy as a function of particle separation at three electrolyte concentrations (van Olphen 1963)

The relative range of the repulsive and attractive energy is shown in figure 2.8. The figure shows that the attractive energy remains practically the same with varying concentration of the electrolyte. The use of Van der Waal's

forces to evaluate the attraction between colloidal particles was proposed by Hamaker (1937). A net potential energy curves could be derived.

2.2.2.1. NET POTENTIAL ENERGY OF PARTICLES INTERACTION

The net potential energy V_T curve of particles interaction is constructed by summation of the attractive and the repulsive energy (V_A & V_R) along the distance between particles, by assuming that the attractive energy is negative and the repulsive energy is positive. The results of these additions for three different electrolyte concentrations are shown in figure 2.9. This can be expressed as follows: $V_T = V_R + V_A$ [2.4]

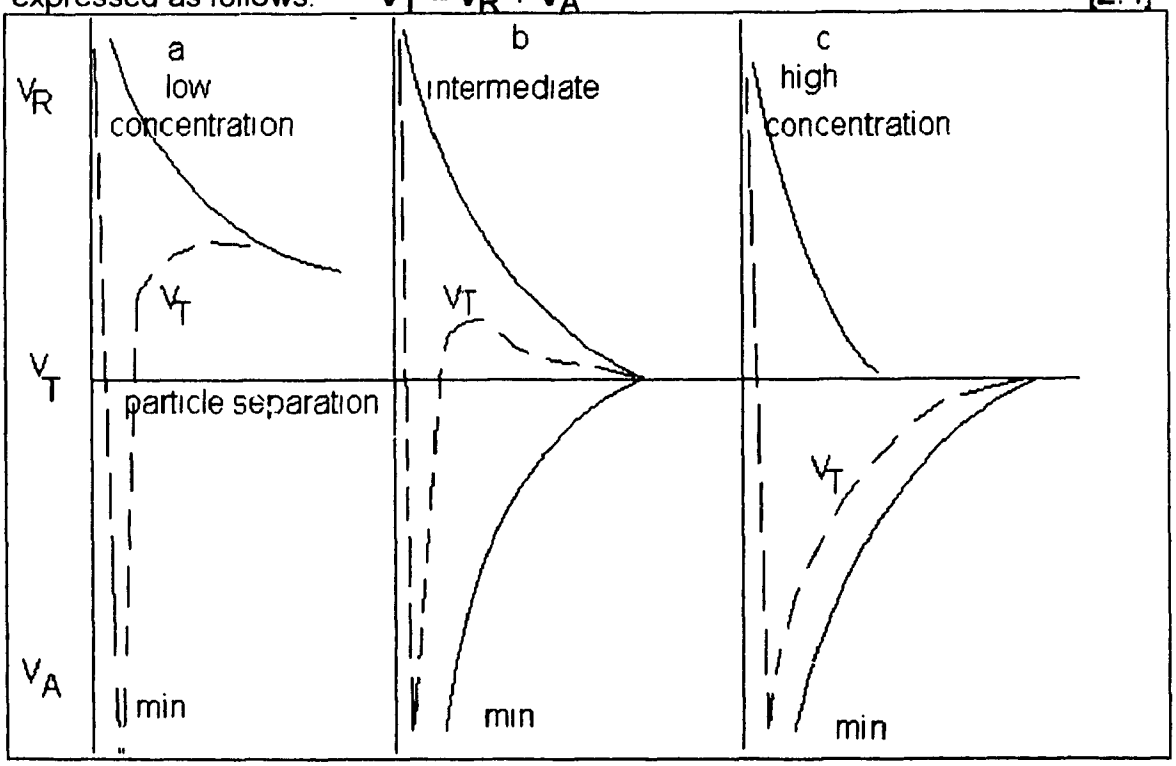

Figure 2.9. Net interaction energy as a function of distance between particles for different electrolyte concentrations (van Olphen 1963)

In constructing these curves, an additional interactive force between the particles is taken into account. This is an interactive force between the crystal

surface and the molecules of water in the medium. This force is effective over a very short range of 10A° or less between the particles. This force is characterized by the steep rise of the potential energy as shown in figure 2.9 at very small values of the particle separation.

The net potential energy of interaction as a function of the distance between two infinite negatively charged, parallel plates with overlapping diffuse ion layers is illustrated in figure 2.10. The curve is characterized by the presence of a single maximum and two minima. The primary maximum is representative of the "energy barrier" against coagulation. DLVO theory states that the particles involved in a collision require an excess of energy equivalent to the energy barrier in order to coagulate. The primary minimum determines the shortest distance between the particles and represents the domination of Van der Waals' attractive forces over electrostatic repulsive forces.

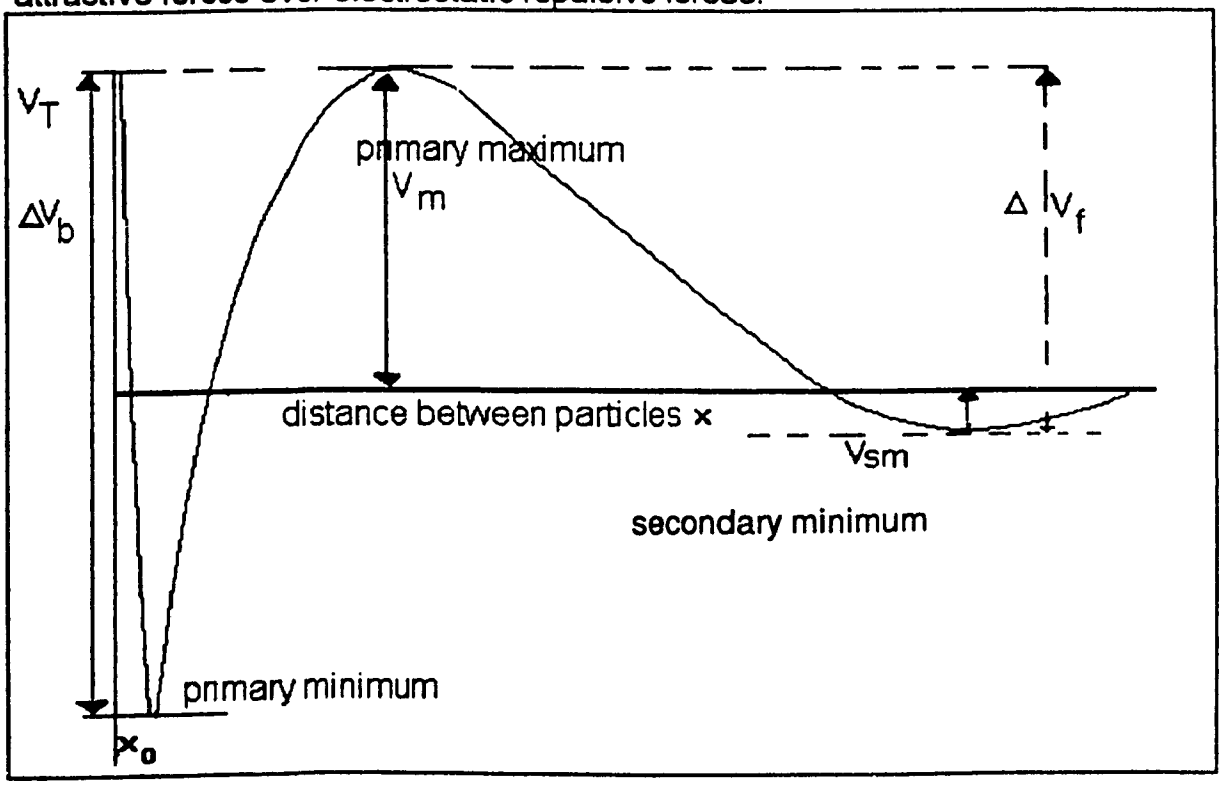

Figure 2.10. Curve of net potential energy ($V_T = V_R + V_A$) as a function of surface separation between two particles, (schematic), (Le Bell 1978)

The energy barrier to coagulation at distances associated with the primary minimum is given by ΔVf. The energy barrier to re-dispersion of a flocculated suspension is given by ΔVb. At larger distances, the electrostatic repulsive force decreases more rapidly than the Van der Waals' attractive force and a secondary minimum is formed.

Negative values for the potential energy of interaction are representative of unstable (flocculated) colloid in which the collision of every particle leads to coagulation. Theoretically, instability is given by the conditions expressed by Equations 2.4 and 2.5 (Derjaguin 1941) :

$$V_T = 0 \qquad [2.5]$$

$$\frac{\partial V_T}{\partial x} = 0 \qquad [2.6]$$

For coagulation conditions to occur, the thickness of the diffuse ion layer must be reduced to such an extent that attractive Van der Waals' forces overcome the electrostatic repulsive forces, i.e. energy barrier against coagulation is diminished. This condition can be obtained by addition of counter-ions to the colloid system to reduce the thickness of the diffuse ion layer and consequently to affect coagulation.

The minimum electrolyte concentration at which coagulation occurs is termed the Critical Coagulation Concentration (CCC) or flocculation value.

2.2.2.2. COAGULATION IN BENTONITE SUSPENSIONS and CCC VALUES

As mentioned above, the coagulation can be obtained by reducing the thickness of the diffuse ion layer by increasing the concentration of electrolyte. This also can be obtained by using counter ions with higher valency. In clay suspensions the presence of oppositely charged basal and edge surfaces

complicates the situation considerably. A small amount of electrolyte might initially deflocculate the clay, while further addition of electrolyte will cause coagulation The structure of the coagulated particles will be dependent upon the conditions under which the suspension changes to coagulated particles (van Olphen 1973)

In the case of montmorillonite, which has a rather high cation exchange capacity, the structure of coagulated particles of the clay will be dependent on the preferential order of the substituting cations if they differ from the ones present on the clay Some typical Critical Coagulation Concentrations (flocculation values) are listed below in table 2.2 (van Olphen 1963). The value of CCC of Ca^{2+} for sodium montmorillonite is not comparable because some of the calcium is used for ion exchange; the value of CCC for Ca^{2+} for calcium montmorillonite gives the correct value. However, the Critical Coagulation Concentrations may be quite sensitive to the source of the material used and its pre-treatment before the experiment.

Table 2.2. Critical Coagulation Concentrations (CCC) of sodium and calcium ions for sodium and calcium montmorillonite suspensions (van Olphen 1963)

	Flocculation value, meq/L	
Suspension (conc. 1/4%)	NaCl	$CaCl_2$
Na-montmorillonite	12-16	2.3-3.3
Ca-montmorillonite	1.0-1.3	0.17-0 23

When a suspension of clay particles flocculates, the mode can either be face-to-face, edge-to-edge or edge-to-face association. The electrical interaction energy differs with different associations. A variety of structures are possible, depending upon the mode of interparticle bonding. Some of the structures of clay particles are presented in figure 2.11 according to van Olphen (1977).

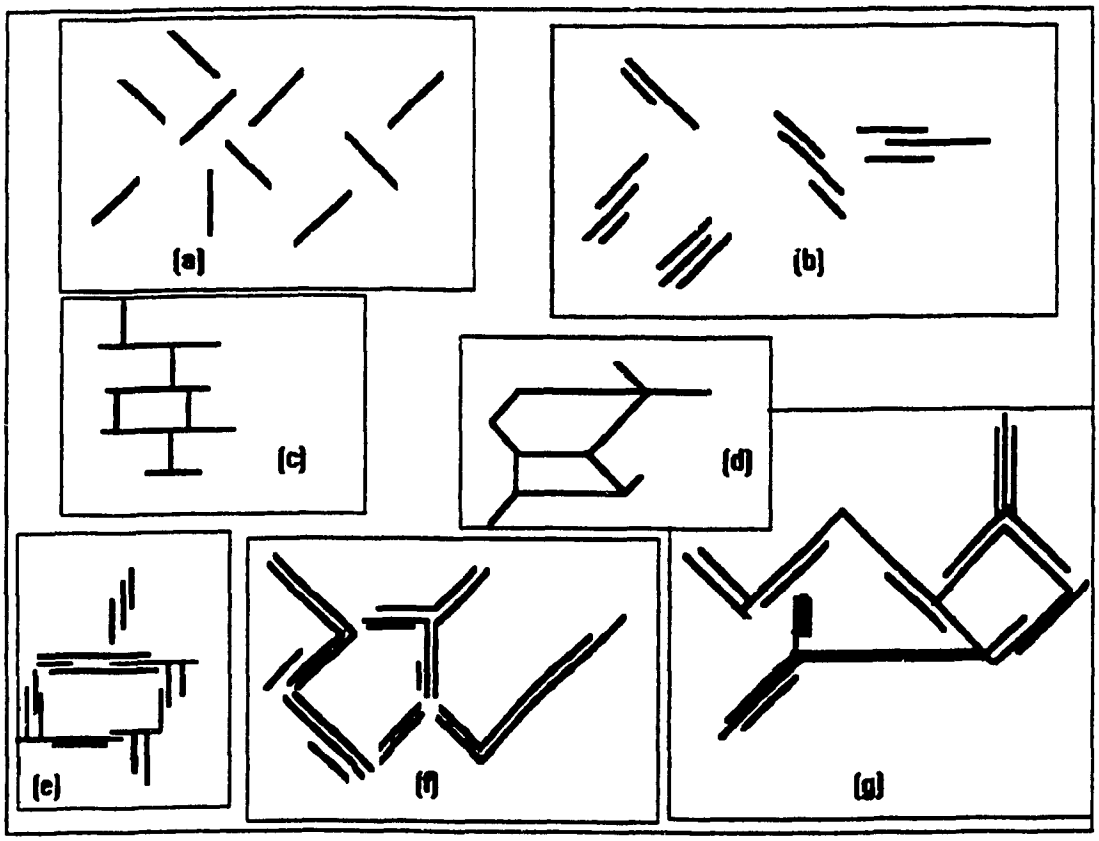

Figure 2.11. Modes of particle association in clay suspensions and terminology (schematical representation) (van Olphen 1977)
(a) "Dispersed" and "deflocculated".
(b) "Aggregated" but "deflocculated" (face-to-face association, or parallel or oriented aggregation).
(c) Edge-to-face flocculated but "dispersed".
(d) Edge-to-edge flocculated but "dispersed".
(e) Edge-to-face flocculated but "aggregated".
(f) Edge-to-edge flocculated but "aggregated".
(g) Edge-to-face and edge-to-edge flocculated "aggregated".

The amount of face-to-face association in the coagulation generally increases with increasing charge of the counter-ions, thus resulting in decreased colloidal stability. The dependence of colloidal stability on pH is due to the effect of pH on the coagulant itself rather than on the clay Generally, the stability increases with increasing pH because the edge-to-face association is broken up In the presence of Ca^{2+}, montmorillonite forms face-to-face stacks and coagulates to form a gel. However, the structure of the gel is not clear Depending on the environment, montmorillonite may exist as independent unit layers or as stacks of layers in particles. In general, the amount of face-to-face aggregation decreases and the interlayer spacing increases with decreasing clay particles concentration, increasing energy between the layers, decreasing electrolyte concentration, and decreasing affinity of the interlayer cations to the outside surface for the clay (Barclay 1970; Warkentin 1962).

The degree of the different modes of association have been estimated in numerous studies by various techniques including rheological, turbidimetric, microscopic and porosity measurements. Van Olphen (1977) suggests that deflocculation can be obtained by a small increase in electrolyte concentration thus breaking the edge-to-face association by decreasing the thickness of the diffuse ion layers. However, face-to-face and edge-to-edge repulsions are not sufficiently decreased to cause this kind of aggregation. If electrolyte concentration is further increase, the diffuse ion layers are reduced enough to cause formation of flocs.

2.3. SWELLING IN Na-BENTONITE CLAYS

2.3.1. PREDICTION

Swelling could be the result of repulsion between adjacent clay particles. Extended swelling is due to osmotic pressure, depending on the ions and the salt concentration. The osmotic pressure decreases with increasing distance between particles, i.e., it decreases as swelling proceeds. The extent of osmotic swelling is dependent upon the interacting surface area. A clay deposited in fresh water has a fabric arrangement with parallel particles orientation, which results in higher swelling than in other conditions. Similarly, for bentonite the parallel orientation of particles results in the greatest swelling than other orientations.

The volume of a sample which allowed to swell freely, increases until forces of attraction balance the forces of repulsion. These forces of attraction include Van der Waals' forces, Coulomb's forces between unlike charges, and forces exerted by organic or inorganic molecules which bond particles.

The volume change of an Na-bentonite is governed by the magnitude of interparticle forces, which is dependent on the charge, surface area and chemical composition of the soil-water system as well as the mode of particle interaction and distances between particle. By simple force equilibrium requirements, if attractive forces exactly balance repulsive forces, the system is at an equilibrium. Disturbing the system, for example, by changing the pore water chemistry, mineralogy, or soil fabric will alter the internal force system; the clay mass will adjust its volume until equilibrium occurs. The magnitude of swelling pressure (or repulsive force) can be measured by applying a confining pressure which will keep the particles at a given distance.

Such experimental studies on swelling have been published by several researchers, (Bolt and Miller 1955; Warkentin, Bolt and Miller 1957; Warkentin and Schofield 1960; and Hemwall 1956). As an example in figure 2.12, Warkentin and Schofield, (1962) measured the swelling pressure for the high-swelling Na-montmorillonite at low salt concentrations and found accordance between the measured and calculated values. At high salt concentrations, the measured pressure was found to exceed the calculated value. This difference probably results from the errors in using concentrations rather than activities of the exchangeable cations, and from neglecting the tactoid structure.

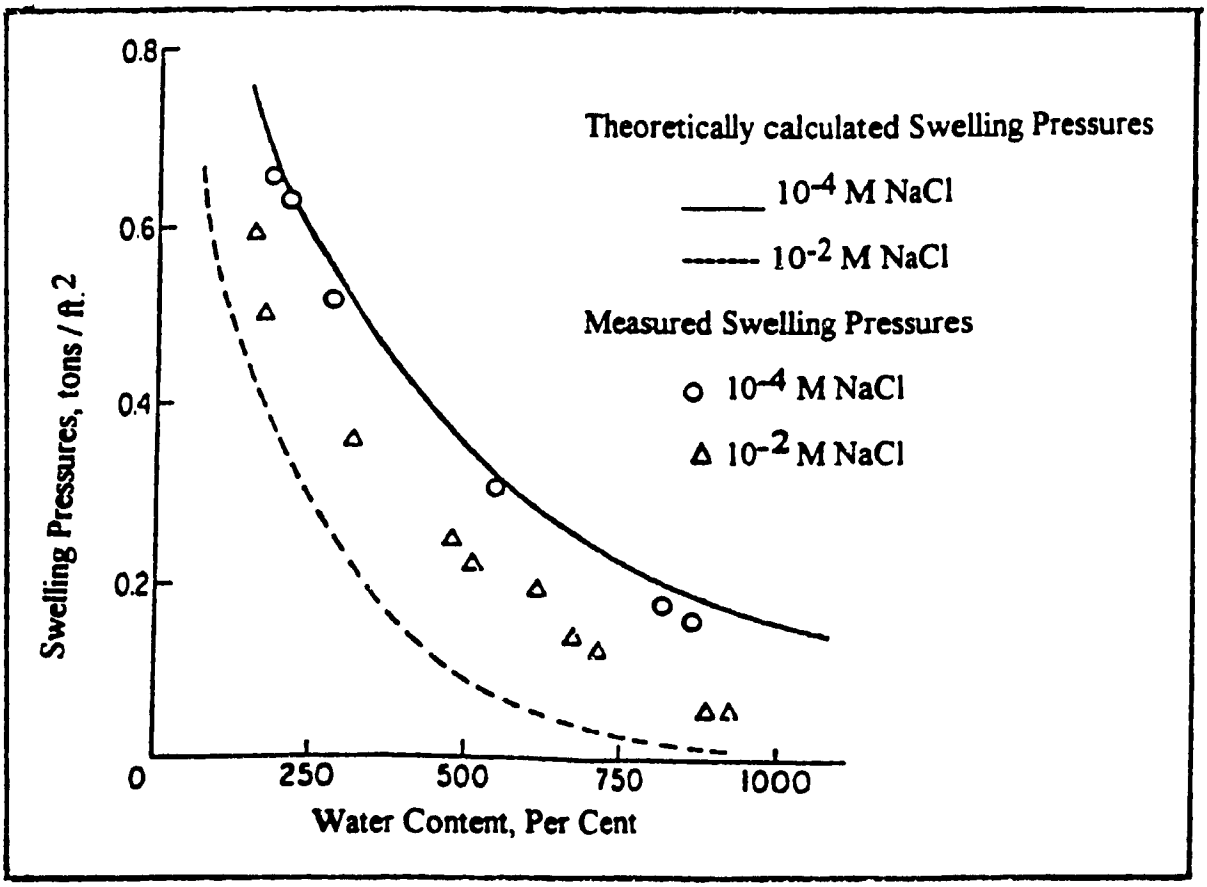

Figure 2.12. Comparison of calculated and measured swelling pressure for sodium montmorillonite at two salt concentrations (Warkentin and Schofield 1962).

According to van Olphen (1977), two different mechanisms are involved in swelling. The first is due to hydration of the dry clay particles and also the ions when water is absorbed between the particles and results in a release of hydration energy The hydration of clays has been treated comprehensively by Forslind and Jacobson (1975) and swelling pressure due to the above hydration has been calculated by van Olphen (1965).

The second is due to diffuse ion layer repulsion, or osmotic swelling, which pushes the particles further apart. Deviations between the calculated and the measured pressures have been found and have been explained differently by van Olphen (1963) and Barclay (1970) to be due to an effect of pressure of non-parallel arrangement of particles or to be due to hydration effects, respectively.

2.3.2. EFFECT OF SALT CONCENTRATION AND COMPOSITION OF PORE FLUID ON SWELLING

The influence of salt concentration and composition of pore fluid on the physico-chemical component of swelling has been explained using Gouy-Chapman theory for mid-plane concentration and expressed in the following equation (Yong and Warkentin 1975):

$$C_C = \frac{\pi^2}{Z_i^2 B (X_d + X_O)^2 10^{-16}} \qquad [2.7]$$

$\mathbf{C_c}$ = concentration of cations midway between two clay plates, in moles/litter.

$\mathbf{Z_i}$ = valence of exchangeable cations

$\mathbf{X_d}$ = half distance between two clay plates, in A^0.

$\mathbf{X_o}$ = correction factor of 1-4 A^0 depending upon ion valence and charge density.

$\boldsymbol{B}$ = 10^{-15} cm/mmole depending upon temperature and dielectric constant.

Based on parallel arrangements of clay particles the relationship between water content, W, and half distance between particles, X_d is given by (Yong and Warkentin 1975):

$$W = \frac{SX_d}{100} \qquad [2.8]$$

where :

W = water content by weight.

S = surface area of clay per unit mass, m2/ g .

X_d = half-distance between two particles, A0.

For γ_C & Gc = soil density and specific gravity g/cm3

For 1 gram of soil

W water = V water = Vsoil - V soil particles = $(\frac{1}{\gamma_c} - \frac{1}{G_c})$

$W = (\frac{1}{\gamma_c} - \frac{1}{G_c}) \times 100$ and

from equation [2.8]

X_d = **100 W/S**

$X_d = 10^4 (\frac{1}{\gamma_c} - \frac{1}{G_c}) \times \frac{1}{s}$ in (A^0)

The swelling pressure can then be calculated from the Van't Hoff equation for monovalent ions as follows (Yong and Warkentin 1975):

$$P = RT(C_c - 2C_o) \qquad [2.9]$$

where :

P = calculated swelling pressure.

R = gas constant.

T = temperature.

C_O = Concentration of salt in the pore water, moles/ litter.

The equations [2.7], [2.9] suggest that an increase in pore-water salt concentration decreases swelling of high-swelling clays generally, especially if monovalent ions are present in the clay. This is due to the reduction in thickness of the diffuse ion layer arising from an increase in electrolyte concentration thus resulting in a decrease in the range of the diffuse ion layers repulsion and the negatively charged particles. In contrary, low salt concentration in pore water with an excess of monovalent cations in the solution will cause high swelling pressure. Accordingly, double layer repulsion can account reasonably well for the swelling behavior of sodium montmorillonite (Bolt 1956). In such a system, the particles are reasonably parallel and attractive forces are small.

In case of divalent cations in the electrolyte, equation [2.7] can account for swelling pressure calculation, using $3C_o$ instead of $2C_o$ equation. Divalent cations tend to restrict the swelling of montmorillonite to a maximum interlayer spacing of about 9A^o (Norrish 1954; Blackmore et al. 1961) where the particles stabilize into tactoids or domains. Electrical double layer theory may account for such behavior if allowance is made for the interparticle water in the tactoids (Shainberg et al. 1971) and if the analysis is based on the external ion distribution.

Very fine fractions (<0.2μm) of illite, kaolinite, and vermiculite may swell in reasonable accordance with theoretical predictions (El Swaify et al. 1967).

For clays consisting of coarser particles of these materials, the swelling curves may indicate little influence of electrolyte concentration or even give results contrary to prediction. This reflects the effect of particle cross-linking due to edge charge influences and non-parallelism of particles.

Practically, soil contains different species of cations. However most experiments and theoretical analysis of osmotic swelling have been made using a single cation species until recently. Thus a study of the system containing various cations species is required. In soils containing a mixture of cations the swelling pressure is closely related to the quantity of sodium in the free pore water relative to divalent species of salt. This may be quantified in terms of the Exchangeable Sodium Percentage (ESP) on clay surface or Sodium Adsorption Ratio (SAR) in pore water, where:

$$ESP = \frac{N^{+}_{a}}{CEC} \times 100 \quad \text{in meq/100g}$$

$$SAR = \frac{Na^{+}}{\left[\frac{Ca^{+2} + Mg^{+2}}{2}\right]^{1/2}}$$

whereby all concentrations are in meq/L .

McNeal et al. (1968) indicated that soils with low salt contents and high SAR and high ESP values (i.e. high sodium contents) exhibit high swelling characteristics. Swelling is generally not appreciable unless the ESP exceeds about 25 or 30 (Aylmore et al. 1959; Shainberg et al. 1971; Quirk 1968).

2.4. DISPERSION IN BENTONITE CLAY

2.4.1. GENERAL

Dispersivity refers to the tendency of soil particles to detach and entrain in a flowing fluid at a bed boundary under the action of drag forces and/or repulsive forces due to diffuse ion layers.

In many geotechnical projects, serious problems have resulted from clay dispersion and subsequent piping or internal erosion of compacted soils (Aitchison and Wood 1965). The conditions for soil dispersion have been identified based on the chemistry and the composition of the pore water (Sherard et al. 1976 ; Arulanandan et al. 1975).

2.4.2. EFFECT OF EROSION, PARTICLE BOND AND DRAG FORCES ON CLAY DISPERSION

Dispersion due to erosion by flowing water was examined by Sherard et al. (1972) for dams. This study classifies Na-bentonite as a sensitive material to erosion process. However, the results for the study cannot be directly applied to the present study due to the differences in the flow conditions and water chemistry. A study of the drag forces on the particles caused by the low water flow and the resisting forces due to bonding between particles is necessary to evaluate the particles dispersion from the gel surface under low water flow condition. The average bond strength of the particles was found to be about 4×10^{-13} N per contact (Osipov 1975; Mitchell 1964). This value of bond strength for the soft gel represents the minimum strength that attributes to the long range

attractive force in the secondary minimum shown in the net energy curve of the DLVO theory mentioned previously, besides the cross linking edge to face (EF) forces (van Olphen 1977). The average drag force has been calculated by Pusch (1983) based on low water flow (10^{-6} to 4×10^{-4} m/s) expected at the disposal location in the rock fissures. The calculated average drag force has been found to be about 4×10^{-15} N at a flow rate of 10^{-6} m/s.

From the above calculations, the bonds in the Na-bentonite are strong enough to balance the drag forces exerted by the flowing water This indicates that erosion of clay by the surrounding groundwater is negligible These results suggest that for low water flow condition that may occur in the disposal vault, the effect of water velocity on particle's detachment by drag forces is insignificant. This justifies the assumption of stagnant water condition used in this study

2.4.3. PARTICLE RELEASE UNDER STAGNANT WATER CONDITION

A frequently debated question is whether spontaneous swelling of the clay would lead to complete disintegration of the gel into a suspension, or that the swelling would be limited and stops as soon as a certain gel volume is reached. This is because it is difficult to perform an experiment in which all external forces are excluded, such as hydrodynamic convection force that tends to disperse the gel particles, and gravity force that tends to operate against the dispersion of these particles. In principle, suspension formation will be spontaneous only if repulsion dominates at any particle distance at any configuration of the particles in space. In reality, however, there are usually some forces that prevent the formation of suspension. These are due to the

attractive forces such as Van der Waals' forces and the edge-to-face cross-linking forces that overcome the repulsion.

However, for Na-montmorillonite gel with high water content, dispersion can occur with low electrolyte concentration and high pH value by breaking the cross-linking force between particles. Le Bell (1978) found that the diffusion coefficient for the colloidal particles released from gel surface of Wyoming bentonite to range from 2×10^{-12} to $< 5\times10^{-13}$ m^2/s in dilute solutions and in distilled water. The results, however, are not sufficient and more data is needed. In addition, the method used in determination of the particle concentration by comparing the results with spherical particles for different materials is a very rough method and gives a relative estimate.

2.5 SUMMARY

The preceding literature review can be summarized in the following:

Forces of attraction and repulsion act between clay particles and they are of importance since the clay particle behaviour is controlled by surface properties not with the weight of the particle. The forces of repulsion are explained by the diffuse ion layer theory for interacting particles and the attraction forces have been introduced to clay particles' interactions by the theory of colloidal stability (DLVO theory) which explains the stability in clay-water system as the net effect between attraction and repulsion forces. If the net effect of forces between the two clay particles is attractive, the two particles flocculate. If the net effect is repulsive they disperse.

The repulsive forces are highly dependent on the characteristics of the system while the attractive forces are not.

The colloidal theories consider only the two types of forces mentioned above and pay no attention to the force arising from the net positive charge at the edges of the clay particle. This force, in case of close approach between particles, can participate in an edge-to-face linkage between particles of electrostatic type. Analytical solutions of swelling pressure and the CCC values by colloidal theories are also limited to the parallel arrangement of clay particles. Practically this is far from the reality and experimental studies are needed.

While the literature review on studying individual clay particles cannot give exact quantitative values or analytical solutions for the problem stated in this study, it serves as a guide to the understanding and interpretation of the direct experimental results.

Dispersion of clay particles from the surface of the clay mass subjected to a flowing water can be affected by the velocity of the flowing water and on the water chemistry of the flowing water. The literature focused on the effect of velocity on dispersion. Except for a study by Le Bell (1978) and by Pusch (1983), little work has been conducted to determine whether the density of compacted bentonite-clay can be maintained for a long period of time when the clay is exposed to a saline groundwater with extremely low flowing velocity and its effect can be neglected.

CHAPTER 3

3. THEORETICAL CONSIDERATIONS

3.1. SAND-CLAY MIXTURES

It has been mentioned that the buffer barrier is a mixture of sand and bentonite. The behavior of sand-clay mixtures is controlled by the dominant surface area. Compared with clays, sand has a very small specific surface area and surface charge density. Thus, in sand-clay mixtures specific surface area for the mixture is almost directly attributed to the clay fraction. Previous work had been demonstrated by Cheung and Dixon (1987) that the flow properties is controlled by the clay portion in the mixture. Consequently, only pure bentonite gel will be considered in the gel penetration into the fissures.

3.2. GEL PENETRATION

From the literature review, swelling of bentonite occurs with water absorption and the expanded gel penetrates through the rock aperture. The distance which the gel can advance into the fissures depends on the environmental conditions (hydrostatic pressure, electrolyte composition, clay flow properties and rock walls friction) which contribute to force equilibrium. Since the swelling process is mainly due to repulsion forces between diffuse ion

layers of bentonite particles, it is expected that the valence of the cations in solution and the solution concentration (ionic strength) are important factors controlling the swelling process as predicted by the diffuse ion theory.

The distance of penetration or the increase in volume due to swelling of the Na-bentonite gel into rock fissures is correlated to many factors such as geometrical properties of the rock apertures, the porewater chemistry (which affects the repulsive and attractive forces) and the flow properties of the clay (Le Bell 1978 and Pusch 1983). Generally, It is found that increasing the salt content in pore water of expanded gel will increase the shearing strength of the clay and increases the resistance of the clay gel (van Olphen 1977; Yong 1975; and Mitchell 1976) and decreases the swelling and expansion. From these theoretical considerations, it is expected that the gel will expand in the rock fissures until equilibrium conditions are reached, but theoretical quantification of the expansion process is difficult because of the many factors affecting the swelling process. These factors cannot be presented in one formula to predict the net resultant of all these factors in order to predict the amount of swell. On this basis, the swelling of the clay bentonite needs to be experimentally examined, approximately simulating the field conditions, where DDW and synthetic groundwater WN-1 of known ionic strength are used for comparison of the results of gel expansion in the two media as will be shown in the experimental part.

3.3. BENTONITE GEL STRUCTURE

From the literature review on clay suspensions, the structure of bentonite gel in contact with water can either be flocculated or dispersed depending, among of

many factors, on the clay particle interaction which occurs through the layers of adsorbed water, diffuse ion layers of exchangeable cations, and direct particle contact. The preceding colloidal theories are based oncertain assumptions in predicting the interparticles interactions, like negatively charged particles of colloidal size with parallel arrangement and treating the particle as a plate of smooth surface, which is not the actual conditions in bentonite clays In addition, the diffuse ion layer theory neglects the positive charge on the clay particle edges which causes a cross-linking bond (edge to face) at short distances between the particles. In addition, the real porewater contains a variety of cations and anions which complicate the problem. Thus, theoretically, it is difficult to predict the structure conditions of the expanding bentonite gel in contact with groundwater in the real field. Experimental data are needed to help evaluation of the state of particles association in the actual conditions By performing sedimentation tests, using a systematic approach through studying the NaCl and $CaCl_2$ solutions with different concentrations in a clay suspension, the CCC of NaCl and $CaCl_2$ can be found. Using the ionic strength for these solutions and that for the real known groundwater, the state of the particles arrangements of the expanded clay gel in real groundwater can be assessed as will be explained in next chapter.

3.4. TRANSPORT PROCESS

3.4.1. DIFFUSION

When the expanding clay gel penetrates in the rock aperture contacting groundwater, some of the clay particles at the interface under the kinetic effect of expansion may release from the gel surface and diffuse away in the solution under the concentration gradient effect The governing equation of

diffusion which can be used to predict the diffusion rate of colloidal particles is that of Fick's second law of diffusion under mass concentration gradient effect only (assuming that velocity effect is neglected) as follow:

$$\frac{\partial C}{\partial t} = D^* \frac{\partial^2 C}{\partial x^2} \qquad [3.1]$$

Assuming C_O to be constant at the gel surface, the solution of this equation is given by (Crank, 1956) as

$$\frac{C}{C_o} = \text{erfc}\left\{\frac{x}{2\sqrt{D^* t}}\right\} \qquad [3.2]$$

C = Concentration of clay particles at distance x from gel surface.

C_O = Concentration of clay particles at the gel surface.

x = Distance above the gel surface.

t = time.

D^* = Diffusion Coefficient of colloidal particles.

The diffusion coefficient D^* can be calculated from equation 3.2 having C, C_O, x, and t.

From the above considerations, there is a need to measure the concentration profiles with time.

CHAPTER 4

EXPERIMENTAL PROGRAM

The purpose of this experimental program is to give qualitative and quantitative data to help accomplishing the objectives of this study by carrying out laboratory tests which simulate the environment surrounding the Canadian Nuclear Waste disposal vault.

The groundwater surrounding the buffer in the Canadian Nuclear Waste disposal vault in the rock shield locations is a saline water named WN-1 or SCSSS of known chemical composition which dissolves mainly Na, Ca, Mg cations in water and has a pH ranging from 7 to 9. The pH values assure that the clay surfaces are negatively charged.

Tests are carried out to determine some important engineering properties of the Avonlea-bentonite as illustrated in (table 4 1) as well as the initial salt content in this material. In addition, sedimentation, swelling, and diffusion tests are carried out which form the major part of this experimental program.

The sedimentation tests are qualitative tests which allow measuring of the critical coagulation concentrations, using different cations, valence and concentration in the solutions, which initiate flocculation in Avonlea-bentonite suspensions.

The swelling tests examine the swelling of Avonlea-bentonite clay in an artificial crack where this clay adsorbs water through the crack only. Two types of water are used; a synthetic solution WN-1, of ionic strength that may occur in the Canadian rock shield and a distilled water (DDW) for comparison purposes

only They are used to compare the effect of water chemistry on swelling of Avonlea-bentonite clay

The diffusion tests aim at evaluating the diffusion coefficients of colloidal clay particles diffused from the gel surface into the solution, using solutions of different concentrations in stagnant conditions. This can be realized by constructing concentration profiles relating the diffused clay concentration with distances measured from the original gel surface as a function of time for each solution.

The materials used and the procedures adopted in the sedimentation, swelling, and diffusion tests are described below.

4.1. MATERIALS

Avonlea bentonite, a montmorillonite-rich clay which is used in the experimental program contains sodium as the main exchangeable cation and has a cation exchange capacity ranging between 80 - 100 meq/100 gm. The specific surface area of the material is 800 m^2/g and the pH of clay suspension is in the range of 8-10 at room temperature. Other engineering properties are summarized in table 4.1.

Table 4.1 summary of some engineering properties of Avonlea-bentonite.

Engineering property	Liquid Limit	Plastic Limit	Plasticity Index %	Specific Gravity
Value	240%	60%	180%	2.69

The above data on Avonlea bentonite indicate that this clay is a very active clay due its high surface area and surface forces. This clay possesses the following properties:

1. High swelling potential.
2. High adsorption capacity, and
3. Very low permeability.

RESIDUAL SALT CONTENT

The soil material in the tests was used without any purification. To check the initial salt content, a sample of 1 gm Avonlea-bentonite was diluted into 50 ml. of DDW and the composition of supernatant solution from the sedimentation is analysed by ionchromatography. The results showed that the residual salt was 38.614 mg/L with 31.35 mg/L sodium and 5.8 mg/L calcium. The complete analysis is illustrated in appendix C.1.

SOLUTIONS

Since groundwater is dominated by Na, Ca and Cl ions; NaCl and $CaCl_2$ solutions (of various molarities), in addition to the deionized distilled water (DDW), are used in the tests as basic solutions for comparison with other solutions representing real groundwater. In addition, synthesized solutions to simulate the Whiteshell Nuclear (WN-1) groundwater and Standard Canadian Shield Saline Solution (SCSSS) are used also with the Avonlea-bentonite in the different tests. The composition of the WN-1 and SCSSS solutions is shown in table 4.2. The calculated ionic strengths (Appendix C.1) are 0.267 for WN-1 and 0.9167 for SCSSS. The ionic strength are used in sedimentation tests as

indication of the total effect of the components of the solution including the valence effect. It is also easy to compare the floculation power of different solutions using their ionic strength.

Table 4.2 . Composition of WN-1 and SCSSS solutions

SAMPLE	WN-1 mg/l	SAMPLE	SCSSS-1 mg/l
Ca	2210±120	Ca	16000±300
Fe	<0.1	Fe	0.74±0.09
K	11.0±0.4	K	43.5±0.3
Mg	58.1±0.7	Mg	215±3
Na	1720±60	Na	4560±200
Sr	15.8±0.3	Si	19±2
Cl	6410±385	Sr	1.94±0.06
NO_3	40.8±1.3	Cl	33200±2000
SO_4	1080±200	NO_3	99.1±6.5
HCO3	28±2	SO_4	758±23
		HCO_3	72±2

From table 4.2, it is clear that SCSSS is a highly saline groundwater of high ionic strength (0.9167) and that WN-1 is a saline water of ionic strength (0.267).

4.2 EXPERIMENTAL PROCEDURES

The procedures and apparatus used for sedimentation, swelling and diffusion tests are described below. In general, various concentrations of NaCl and $CaCl_2$ solutions and synthetic groundwater are used to cover the cation types and the range of concentrations in the ground water.

4.2.1. SEDIMENTATION TESTS

Sedimentation test series are performed to show the effect of the environmental factors on the coagulation and dispersion process in Avonlea-bentonite suspensions and to study the structure of the bentonite gel in contact with water by studying the effect of salt concentration and the valence of salt cations on the sedimentation process.

In spite of the simplicity of these tests, they are very important to explain the concepts of the colloid theory of stability and to determine the flocculation values of different electrolytes in the bentonite suspensions. Sedimentation tests are necessary to understand and to explain the electrolyte effect on the coagulation and sedimentation of colloidal particles and how the amount of the salt is very sensitive to the sediment properties and on the particles arrangement. These tests also give a qualitative description for the gels formed in the sediment volume.

Two types of tests are carried out to investigate the coagulation and sedimentation of the Avonlea-bentonite, these are termed the gravity and centrifugation tests. The gravity test is used to examine sedimentation occurring

under gravity effect in various electrolytes; the centrifugation test is devised as a controlling test on the gravity tests in addition to time saving by using these tests

4.2.1.1. GRAVITY TESTS

These tests include a series of flocculation tests which enable the determination of CCC values associated with different cations.

In the flocculation tests, 2% by weight of Avonlea-bentonite is mixed by shaking with DDW containing a range of concentrations of one type of electrolyte, for example, NaCl. The same suspension volumes are made in identical test tubes for ease of subsequent comparison of sediment volumes of the clay in the different solution concentrations after a period of settlement, which has been arbitrarily taken as 18hrs, since it is considered to give satisfactory results in such time period. One of the test tubes is identified as having the Critical Coagulation Concentration (CCC) that initiates flocculation of particles when the top of the sediment is clear and the supernatant looks clear also. Usually the concentrations in two adjacent tubes would denote the upper and lower limits of the CCC value.

Table 4.3 Various concentrations of NaCl and $CaCl_2$ used in the sedimentation tests

DDW	DDW
10^{-5} M $CaCl_2$	10^{-5} M NaCl
10^{-4} M $CaCl_2$	10^{-4} M NaCl
10^{-3} M $CaCl_2$	10^{-3} M NaCl
10^{-2} M $CaCl_2$	10^{-2} M NaCl
10^{-1} M $CaCl_2$	10^{-1} M NaCl
10^{-0} M $CaCl_2$	10^{-0} M NaCl

By repeating the above procedures using smaller concentration intervals between the upper and the lower limits for a number of times, the CCC value for Na+ can be more precisely determined.

The above procedures are also carried out for $CaCl_2$ solutions thus obtaining CCC value for Ca^{2+}.

DDW and different salt types and concentrations used in the gravity tests are illustrated in table 4.3.

Details on sedimentation tests procedures and CCC values and tables are listed in appendix C.

4.2.1.2. CENTRIFUGATION TESTS

The procedures of this test is similar to that of the gravity test. The main differences being the time for testing is shortened by centrifuging the suspension for a maximum 3hrs at a speed of 2500 r.p.m. In addition, WN-1 and SCSSS water are also used in the test. The sediment volumes associated with the two types of water are also recorded for comparison with corresponding volumes associated with the CCC value obtained for Na+ and Ca^{2+}.

The sediment volumes as a percentage of initial suspension in DDW, and SCSSS and WN-1 water are plotted against the different salt concentrations and ionic strength, Tables and charts are illustrated in next chapter in the results and discussion. More data on centrifugation tests and procedures are reported in appendix C.

4.2.2. SWELLING TESTS

In these tests, two cells are used to immerse Avonlea-bentonite in DDW and WN-1 media respectively. Each cell consists of two plastic plates clamped vertically together with a clear distance of 0.5 mm between them, by the use of spacers, to simulate the crack. The lower plate has a 50 mm diameter and 12 mm thick cavity in which a sample of compacted Avonlea bentonite is placed (figure 4.1).

The swelling of compacted Avonlea bentonite in the artificial crack was followed by measuring the distance of the advanced gel front at different times from the initial boundaries of the original sample in DDW and in WN-1 water, for an arbitrary time of 30 days.

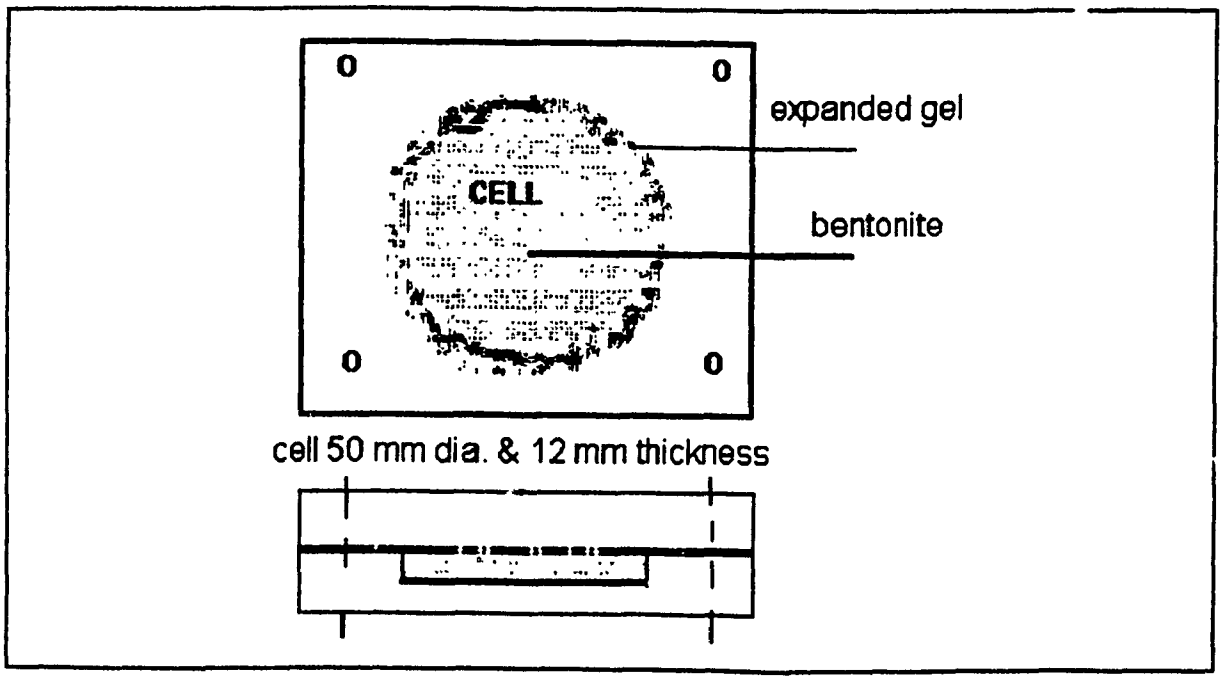

Figure 4.1 Shows schematic diagram of cell used in bentonite swelling test.

4.2.3. DIFFUSION EXPERIMENTS

Preliminary investigations of 15% clay gel of same volume placed in test tubes in different dispersion media, indicated an increase in volume with different amounts depending on the dispersion media. In the mean time, these investigations indicated that the concentration of bentonite particles released from the gel into solutions would be extremely dilute. Therefore a Laser technique was used in the diffusion tests to detect the concentration of Avonlea-bentonite particles at different distances away from the clay gel (15% bentonite by weight in DDW) surface at different times. The dispersion media is chosen using the basic solutions NaCl and $CaCl_2$ of different concentrations besides the DDW to show the extreme case in dispersion media The grounwaters expected at the Canadian Shield are simulated using solutions of similar composition as WN-1 and SCSSS as dispersion media (table 4.4). This technique has an additional advantage of not disturbing the sample. In addition, it gives the intensity at various fixed levels in the test tube. Different dispersion media (table 4.4) are used for measurements of the diffused particles concentration in order to construct the concentration profiles.

Table 4.4 Gel concentration with different dispersion media in Diffusion Tests

1)	15 wt % bentonite gel prepared in DDW dispersing into
i)	DDW
ii)	WN-1
iii)	SCSSS
iv)	0.1 M Na
v)	0.01 M $CaCl_2$
vi)	0.001 M NaCl
vii)	0.0001 M $CaCl_2$

Table 4.4 shows the clay gel used in diffusion tests to be 15% (1.5×10^5 mg/L), i.e. with a water content of about 670%, this is the most diluted form of the gel to

be expected during an expansion process, i.e. the worst conditions of gel dilution for the sake of a safety study. The method of preparation of gel samples is as follows.

4.2.3.1. SAMPLE PREPARATION

1. The stock Avonlea-bentonite was sieved to separate particles of 45μm and smaller using standard American sieve sizes (sieve size limit of No.325 standard). In addition, the dry weight of the stock bentonite is determined by drying a sample at 105°C for 24 hrs. The water content of the stock sample is calculated as a weight percentage.

2 Three different weight percentages 15%, 30%, and 40% of sieved bentonite are mixed in DDW, WN-1 and SCSSS. The weight of water used is derived from the volume used assuming the density of the three types of water to be 1 g/ml.

3. Each gel is allowed to swell for approximately 48 hrs with stirring at various time intervals. Stirring is to ensure a uniform distribution of water in the gel to minimize remaining agglomeration

4. Portions of the gels are then transferred into glass "plugs" in preparation for insertion into the sample test tubes. The gels were allowed to swell and settle in the plugs for approximately 24 hrs.

5 The top of the swollen gels are sheared to level the plane surface of the glass plugs. This provides a constant reference height for subsequent dispersion measurements.

6. Sample test tubes are thoroughly cleaned in DDW and acetone to ensure that both the interior and exterior of the tubes are free of markings and dust particles The test tubes are individually inspected both visually and with the

laser to detect flaws which would distort the general optical properties of the tubes.

7. The glass plugs containing the gel samples are then inserted into the test tubes (figure 4.3).

8. A constant volume of 25 ml is used for each dispersion medium (table 4.4) to submerge the gel in the test tube. Each dispersion medium is added by directing along the side of the tubes to minimize the disturbance to the gel surface.

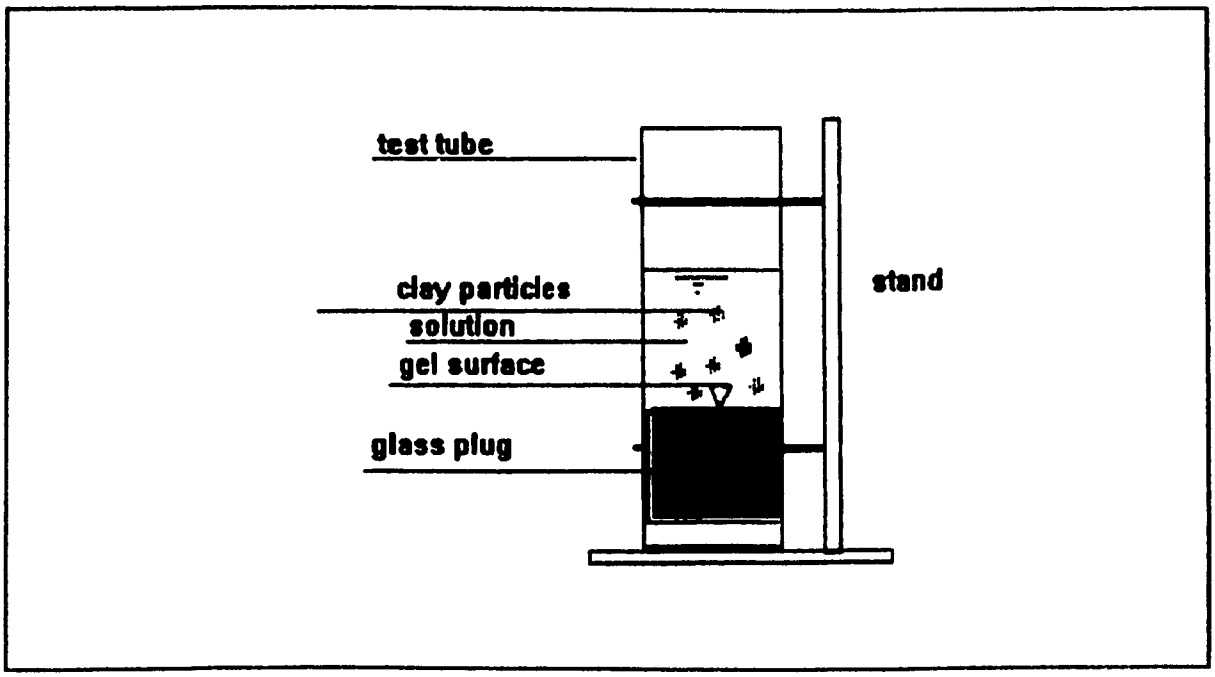

Figure 4.2. Schematic diagram showing the stand holder of test tube sample.

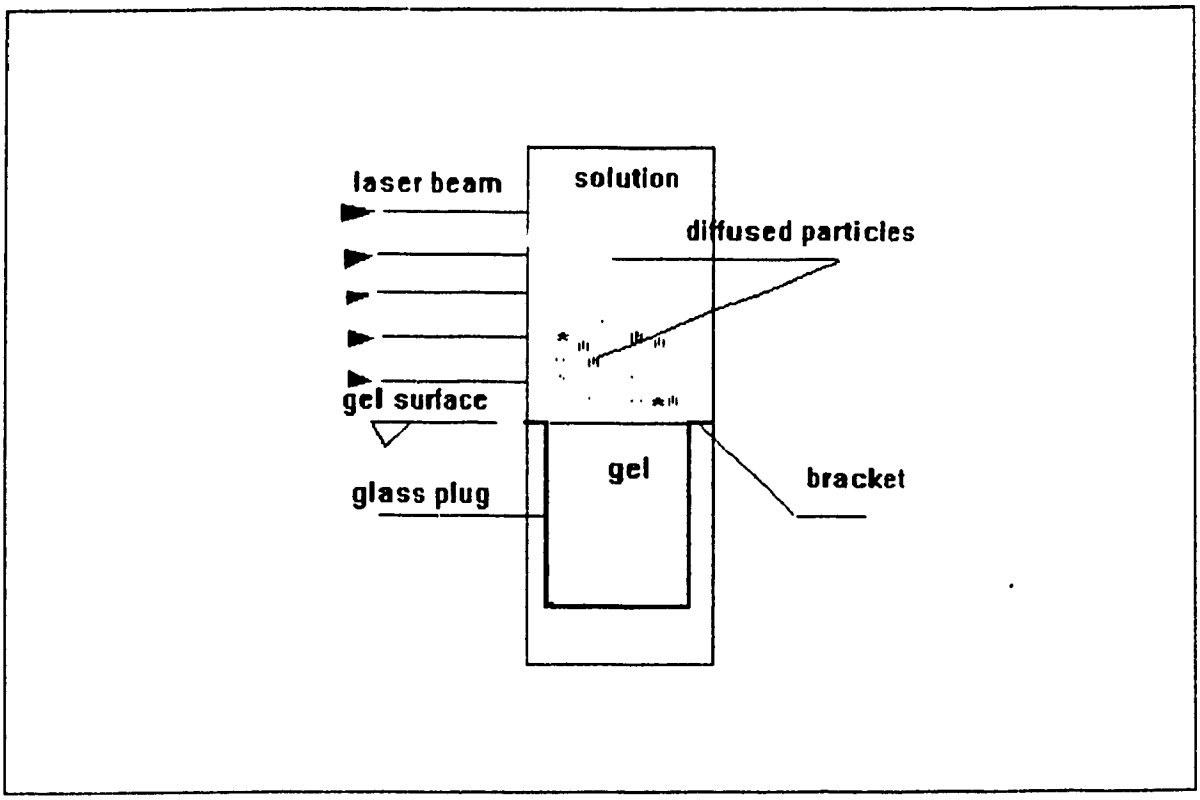

Figure 4.3. Schematic diagram showing the test tube containing the gel in the glass plug and particle release in solution medium .

4.2.3.2. APPARATUS

A schematic diagram of the laser light scattering apparatus designed for the dispersion measurements is illustrated in figure 4.4.

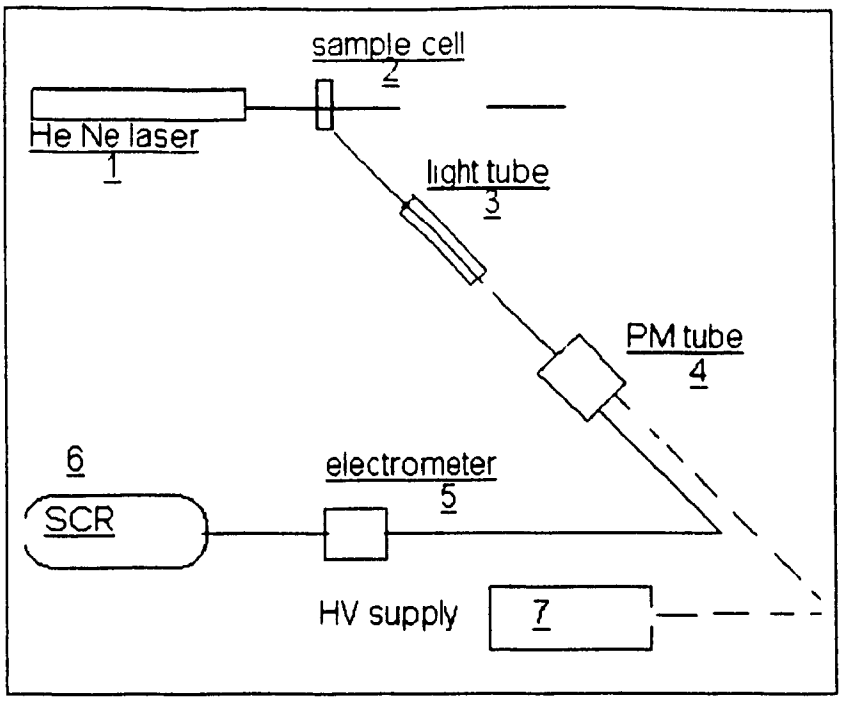

Figure 4.4. Schematic diagram of the dispersion apparatus

The light source is a He-Ne laser (1) further collimated through the presence of a small aperture. Light incident on the sample cell (2) and scattered by suspended particles is collected and transported to a photo multiplier (PM 4) tube through the use of a light pipe (3) oriented at an angle of 45° from the collimated beam. An electrometer (5) amplifies the signal from the photo multiplier tube and provides a voltage to a strip chart recorder (6) The voltage output is directly proportional to the scattered light intensity

4.2.3.3. CALIBRATION OF CLAY SUSPENSION CONCENTRATION

Standards are made using different known concentrations of Avonlea-bentonite. Suspensions, of size 2 μm which is expected to diffuse from the gel surface, in DDW which provide the basis for a calibration between bentonite particle concentration and scattered light intensity. The standards are

subsequently used to normalize dispersion data. Normalization of the dispersion data is required to minimize the effect of minute positional changes of the optical components of the apparatus. A sedimentation technique is employed to obtain a colloidal suspension of 2μm bentonite particles in distilled water for calibration.

Figures 4.5 is a calibration curve drawn from the data in table 4.5. The data in the figure are normalized to the DDW reading of scattered light intensity as also shown in table 4.5

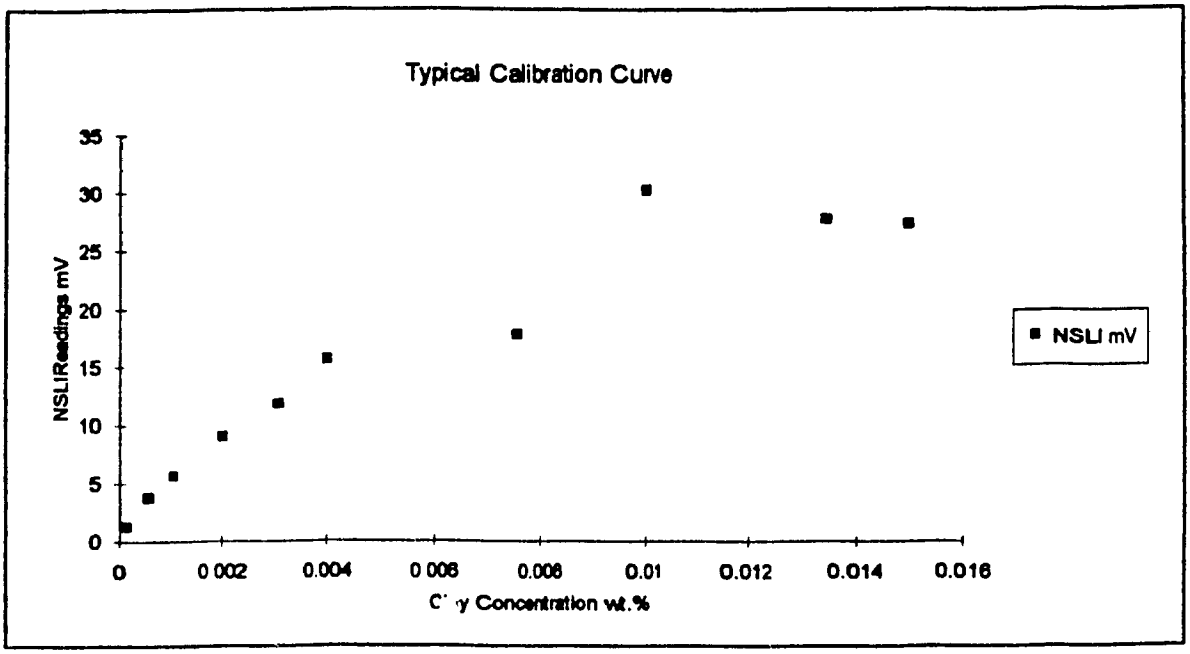

Figure 4.5. Typical Calibration Curve (normalized data to DDW)

Table 4.5 Data of Calibration of Standard Suspensions in figure 4.5

Standard wt%	Reading mV	Normalized reading mV to DDW
DDW	0.775	1
0.0001	0.975	1.27
0.0005	2.92	3.79
0.001	4.375	5.68
0.002	6.96	9.04
0.003	9.12	11.84
0.004	12	15.58
0.0075	16	17.79
0.01	23.26	30.21
0.0135	22.1	27.68
0.015	20.97	27.28

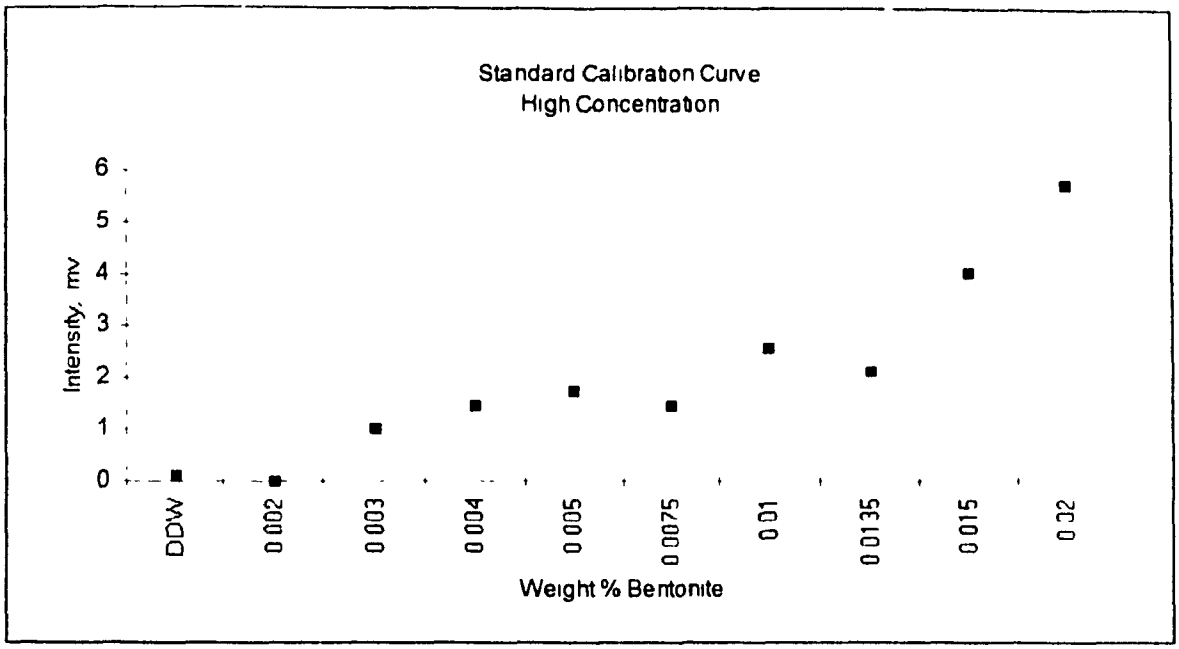

Figure 4.6. Standard Calibration Curve (data not normalized)

Figure 4.6. Shows a typical calibration curve drawn for high clay concentrations versus readings in mV without normalization as shown in table 4 5

Table 4.6 Data of Calibration of Standard Suspensions in figure 4.6

Standard Calibration ....Higher Concentration

1330 V .....10^{-7} amps..... ..... 5-50 V

Standard wt% Bentonite in DDW	Reading mV
DDW	0.1
0.002	
0.003	1
0.004	1.455
0.005	1.725
0.0075	1.475
0.01	2.575
0.0135	2.115
0.015	4.025
0.02	5.75

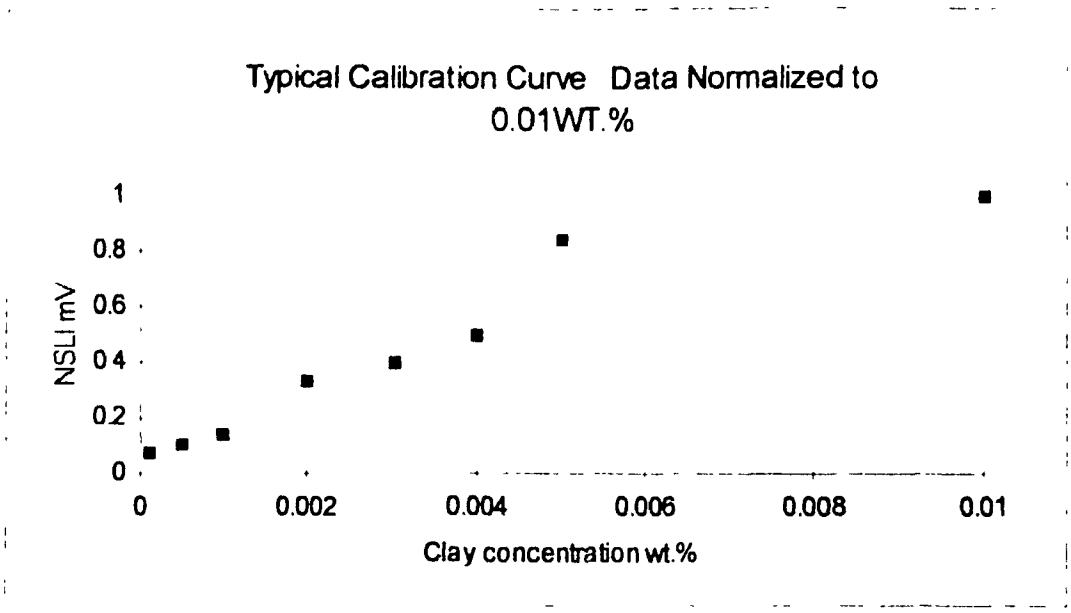

Figure 4.7. Typical Calibration Curve (normalized data to 0.01wt%)

Figure 4.7 shows a typical calibration curve for low concentrations vs. normalized scattered light in mV, the normalization is to 0.01 wt% as also shown in table 4.7 This curve can be used in finding the clay concentrations of released particles, if the normalized scattering readings are determined from the laser apparatus measurements in the diffusion tests. This curve is used for calculation of the clay particle concentration in the concentration profiles when needed in chapter 5 to show the amounts of diffused particles.

Table 4.7 Data of standard clay suspensions used in figure 4.7

Standard Clay Suspension wt%	Standard Clay Suspended mg/L	Normalized Scattered Light Intensity mV
0.0001	1.0	0.074
0.0005	5.0	0.1
0.001	10.0	0.14
0.002	20.0	0.33
0.003	30 0	0.4
0.004	40.0	0.5
0.005	50.0	0.84
0 01	100.0	1

CHAPTER 5

EXPERIMENTAL RESULTS AND DISCUSSION

This chapter discusses the effect of electrolyte (type and concentration) on bentonite clay in terms of particles arrangements (fabric) which are dictated by the repulsive and attractive forces during sedimentation, swelling and the diffusion process in light of the tests results.

5.1. SEDIMENTATION TESTS

5.1.1. GRAVITY TESTS

In these tests, clay suspensions of 2% concentration in basic solutions of NaCl and $CaCl_2$ of various molar concentrations are prepared and the sediment volumes are measured after a settling time of 18 hrs. Data of measured sediment volumes in (ml) and the corresponding electrolyte concentration in mole/L are plotted. In addition, the ratio of the sediment volumes to the initial volume are calculated and also plotted as (percentage sediment volume) in the same figures. Figures 5 1 and 5.2 are drawn for both NaCl and $CaCl_2$ In these figures, the vertical axes represent the sediment volume in ml. and the percentage of the sediment volume (%), while the horizontal axes represent the electrolyte concentration in mole/L. From the results of gravity tests shown in figure 5.1, it is observed that the range of the minimum NaCl concentration which initiated coagulation in the 2% Avonlea-bentonite suspension (CCC) was visually lying between 0.01 and 0.03 M for a settling period of 18 hrs. This result

was obtained from visual observation of the sediment and the solution for the case where the upper solution over the sediment changed from cloudy to clear.

At salt concentrations much lower than the CCC, the sediment volume is small and the suspension is cloudy. This is because at dilute concentrations, the repulsive forces between the diffuse ion layers are dominant and the clay particles are mainly dispersed. As NaCl concentration increases (< CCC), the sediment volume increases due to more flocculation occurring between particles leading to more sedimentation. As the concentration is increasing to just below CCC, the increase in volume is more noticeable. This was explained by van Olphen (1977) to be due to the breaking of the edge-to-face cross linking between the particles causing de flocculation between particles leading to an apparent increase in sediment volume. As the salt concentration increases beyond CCC, the volume decreases. This is due to the reduction of the diffuse ion layer thickness by the increasing cation concentration, which results in a decrease in sediment volume in accordance with the diffuse ion layer theory.

In the case of $CaCl_2$ solution (divalent Ca^{+2}), for the same molar concentration as in NaCl solution (univalent Na^{+}), the CCC value is in the range of 0.003 to 0.005 M (figure 5.2), which is much less than that of NaCl solution. This result demonstrates the importance of the cation valence in the electrolyte in the flocculation process. In addition, the volume of sedimentation decreases with increasing salt concentration in the case of $CaCl_2$ which is different from the trend observed for the NaCl case. This is because face to face orientation (aggregation) of clay particles is formed initially at dilute Ca^{+2} concentrations due to the di-valence effect. In the test tubes of higher concentration, the effect of increased concentration decreases the thickness of the diffuse ion layer in clay particles in the suspension, consequently, the interparticle distance decreases

effectively due to the valence and concentration effect and leads to coagulation. The magnitude of reduction in the diffuse ion layer thickness, using divalent Ca^{+2} instead of univalent Na^{+}, is approximately one half as shown in table 2.1. The result of using Ca^{+2} as electrolyte is that the overall sedimentation volume decreases and the particles in the sediment are arranged in a flocculated and aggregated mode as suggested by figure (2.11 e, f, g). Also it is noticed that, in case of $CaCl_2$ electrolyte, the rate of coagulation is faster than that using NaCl electrolyte. This is also attributed to the efficient reduction in the diffuse ion layer, which in turn, reduces the repulsion between particles and as a result, the attractive forces dominate. Consequently, each collision between the particles will lead to coagulation.

These results are in agreement with the diffuse ion layer theory which predicts the effect of the cation valence and cation concentration in reducing the thickness of the diffuse ion layers which reduces the repulsion forces Consequently the attractive forces dominate, causing the flocculation of the particles and leading to sedimentation. This final result (attractive forces domination) is also in agreement with the theory of stability (DLVO theory). From the above tests results, it is resumed that the two types of interparticle forces discussed are the repulsive and attractive forces which are considered by the colloidal theories.

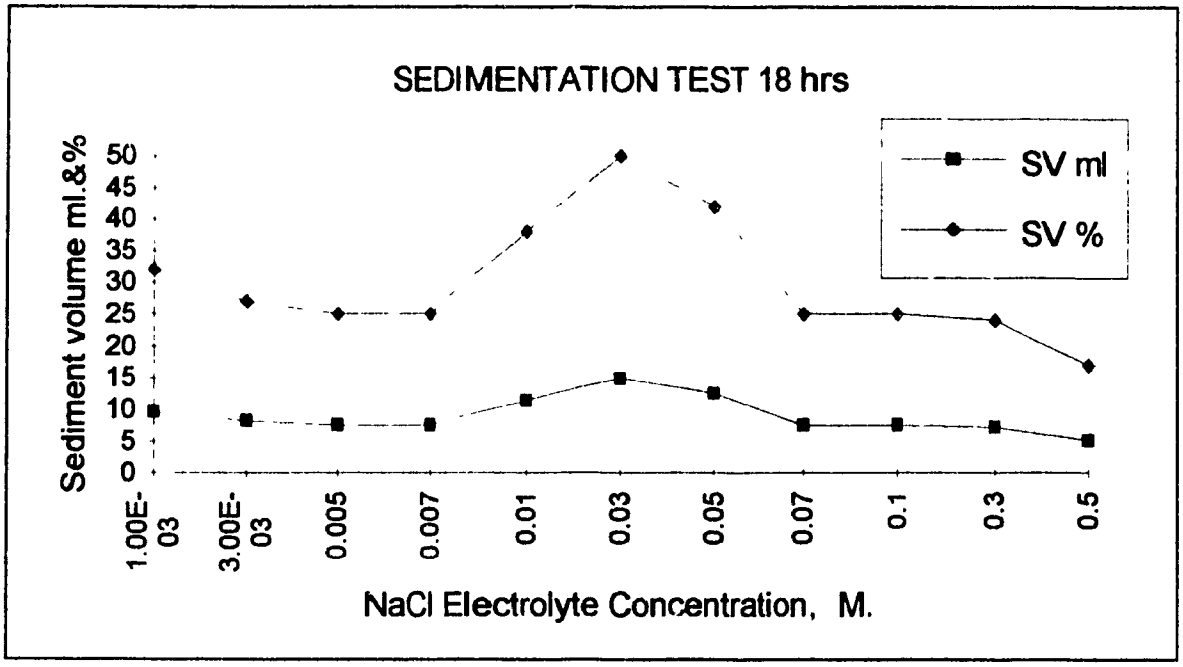

Figure 5.1. Sedimentation test results using NaCl electrolyte with various concentrations for a settling time of 18 hrs

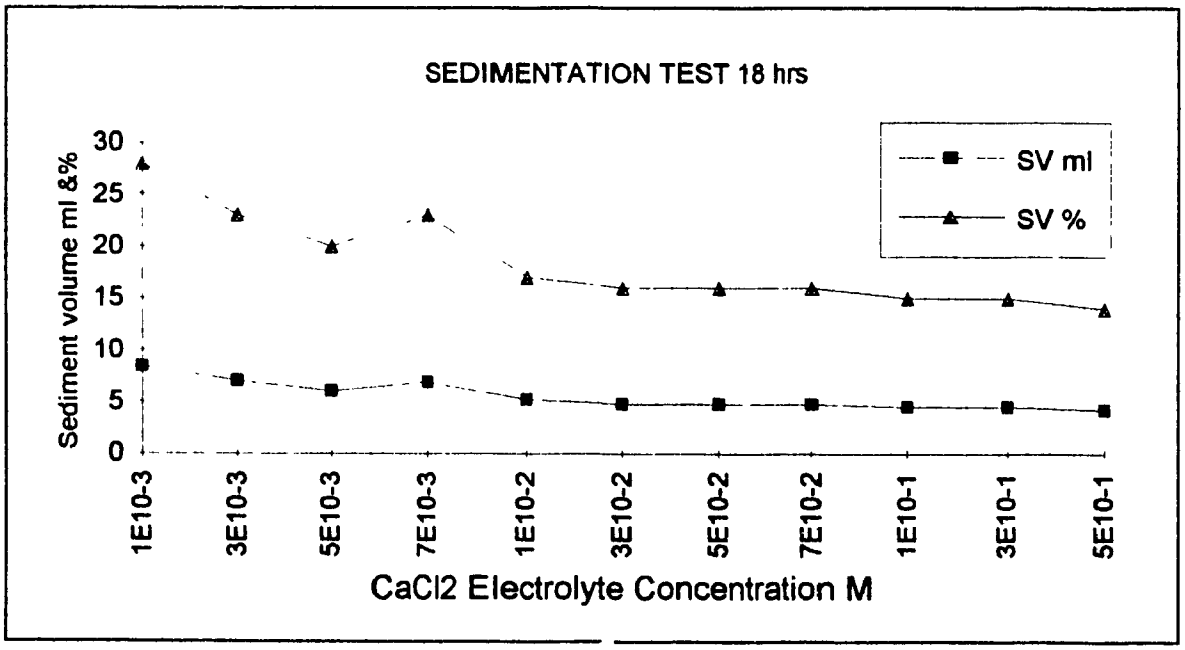

Figure 5.2. Sedimentation test results in $CaCl_2$ electrolyte with various concentrations for settling time of 18 hrs

5.1.2. CENTRIFUGATION TESTS

As previously mentioned, centrifugation tests are performed as controlling tests and can be run in shorter time than the gravity tests. In these tests, the sediment volumes are measured in (ml) at the beginning of centrifugation, and after 9 hrs. of settling and are indicated in tables 5.1 & 5.2 as (0 hr.) , volume (V1). In addition, sediment volumes and percentage to the initial volume (%sed.) are measured after 1 hr. and 2 hrs. centrifugation (Vol. 2 & Vol. 3) are also shown in tables 5.1 & 5.2. where the sediment volume decreases with time of centrifugation until it became constant.

The electrolyte ionic strength is used in tables 5.1& 5.2 to show the total effect of different species contained in the solution and for the ease of comparison of the results of the flocculation power for various solutions

The tests results are shown in tables 5.1, 5.2 and in figures 5.3, 5.4. In figure 5.3 & 5.4, the sediment volumes in (ml) are drawn against electrolyte ionic strength (in moles).

The results show that, in the case of $CaCl_2$ electrolyte, the sediment volume tends to decrease with increasing ionic strength, or increase in molar concentration. For NaCl electrolyte, this trend increases from low concentration to that indicated by CCC and then decreases. These trends correspond to those found in the gravity tests. This can similarly be explained by the effect of increase in cation valence and electrolyte concentration which reduce the thickness of diffuse ion layer and consequently reduce repulsive forces. The reduction of repulsive energy will cause the net energy to be an attractive energy and lead to particle association by decreasing the distance between the particles as previously discussed by the net energy curve in the DLVO theory of colloidal stability.

In addition, it can be seen that the flocculation power of WN-1 is higher than that provided by the concentration of $CaCl_2$ indicated by the CCC (0.003-0.005) due to the high concentration of divalent cations in this saline water which reduces effectively the thickness of the diffuse ion layer leading to particles coagulation. These values are in accordance with other investigations reported in literature.

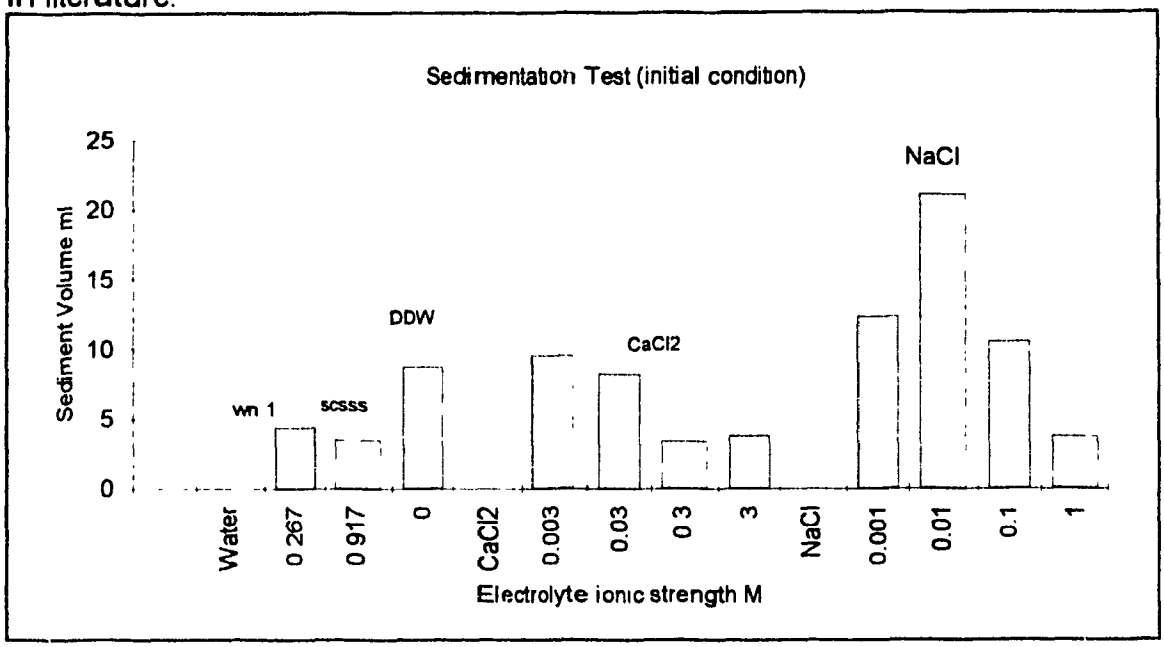

Figure 5.3. Effect of electrolyte ionic strength on sediment volume of clay suspensions 9 hrs (initial condition) before centrifuge.

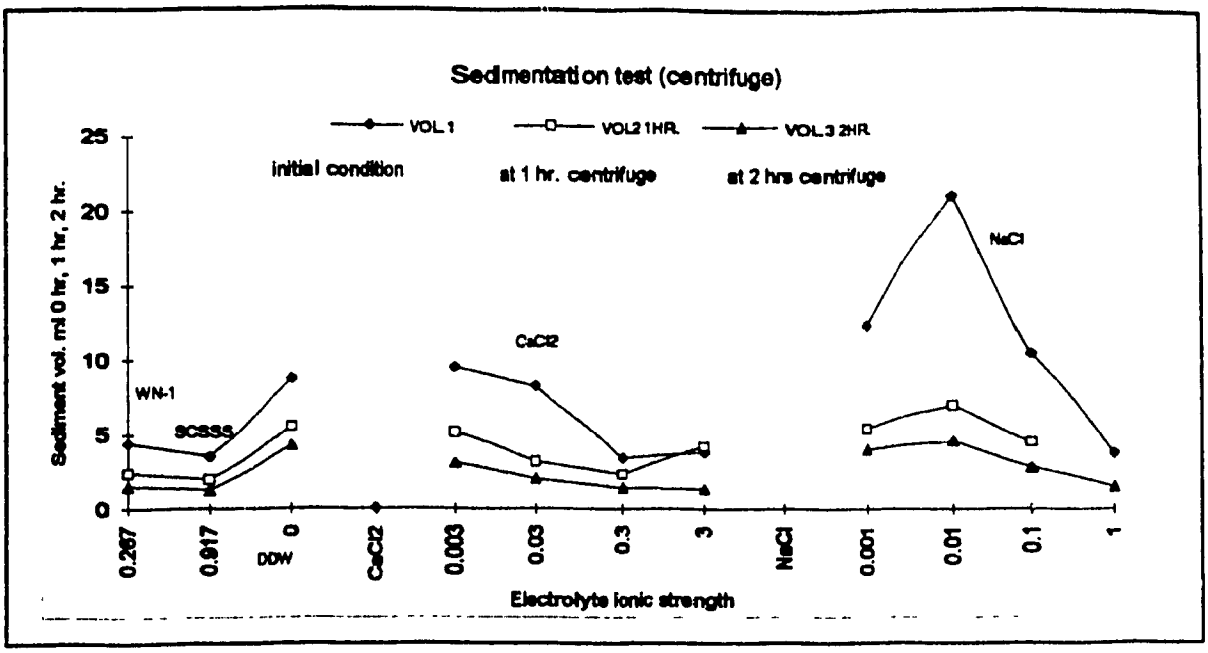

Figure 5.4. Sedimentation volume for 1hr, 2hrs centrifuge and electrolyte ionic strength for different solutions

The decrease of sediment volume in case of saline water is an indication of its flocculation power due to the high divalent cations in these saline waters that compress the diffuse ion layer. It is also noted that the flocculation rate in solutions of concentration values greater than the CCC is faster, the reason is that the coagulation velocity between the colliding particles is increased due to the strong reduction in the thickness of the diffuse icn layer and the domination of attractive forces between the moving particles in the suspension.

Table 5 1 Sedimentation tests data in WN-1, SCSSS, and DDW.

Sample	vol1 initial volume	vol2 1hr	%SED.	vol3 2hrs	%SED.
I=ionic strength Molar	ml	1hr. ml		2hrs ml	
WN-1 I= 0.267	4.4	2.37	7.9	1.5	5
SCSSS I= 0.917	3.5	1.95	6.5	1.25	4.2
DDW I= 0	8.75	5.5	18.3	4.25	13.3

Table 5.2 Sedimentation test data & results in NaCl & $CaCl_2$ electrolytes of different ionic strength.

Sample	vol1 0hr ml	vol2 1hr ml	%SED.	vol3 2hrs ml	%SED.
$CaCl_2$ I=ionic strength. Molar					
I= 0.003	9.5	5.15	17.2	3.1	10.3
= 0.03	8.25	3.15	10.5	2	6.7
= 0.3	3.4	2.3	7.72	1.4	4.7
= 3	3.8	4.2	14	1.35	4.5
NaCl					
I=0.001	12.3	5.4	18	4	11.7
= 0.01	21	7		4.6	15.3
= 0.1	10.5	4.5	15	2.8	9.3
= 1	3.75			1.5	5

From the above results and discussions concerning the sedimentation tests, it can be concluded that the Critical Coagulation Concentration is considered a measure of the suspension's conditions before they are brought to flocculation, i.e. the original stability of this suspension. The higher the original stability, the greater the amount of electrolyte (CCC) required for reduction of the stability to the given level which is fixed by the conditions of the test In addition, the CCC value gives an estimation for the flocculation power of the electrolyte used to flocculate the suspension

The use of NaCl and $CaCl_2$ as basic solutions in the sedimentation tests is considered as a systematic approach in predicting the state of bentonite gel at interface penetrating in the rock fissures and contacting with the groundwater in the Canadian Nuclear Waste disposal vault. The groundwater contains Ca^+, Na^+, and Cl^- as main cations and anions in the water dissolved salts A knowledge of the CCC for NaCl and $CaCl_2$ in bentonite suspensions as found above, and knowing the composition of the groundwater WN-1 or SCSSS, in addition to using the ionic strength for all solutions, one can easily predict the clay fabric in contact with these groundwaters As shown in the tables and figures above, it is clear that the ionic strength of WN-1 and of SCSSS are greater than those of the CCC either of NaCl or $CaCl_2$, and this results in efficient compression of the diffuse ion layer and the attractive forces become dominant. This leads to an efficient coagulation and the clay particles at the clay-water interface are strongly attracted together. These results lend support to both swelling and diffusion tests

5.2. SWELLING TESTS

In these tests, two waters (DDW& WN-1) are used for the sake of comparison to show the salinity effect on swelling, so these tests planned to show the swelling of clay in small cracks and to see if a possible particle release in the crack during the expansion process may occur. Results have shown that bentonite gel does swell and penetrate into narrow cracks. The rate of swelling in distilled water is rapid at the beginning of the test and then decreases with time, until it reaches an equilibrium state (repulsive and resisting forces become equal). The time required to reach this equilibrium state is not known. The expansion of the bentonite sample exceeds the boundaries of the frame designed for the cell after 30 days and no measurements were taken thereafter. The trend of the expansion is increasing at the beginning as previously mentioned and the rate then decreased to be very slow. This result is in accordance with the diffuse ion theory, where the thickness of the diffuse ion layer is maximum and the water is free of salt, the result is a maximum particle interaction and maximum swelling.

In WN-1 solution, it is observed that very small penetration occurs due to swelling (1-2 mm) and after that the sample does not swell. The major factor in minimizing the swelling is the divalent cations in the groundwater which compress the diffuse ion layers thus significantly reduce the swelling pressure until the penetrating clay and the WN-1 groundwater are in equilibrium conditions These results are in agreement with the behavior predicted by the diffuse ion layer theory in terms of swelling and the importance of the water chemistry on the swelling and volume change This effect was explained by the theory on the basis of reducing the thickness of the diffuse ion layer.

The WN-1 water, after the clay expansion, was noticed to be very clear, and no particle release was observed, through visual examination, from the clay mass.
In the case of DDW, the expansion of clay continued and reached the cell boundaries and consequently no precise measurement was obtained.
In the Canadian Nuclear Waste Management Program, the groundwater is a saline water as shown before, and the expansion of clay as a gel in the rock fissures is expected to be limited depending also on the geometry of the rock fissures and on the pressure at the buffer The expanded bentonite will seal the cracks and the surrounding rock around the buffer and will exert pressure on the upper backfilling ensuring the sealing of the cracks in the entire area surrounding the barrier .

5.3. DIFFUSION EXPERIMENTS

All the tests results are shown in Appendix D. Only three groups of test results are considered representative fcr discussion purposes.

RESULTS OF DIFFUSION TESTS

GROUP NO. 1

CONCENTRATION PROFILES OF DISPERSED PARTICLES WITH RESPECT TO DIFFERENT ELECTROLYTES AND CONCENTRATIONS

Dispersion data have been collected for a period of 164 hrs A plot of the normalized scattered light intensity versus distance from the gel surface after

one hour of diffusion (Figure 5.5) provides an indication of the relative initial particle concentrations in the different electrolytes. It is noted that the particle concentration decreases with increasing distance from the gel surface. It is also noted that the higher the ionic strength of the dispersive medium the fewer particles exist in suspension at the same time.

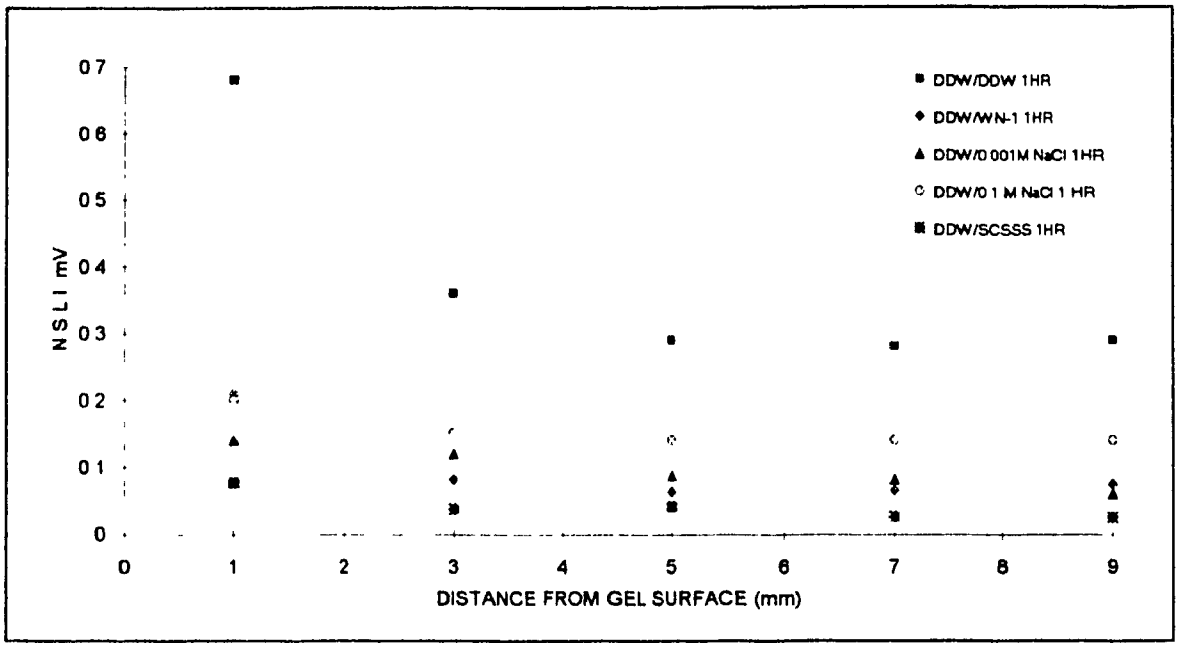

Figure 5.5 Concentration Profiles for various electrolytes measured after 1 hr

These results can be explained by the diffuse ion layer theory to be due to the influence of valences of cations and the associated salt concentration in the media. From figure 5.5, the following can be concluded:

1. It is obvious that the influence of the divalent cations is extremely important in the particles diffusion process.

2. The data shows that the primary light scattering intensity, from the concentration profile obtained for bentonite gel sample mixed with the saline water SCSSS, is extremely low although the dispersion medium is deionized

distilled water. This result is in good agreement with the results obtained from the sedimentation tests using the saline solution SCSSS where the sedimented gel is compressed as explained before and the particles at gel surface are strongly attracted together.

3. The concentration profile, for the bentonite gel mixed in DDW and using WN-1 as dispersion medium, shows that the amount of particles released from the gel surface is little higher than those obtained in SCSSS This result is in accord with the fact that WN-1 is less saline than SCSSS and its ionic strength value is much smaller than that of SCSSS This also indicates that the flocculation state at gel interface in SCSSS is relatively stronger than that in WN-1, and consequently the possibility of particle release is lower as the profiles show

4. Following the same argument, concentration profiles for other dispersion media (0.1M NaCl, 0.001M NaCl, and DDW) can be similarly explained The trend of these profiles is increasing as the concentration of the dispersion media decreases. The maximum increase is obtained for deionized distilled water

5. An important remark on these profiles is that the concentration gradient becomes constant and in equilibrium after a certain distance from the gel surface for all dispersion media.

6. A conclusion can be drawn from the above discussion, which is related to the importance of the divalent cations in the groundwater. This gives the groundwater a high flocculation power which keeps the clay particles attracted to each other in a short time during the expansion process

7. The values measured at 1hr can be expressed in terms of concentration units (mg/l) using the calibration curve illustrated in chapter 4 where the normalized

data in (mV) can be related to (mg/l). On the basis of the calibration curve values, the calculations showed that the concentration of the particles released, for 1 hr time, in the lower curve (SCSSS) range from 1.46 mg/l at 1mm from the gel surface to 0.34 mg/l at 9 mm. The amounts of particles concentration released in case of DDW (the higher curve) are in the range of 45.6 mg/l at the gel surface to 17.85 mg/l at 9 mm.

GROUP N0. 2

CONCENTRATION PROFILES OF DISPERSED PARTICLES IN DDW WITH RESPECT TO TIME

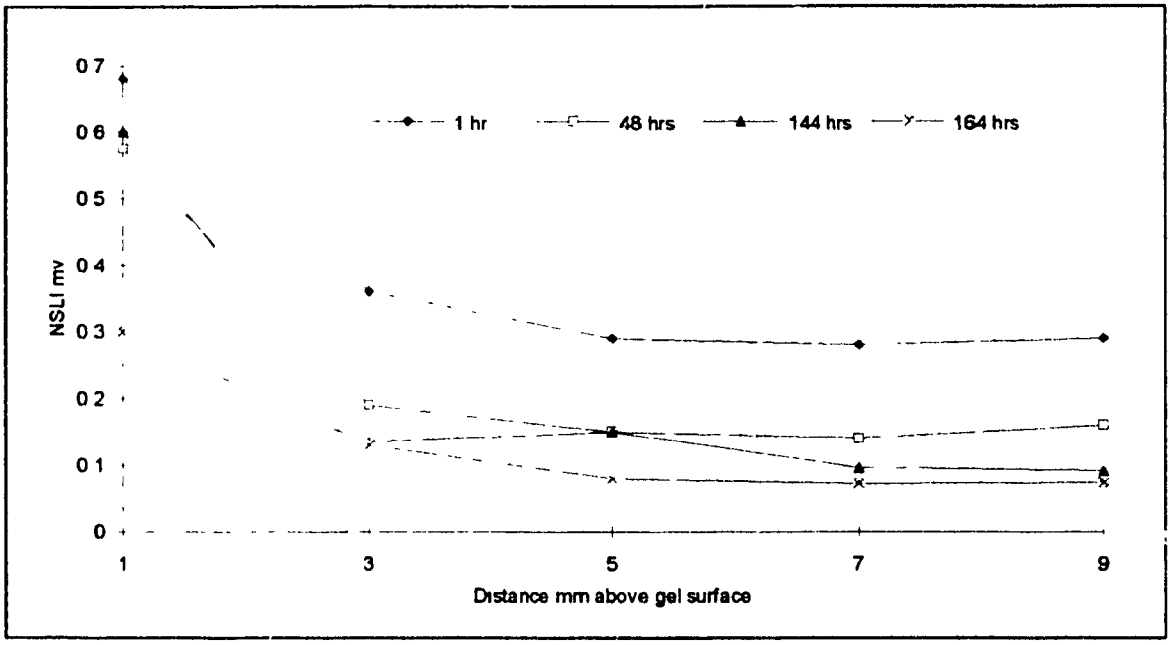

Figure 5.6. Concentration profiles as a function of time in DDW dispersion media

Figure 5.6 shows the concentrations of clay particles released at different distances from the gel surface in terms of normalized scattered light intensity. The dispersion medium in this test is deionized distilled water and the

measurements of concentrations were obtained for 1hr, 48 hrs, 144 hrs, and 164 hrs.

The results show that the concentration of the dispersed particles decreases with distance from the gel surface. The concentration of released particles is also decreasing with time against what was expected from a real diffusion case (increase in concentration of diffused particles with time) This result is found to be in conflict with other research, where the results showed an increase in release of particles in DDW dispersion medium. Accordingly, a test was performed on the bentonite clay sample to check the salt content in this sample. Results showed that a residual salt concentration calculated for 15% clay gel was found to be in the range of the CCC of NaCl obtained in sedimentation tests. The above residual salt will help flocculation of particles and decrease the possibility of particle release.

Explanation for the difference in results in this study and in other studies may be attributed to the initial salt content in the samples used in this test as explained above. On the basis of this result, it is important to be aware of the presence of salt in the clay used which will exert an adverse effect in the understanding of dispersion behavior in the distilled water

GROUP NO. 3

CONCENTRATION PROFILES OF DISPERSED PARTICLES WITH RESPECT TO TIME

Concentration profiles for group No.3 as function of time in dispersion media, WN-1, 0.01 M $CaCl_2$, and SCSSS are selected as a representative sample among the concentration profiles obtained for different dispersion media

and different porewater compositions. All the figures of concentration profiles and tables of obtained data are illustrated in appendix .D

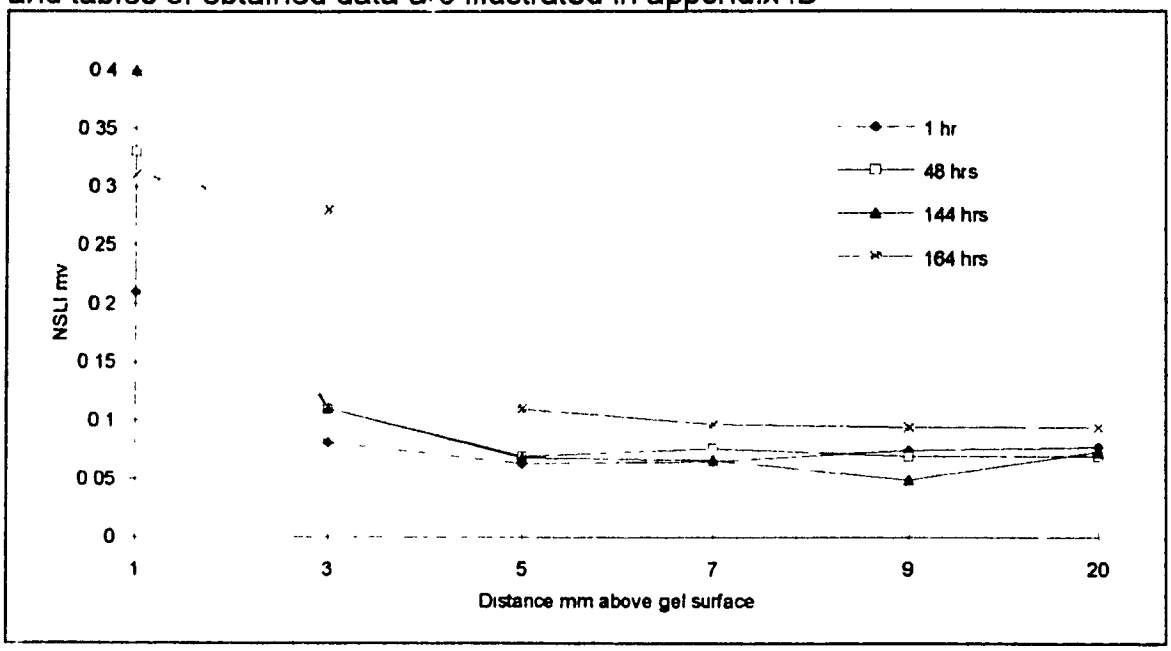

Figure 5.7 Concentration profiles as a function of time in WN-1 saline water as a dispersion media

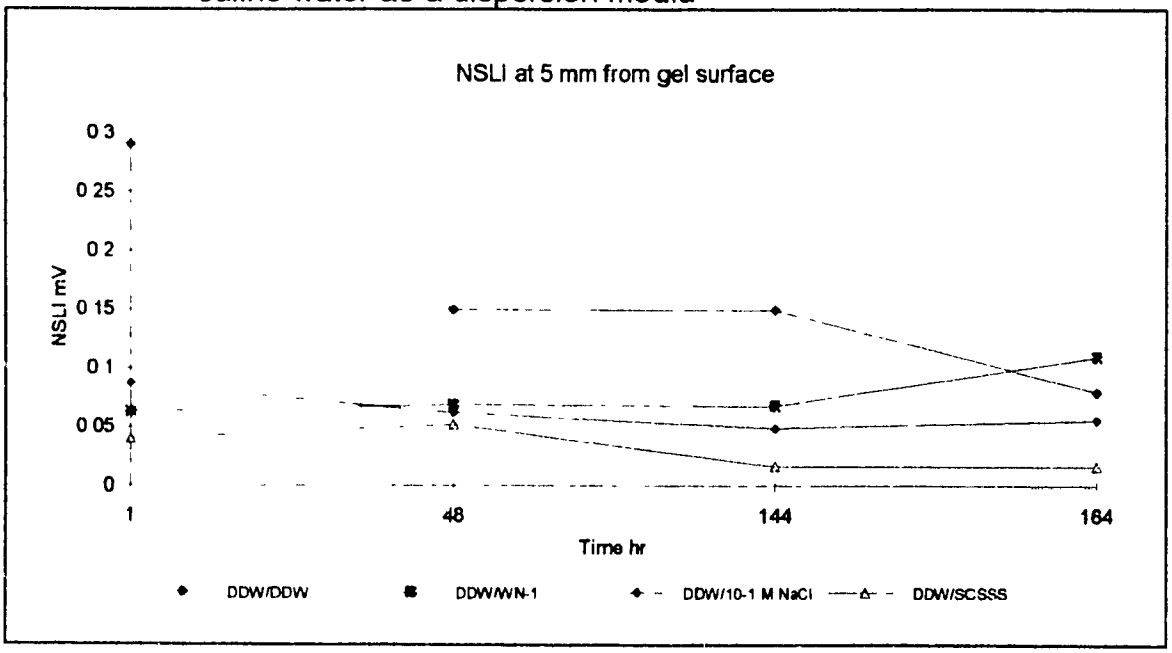

Figure 5 8 The concentration of particles 5 mm from the gel surface as a function of time

Results of group 3 show that concentrations of particles released from the gel surface are lower than those obtained from group No.1, where the dispersion medium is distilled water. Results of group 3 show that the concentration of diffused particles decreases with time at the same distance from the gel surface In the case of a real diffusion process, an increase in the concentration of diffused particles with time is expected, and accordingly, one can assess the diffusion coefficient from these concentration profiles as was planned in the theoretical considerations. This implies a resultant settlement rather than particle diffusion. This phenomenon is due to the 'kick-off' effect of addition of media into the test tubes caused by the disturbance of the gel particles on the interface, each time initiating particles dispersed from the gel surface. These particles eventually settle under gravity thus explaining this phenomenon. In effect, the scattered light intensities detected is more likely due to the settling particles released by the 'kick-off' effect. This is illustrated in figures 5 7, 5.8;5.9 and 5 10 and in other figures in appendix D.

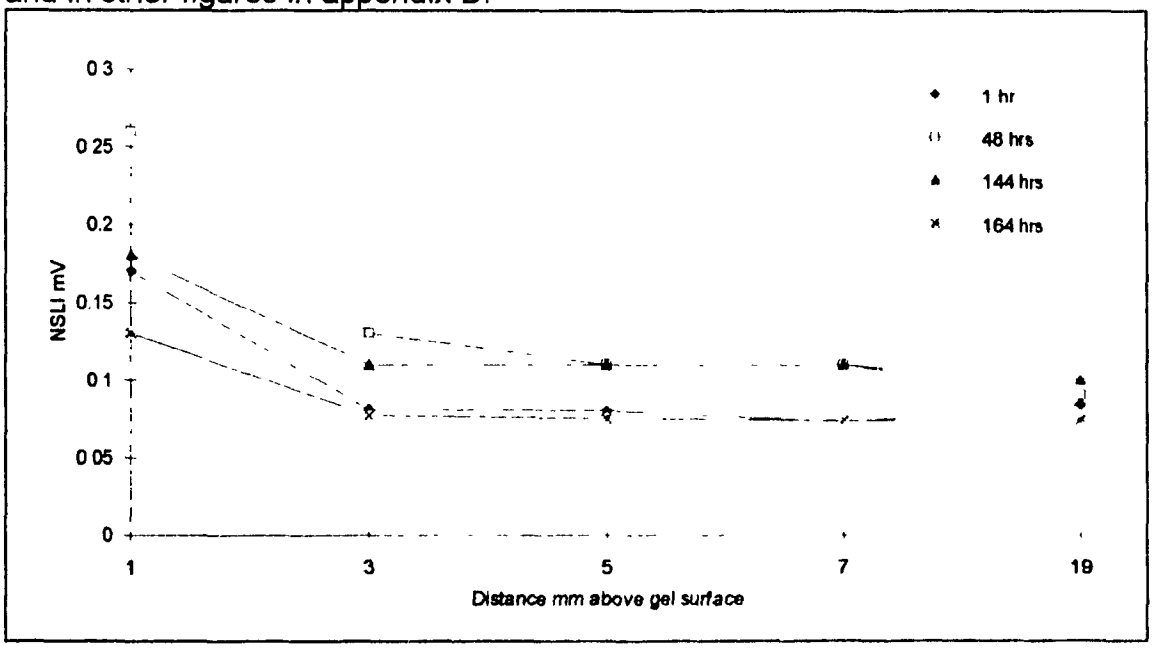

Figure 5.9 Concentration profiles as a function of time in 0.01M $CaCl_2$ dispersion media.

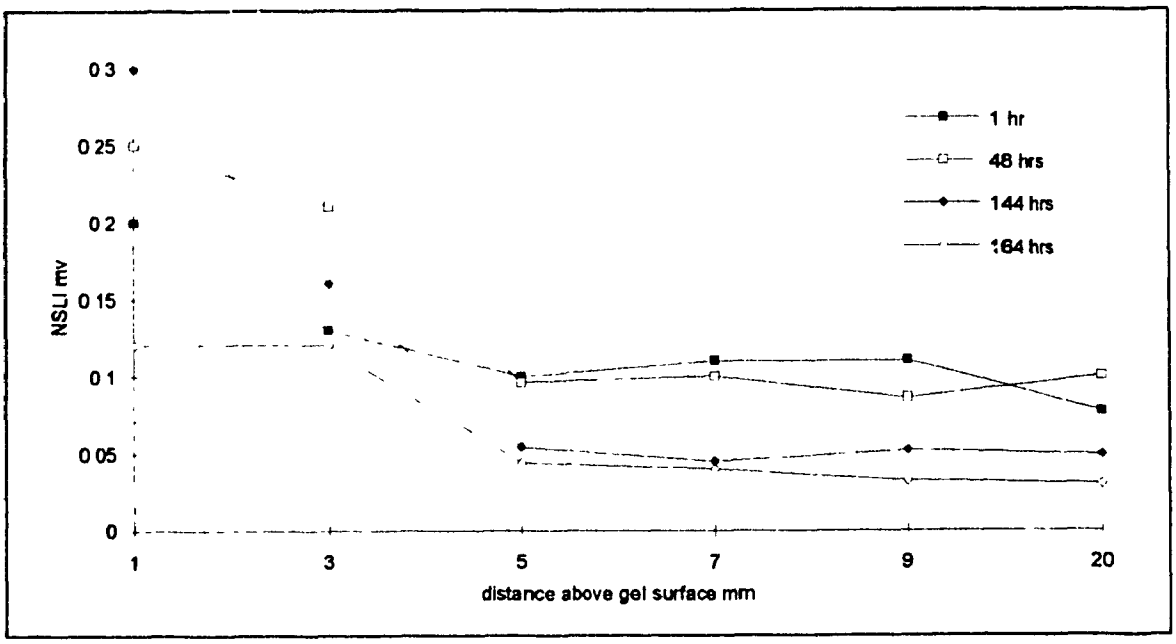

Figure 5.10 Concentration profiles as a function of time using SCSSS as porewater and dispersion media.

In general, the results show that higher ionic strength of dispersion media, and of the mixing solution (porewater) would lead to lower concentrations of dispersed particles as would be predicted by the diffuse ion layer theory. The high concentration of dispersion media and of the porewater, and the high valence of cations in these media will result in reducing the thickness of the interacting diffuse ion layers, and this in turn reduces the repulsion between the clay particles and leads to the overcoming of the repulsion energy barrier previously discussed in the net potential curve of the DLVO theory. This leads to trapping the clay particles in the deep minimum of attraction in the above potential curve and they are coagulated and in a flocculated state.

However all the tests do not show an obvious diffusion rather than settlement of kicked off particles. Finally, the results associated with DDW medium show a similar trend to that of other media, which is not expected. This unexpected result for DDW is due to the effect of residual salt in the clay

material which effectively converts DDW into saline solution and reduces the thickness of the diffuse ion layers in the clay particles. This leads to domination of the attractive forces and decreases the distance between particles The final result is a coagulated gel with particles associated in flocculated and aggregated state. This type of structure is relatively strong enough to prevent any particle release.

Summary of experimental results:

1. The use of NaCl and $CaCl_2$ solutions (which are containing the main cations of dissolved salts in groundwater) as a systematic approach in sedimentation tests was necessary for comparison of the coagulation effect of other groundwaters or flocculants in general..

2. The results obtained from the sedimentation test showed that the CCC can be considered as an important measuring scale for the flocculation power of different electrolytes.

3. The value of CCC of NaCl solution found to be in the range of 0.01 to 0.03 M, whereas the value of CCC of solution found to be in the range of 0.003 to 0 005 M. The values show the flocculation power of Ca as a divalent cation This is in agreement with diffuse ion layer theory and with flocculation values obtained by others in literature (van Olphen 1977).

4. The sedimentation experiments showed that the flocculation power of synthetic solutions of similar composition as that of groundwater in the Canadian Shield is higher than the CCC of the $CaCl_2$ and NaCl used before This is attributed to the higher ionic strength of this groundwater.

5. From the above explanations it is expected that, in the Canadian Nuclear Fuel Waste Management Program, the bentonite gel in contact with groundwater to be in a flocculated state.

6. Swelling tests showed expansion of clay gel in distilled water in the crack, while the saline water WN-1, showed much less expansion for the same conditions. This will ensure that in the Canadian Nuclear Fuel Waste Management Program, the clay gel will expand and fill the cracks of adjacent rock and this expansion will stop at a certain distance depending, besides the groundwater salinity, on other factors like the rock fissure geometry.

7. Diffusion tests showed that the number of particles released from the gel surface are decreasing with time, whereas an increasing trend was expected as in real diffusion conditions. This particle release thought to be due to kick-off effects resulting from the gel surface disturbance during addition of dispersion solutions.

8. The general trend of all concentration profiles is of decreasing trend with time. Even for distilled water, it gives the same trend although the clay in suspension showed a turbid suspension and particles remained in suspension. This unexpected result was explained to be due to the residual salt effect in the gel of higher clay concentration (15%) than that in suspension (2%).

9. From the obtained concentration profiles, it is noted that the values of released particles are much lower in the cases were the concentration of dispersion media or porewater are higher or containing higher valence in the cations.

10. The diffusion results confirm that clay particles of the gel under an expanding state are attracted together and they form a flocculated structure in the presence of salt concentrations beyond the CCC values of NaCl and $CaCl_2$.

11. In the Canadian Nuclear Fuel Waste Management Program, the groundwater concentration is beyond the CCC of the basic solutions (NaCl, $CaCl_2$) and this suggests that the clay gel surface will be in flocculated state and the surface will not release particles.

CHAPTER 6

CONCLUSIONS AND RECOMMENDATIONS

6.1. CONCLUSIONS

The following conclusions can be drawn from the previous experimental results and discussions:

1. Particles' interaction in clay-water suspension depends on particles' concentration in the suspension, on the water salinity, and on types of ions species. From the systematical study in the sedimentation tests using NaCl and $CaCl_2$ solutions, it is found that the CCC values of these solutions in the 2% Avonlea-bentonite clay suspensions lie in the range of 0.01-0.03 M and 0.003-0.005 M, respectively,

2. For a given groundwater solution, the association of particles can be predicted by considering the ionic strength of this solution. This is supported experimentally and proven by results obtained from sediment volume tests of Avonlea-bentonite suspension in the Canadian shield groundwater. These results suggest that the clay gel is flocculated.

3. Diffusion tests data showed that no particles released from the gel surface for various solutions including the groundwater expected in the Canadian shield The concentration profiles are related to the particles disturbance and not to diffusion. This implies that particles are not released from the expanded state of the clay mass and suggest that the gel is flocculated.
Based on above results, it can be confirmed that the clay gel is flocculated and the long-term performance can be achieved.

4. The lack of release of bentonite particles from the gel surface (to be expected from the theory in case of distilled water) is attributed to the high initial salt content (higher than the CCC) which tends to flocculate the gel.
This important conclusion reflects the importance of the material properties to be used.

5. The laser technique is useful to study the time dependent concentration profiles in clay suspensions.

6. Of particular significance, by using the above results, it is possible to predict the particle release from a clay barrier under a given groundwater condition by considering the water salinity, type of ions species in the solution and the residual salt content in the clay.

6.2. RECOMMENDATIONS

1. Further research is needed by repeating the diffusion tests on Avonlea-bentonite samples, using distilled water as a dispersion medium, and after purification of clay sample to obtain a salt-free clay sample and to examine the diffusion results. The objective of the further research is to explain the contradiction in results obtained in distilled water as mentioned before in this study and to confirm the effect of the residual salt on diffusion process in distilled water.

2. Using the Laser technique, a model can be developed to predict the rate of sedimentation of clay particles in a suspension by measuring the concentration profiles as a function of time.

3. It is recommended to develop a technique to minimize the disturbance of the clay gel surface (kick-off effect) resulting from addition of solution.

REFERENCES

Aitchison, G.E., and Wood, C.C. (1965). Some interactions of compaction, permeability, and post-construction affecting the probability of piping failure in small earth dams, proc. 6th int. conf soil mech. and found. eng., Montreal, vol.2, p.442.

Arulanandan, K., Loganathan, P., and Krone, R. B., (1975). Pore and Eroding Fluid Influences on Surface Erosion of Soil, Journal of Geotechnical Engineering Division, ASCE, Vol. 100, No GT1, pp. 51-66.

Aylmore,L.A. G. and Quirk, J. P. (1959). Swelling of Clay Systems.Nature, No.183 : pp.1752 - 53.

Barclay, L. M. and Ottewill, R. H. (1970). Interparticle Forces in Montmorillonite Gels. Spec. Faraday Disc., No. 1 : 138.

Brackley, I.J.A. (1973). Swell pressure and free swell. proc. 3. int. conf Expansive Clays. Israel 1973, vol. 1.

Bolt, G. H. (1956). Physico-Chemical analysis of the compressibility of pure clay, Geotechnique, Vol.6 No.2, pp. 86-93.

Bolt, G.H. and Miller, R.D. (1955) . Compression studies on illite suspensions. Proc. American Soil Science Society 19: pp285.

Chapman, D. L. (1913). A contribution to the theory of electro-capillarity, Phil Mag. 25, 6th Series : pp. 475-481.

Cheung, S.C.H., Gray, M.N. (1989). Mechanism of ionic diffusion in dense bentonite. Scientific basis for Nuclear Waste Management, Proc. Matls. Res. Soc., 127: pp. 677-681.

Cheung, S.C.H, Gray, M.N. and Dixon, D.A. (1987). Hydraulic and Ionic Diffusion Properties of Bentonite/Sand Buffer Materials in Coupled Processes Associated with Nuclear Waste Repositories, Vol. 30, 393-407, Academic Press Inc.

Crank, J. (1975). The Mathematics of diffusion, Clarendon Press, Oxford, 2nd ed. p 414.

Derjaguin, B. and Landau, L. D. (1941). Acta Physiachim, USSR, No. 14 pp 633.

El-Swaify, S. A. and Henderson, D. W. (1967). Water Retention by Osmotic Swelling of Certain Colloidal Clays with Varying Ionic Composition. J. Soil Sci., Vol. 18, No. 2 : pp. 223 - 32.

Forslind, E. and Jacobsson, A. (1975). Water, A Comprehensive Treatise. Ed. F. Franks, Vol. 5, Plenum Press, New York.

Forslind, E. and Jacobsson, A. (1975). Water, A Comprehensive Treatise. Ed. F. Franks, Vol. 5, Plenum Press, New York.

Friberg, S. (1976). Food Emulsions. Marcel Dekker Inc., New York and Basal.

Freeze, R.A. and Cherry, J.A. (1979). Groundwater . Printice-Hall Inc. London

Gouy, G. (1910). Sur la constitution de la charge electrique a la surface d'un electrolyte, Ann. Phys. (Paris), Serie 4, 9, pp. 457-468

Gohl, W.H. (1980). Volumetric stability and unsaturated flow in an expansive South African soil. Master Thesis of McGill University.

Grim, R. E. (1968). Clay Mineralogy, 2nd Ed., McGraw-Hill.

Hamaker, H. C. (1937). The London-Van der Waals attraction between spherical particles, Physica, Vol. 4 : pp. 1058-1072.

Hemwall, J. B. and Low, P. F. (1956). Swelling of Na-montmorillonite. Soil Sci., No. 82 : p. 135.

Hancox, W.T. (1986). Proceedings of the 2nd international conference on radioactive waste management, Winnipeg, Manitoba, pp 1-9 Canadian Nuc;ear Society, Toronto.

Kahn, A. (1958). The flocculation of sodium montmorillonite by electrolyte, J. Colloid Sci., No. 13 : pp. 51-60.

Kruyt, L. (1952). Colloid Science I : Irreversible System. Elsevier, Amsterdam.

Langmuir, I. (1938). Role of Attractive and Repulsive Force in Formation of Tactoids and Thixotropic Gels. J Chem. Phys. No. 6.

Lambe, T. W., and Whitman, R. V. (1979). Soil Mechanics, SI Version, John Wiley & Sons, Inc.

Le Bell, J. C. (1978). Colloid Chemical Aspects of the Confined Bentonite Concept. KBS Teknisk Rapport. Ytkemiska Institutet., Stockholm, No. 97.

Low, P. F. (1980). The Swelling of Clay : II. Montmorillonites. Soil Sci. Amer. J., Vol. 44, No. 4 : pp. 667 - 76.

Low, P. F. and Margheim, J. F. (1979). The Swelling of Clay : I. Basic Concepts and Empirical Equations. Soil Sci. Amer. J., Vol. 43 : pp. 473 - 81.

Mitchell, J. K. (1964). Shearing resistance of soils as a rate process. J. Soil Mech. and Found. Div., Am. Soc. Civ. Eng. , Vol. 90, No. SM1, pp. 29-61.

Mitchell, J. K. (1973). Influences of Mineralogy and Pore Solution Chemistry on Swelling and Stability of Clays. Proc. III Int'l. Conf. on Expansive Soils, Haifa, Israel. Vol. 3 : pp. 11 - 25.

Mitchell, J. K. (1976). Fundamentals of Soil Behavior. John Wiley and Sons.

Mouradian, A., (1993). Modelling of environmental effects on clay permeability Master Thesis. Concordia University, Montreal. Quebec, Canada.

Nickel, S.H. (1977). A rheological approach to dispersive clays. ASTM., STP 623, J.L. Sherard and R.S. Decker, eds. Amer Soc. for Testing and Materials. pp. 303-312.

Norrish, K. (1954). The Swelling of Montmorillonite Disc. Faraday Soc., No. 18: pp. 120 - 34.

Osipov, V.I. (1975). Structural bonds and the properties of clays Bull. Eng. Geol. No. 12, pp 13-20.

Pusch, R. (1983). Stability of Bentonite Gels in Crystalline Rock-Physical Aspects. Division of Soil Mechanic, University of Lulea.

Quirk, J. P. (1968). Particle Interaction and Soil Swelling. Isr. J. Chem., Vol 6 : pp. 213 - 34.

Shainberg, I., Bresler, E., and Kaiserman, A. (1971). Studies on Na/Ca Montmorillonite Systems I. The Swelling Pressure. Soil Sci., Vol. 111 , pp. 214 -219.

Sherard, J.L., Decker, R. S., and Ryker, N.L. (1972). Piping in earth dams of dispersive clay, proc. of the ASCE specialty conference on the performance of earth and earth-supported structures, Purdue University, pp. 589-626.

Sherard, J.L., Dunnigan, L.P., and Decker, R.S. (1976b), Identification and nature of dispersive soil. journal of the geotechnical division, ASCE , Vol.102, No. gt4, pp. 287-301

Shaw, D.J. (1966). Introduction to Colloid and Surface Chemistry. Butterworths. London.

Stern, K. (1924). Etschr. Elecktrochemie : 497.

Swartzen-Allen, L. and Matijevic, E. (1975). J. Colloid Interf. Sci., No. 50 : pp. 143.

Taylor, L. O. (1962). The Effect of Depressed Temperatures on the Swelling Pressure of Na-montmorillonite. McGill University thesis, Montreal.

Van Olphen, H. (1952), A tentative method for the determination of cation exchange capacity of small samples of clay minerals, Clay Mineral Bull., 1, pp. 169-170

Van Olphen, H. (1954). Interlayer forces in bentonite. Clay and Clay Minerals, 2, pp. 418-438.

Van Olphen, H. (1956). Force Between Suspended Bentonite Particles. Clay and Clay Minerals; National Research Council, Nat'l Acad. Sci. (U.S.A.); Publication No. 456, Washington, D. C.

Van Olphen, H. (1962) Unit Layer Interaction in Hydrous Montmorillonite Systems. J Coll. Sci., Vol. 17

Van Olphen, H. (1963). Compaction of clay sediments in the range of molecular particle distances. Clay and Clay Minerals, Vol. 11, pp. 178-187

Van Olphen, H. (1964). Internal mutual flocculation in clay suspensions. J Coll Sci., Vol. 19, pp. 313-322.

Van Olphen, H. (1965). Swelling Pressure Calculation at Short Separation. J. Colloid Sci., Vol. No. 20: pp. 822.

Van Olphen, H. (1973). Unit layer association and dissociation in suspensions of montmorillonite clays, particle growth in suspensions, A.L. Smith, Editor, pp. 83-94, Academic, New York.

Van Olphen, H. (1977). An Introduction to Clay Colloid Chemistry. second edition, Inter-Science Publishers, New York.

Verwey, E. J. W. and Overbeek, J. Th. G. (1948). Theory of the Stability of Lyophobic Colloid. Elsevier, Amsterdam.

Warkentin, B. P. (1956). Bonding Between Montmorillonite Clay Particles Cornell University Thesis.

Warkentin, B. P., Bolt, G. H. and Miller, R. D. (1957). Swelling Pressures of Montmorillonite. Soil Soc. Amer. Proc., Vol. 21 : pp. 495 - 97.

Warkentin, B P and Schofield, R. K. (1960). Swelling Pressure of dilute Na-montmorillonite pastes. Clay, Clay minerals, Vol. 7, pp. 343-349.

Warkentin, B. P. and Schofield, R. K. (1962). Swelling Pressure of Na-montmorillonite in NaCl Solutions. Jour. Soil Sci., Vol. No. 13: pp. 98 - 105.

Williams, B.G. and Drover, D.P. (1966). Factors in gel formation in soil suspensions. Soil Science., USA. Vol. 104, No. 5

Yong, R. N., Sethi, A. J., Ludwig, H. P., and Jorgensen, M. A. (1978). Physical Chemistry of Dispersive Clay Particle Interaction. A.S.C.E. Preprint 3379, Chicago.

Yong, R. N. and Warkentin, B. P. (1975). Soil Properties and Behavior Development in Geotechnical Engineering. Elsevier Scientific Publishing Co., Amsterdam, Oxford, New York.

Yong, R. N. , Mohamed, M. O. and Warkentin, B. P. (1992). Principles of contaminant Transport in Soils.

APPENDIX A

CLAY MINERALS

TABLE OF CONTENTS

LIST OF FIGURES

A.1 SHAPE AND STRUCTURE

Concerning the various techniques of observing particles in a clay suspension, other step in magnifying power is realized by use of the electron microscope. With this instrument, which operates at high vacum, a picture of the dry clay particles is obtained. The particles appear to be large thin plates and some times lath-, rod-, or needle-shaped.

The final step in magnification is crystal structure analysis from X-ray diffraction patterns, which supplies a picture of the crystalline regularities in the arrangement of the atoms.

The knowledge concerning the crystal structure of different clays has been contributed greatly to an understanding of their surface properties, which are of primary importance in the colloid chemical behavior of clay suspensions Therefore, the main structural principles will be described in some details

According to Pauling, who was the first to describe the structure of clay minerals, each platelike clay particle consists of a stack of parallel layers Each layer is a combination of tetrahedrically arranged *silica sheets (T)* and octahedracilly arranged *alumina* or *magnisia* sheets (O).

2:1 layer clays (montmorillonite and illites) are built of layers composed of two tetrahedral sheets with one octahedral sheet in between (T-O-T); 1.1 layer clays (kaolinite) are built of layers consisting of one tetrahedral and one octahedral and one octahedral sheet (T-O).

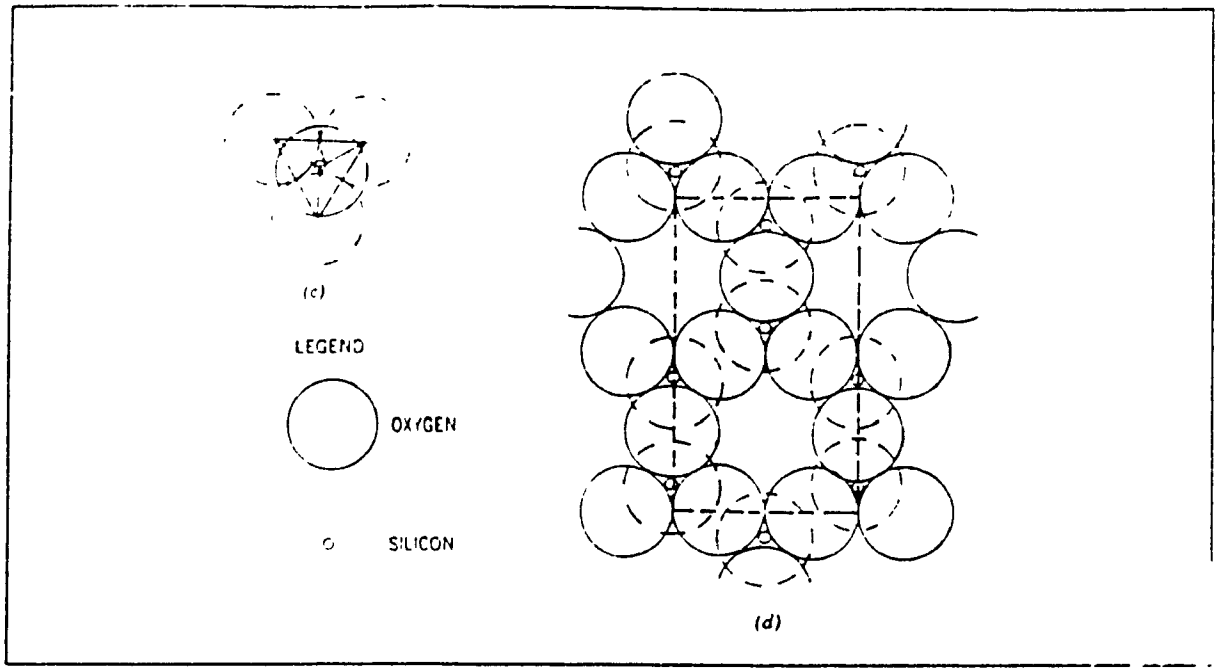

Figure A 1a Structure of tetrahedral sheet (dotted line: unit cell area).

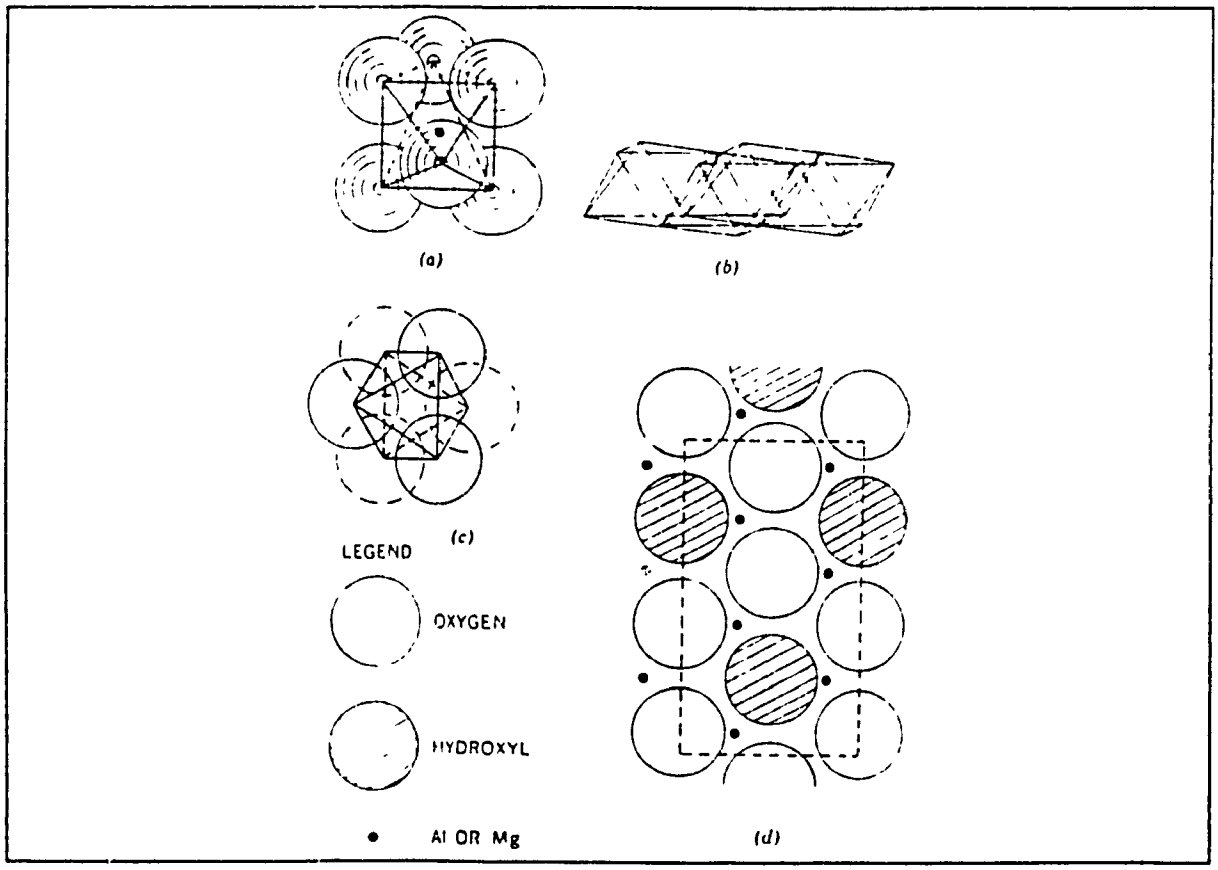

Figure A.1b. Structure of octahedral sheet (dotted line: unit cell area).

A.2 MONTMORILLONITE CLAYS ((2:1 LAYER CLAYS)

The atom arrangement in a 2:1 layer clay is shown in the schematic drawing in figure A.2., representing a unit of structure which repeats itself laterally in the layer. All valences of the atoms are satisfied in the sketched structure Of the three possible octahedral positions, two are occupied by trivalent Al (*dioctahedral arrangement*). Alternatively, all three positions may be filled by divalent Mg (*trioctahedral arrangement*). These electroneutral structures represent the compositions of the micaceous minerals pyrophyllite and talc, respectively.

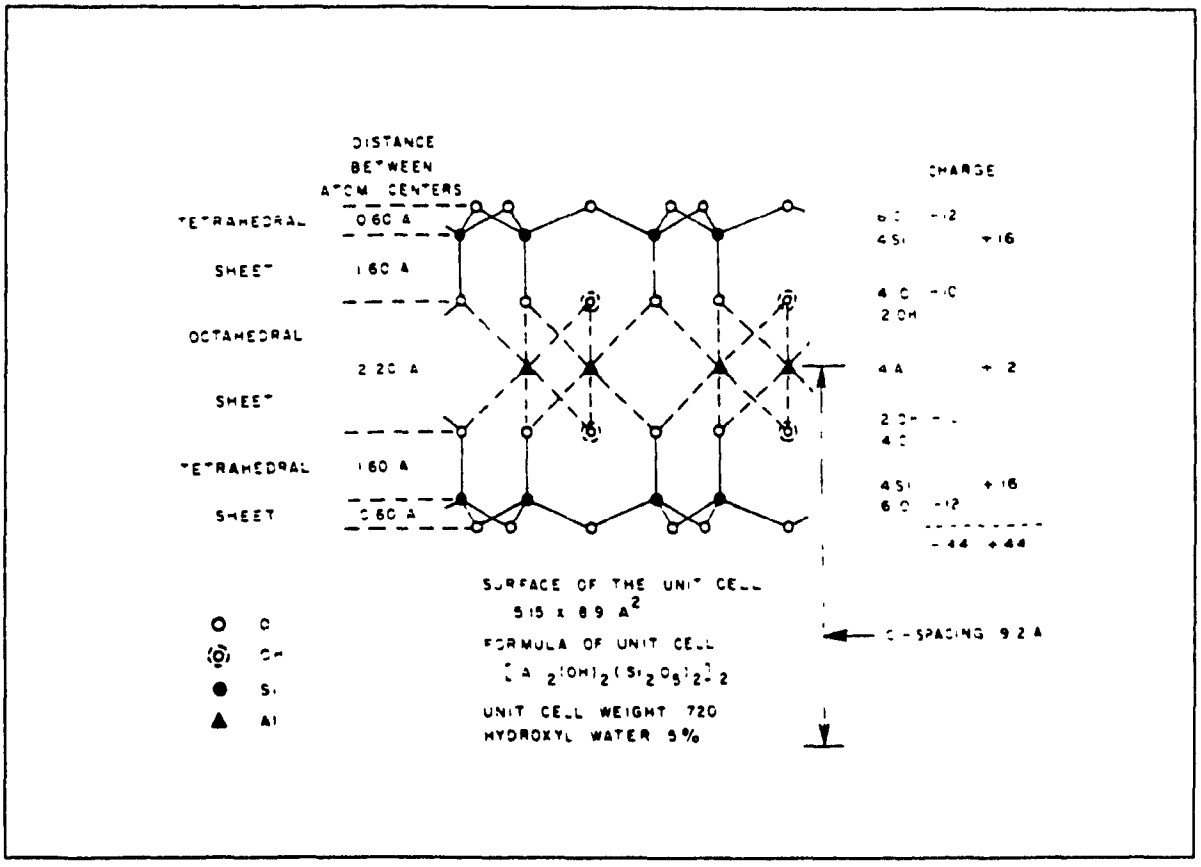

Figure A.2 Atom arrangement in the unit cell of a 2:1 layer mineral(schematic) (van Olphen 1977).

Montmorillonite clays are derived from these two prototype minerals by substitution of some of the elements by others; for example, tetravalent Si is replaced partly by trivalent Al, or Al in the octahedral sheet is partly replaced by divalent Mg without the third vacant position being filled. Such substitutions of electropositive elements by those of lower valence result in an excess of negative charge of the layers. The net negative charge is compensated by the adsorption of cations on the layer surface, both on the interior and on the exterior surfaces of the stacks.

The most typical property of montmorillonites is the phenomenon of *interlayer swelling* (or *inter crystalline swelling)* with water. In the presence of water or water vapor, the dry clay takes up water which penetrates between the layers and pushes them apart a distance equivalent to one to four monomolecular layers of water. Owing to this effect, the layer-repetition distance in the stack increased from about 10 A° for the dry clay to approximately 12.5-20 A° for the wet clay

The compensating cations which are adsorbed on the layer surfaces may be exchanged for other cations; therefore, they are called the exchangeable cations of the clay. The amount per unit weight of clay is the cation exchange capacity (CEC) of the clay, which is usually of the order of 80-100 meq per 100 g for montmorillonites. The CEC is a measure of the amount of substitution in the crystal.

Common size of Montmorillonite particle

Typical thickness = 30 A°

Typical diameter = 1000- 10000 A°

Specific surface = 0.8 Km^2/kg

Typical shape : Sheets of unit thickness

Montmorillonite Surface Area and Surface Charge Density (van Olphen 1977)

As an example, consider a montmorillonite clay in the sodium form having the following unit-cell formula:

$$(Si_8)(Al_{3.33}Mg_{0.67})O_{20}(OH)_4$$

$$Na_{0.67}$$

The unit-cell weight for this formula is 734. Therefore, 734 g of this clay contains 6.02×10^{23} unit cells (Avogadro's number).

Each cell has a surface area of 5.15×8.9 A^{o2} on each side. (The dimensions of the unit cell are slightly dependent on the type of isomorphous substitutions in the lattice).

Thus, the total surface area of 1 g of clay is

$$\left(\frac{1}{734}\right) \times 6.02 \times 10^{23} \times 2 \times 5.15 \times 8.9 A^2/g = 752 m^2/g$$

Alternatively, the surface area per cation follows immediately from the unit-cell formula and the unit-cell dimensions:

$$\frac{(2 \times 5.15 \times 8.9)}{0.67} = 136 A^2/\text{ion}$$

The interlayer area per cation is ½ x 136 + 68 A^2/ion.

In general, there is about ⅔ of a monovalent cation per unit cell.

For divalent cations, the surface area per ion is twice as large as for monovalent cations.

The surface charge density can be computed as follows: On each sq. cm of surface area, there are $10^{16}/136$ elementary charges. This is equivalent to a charge density of 3.5×10^4 esu/cm^2, or 11.7 $\mu C/cm^2$.

A.3 ILLITES (2:1 LAYER CLAYS)

Illites have the same basic structure as montmorillonites, but do not show interlayer swelling. The total amount of isomorphous substitution is usually larger than that for montmorillonites. Substitution of Si by Al in the tetrahedral sheet is predominant. The compensating cations are mainly potassium ions. The lack of interlayer swelling is attributed to the strong electrostatic attraction between the potassium ions and the two charged layers on each side, owing to a favorable geometric arrangement and the large number of potassium ions. Because of the lack of the interlayer swelling, the cations between the layers are not available for exchange, as in montmorillonites; therefore, the CEC involves only the ions on the exterior surfaces of the stack. Hence, the CEC is lower than for montmorillonites (about 20-40 meq per 100 g) despite the greater charge deficiencies in the crystal.

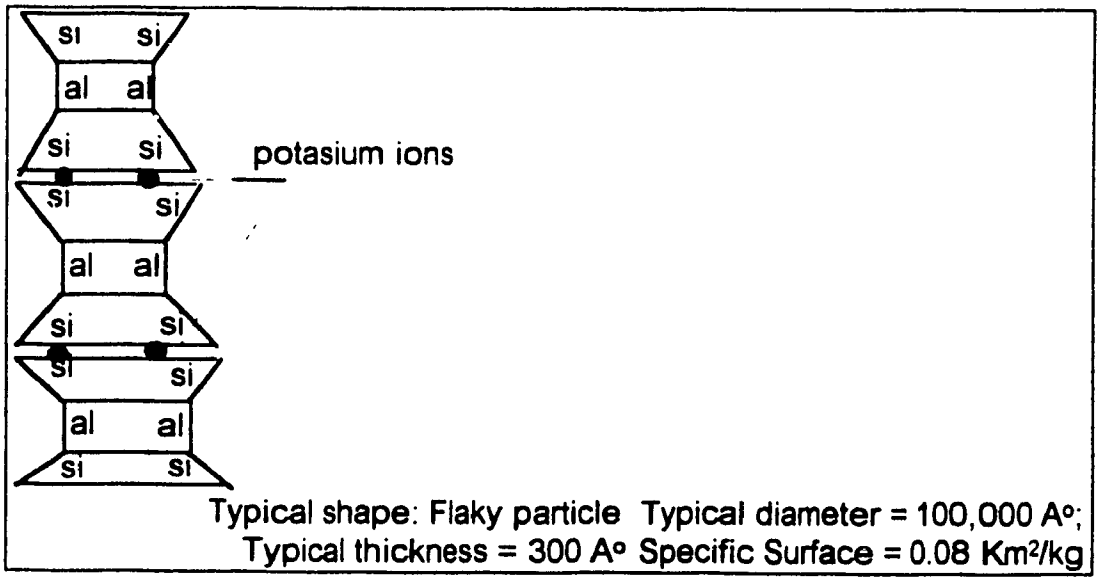

Figure A.3. Schematic representation of typical illite structure

(Yong and Warkentin 1975)

A.4. KAOLINITES (1:1 LAYER CLAY)

The arrangement of atoms in the layers of 1:1 layer minerals, the kaolinites, conform very closely with the sketched electroneutral structure The small amount of isomorphous substitution, which usually escapes precise analysis, is compensated by exchangeable cations located exclusively on the exterior surfaces of the layer stacks. The CEC is of the order of 2-10 meq per 100 g. Alternatively, the charge may originate from adsorbed silica-alumina compounds.

The species in any group of minerals differ in the degree and type of substitution and in the geometry of stacking of the layers in the particle. In many clays, layers of different types of clay are stacked in the same particle. these are called *mixed-layer clays.* The number of layers stacked in a single particle is usually small in montmorillonites(say two to five) and is larger in illites. The thickest particles occur in kaolinite suspensions.

Typical thickness = 500- 20,000A°, Typical diameter = 3000-40,000A°

Specific Surface = 0.015 K m2/ kg, Typical Shape : Stacked 6 sided plates

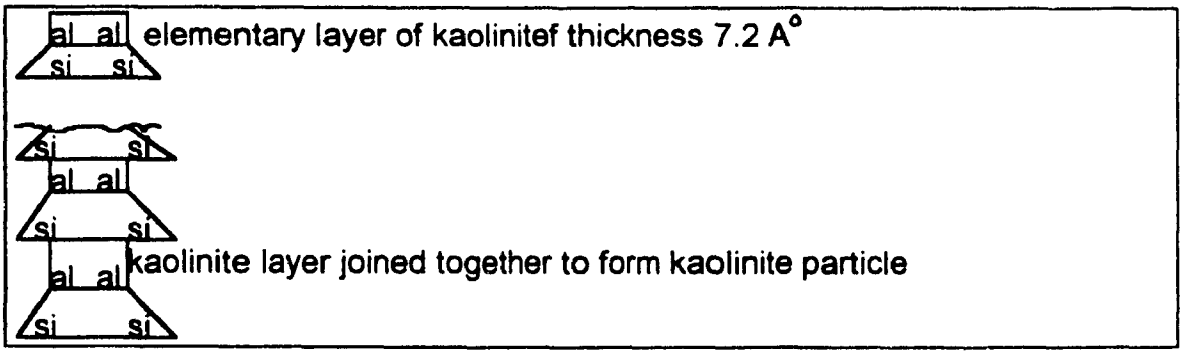

Figure A.4. Schematic Representation of typical Kaolinite structure

(Yong and Warkentin 1975)

A.5. ELECTRIC CHARGE OF CLAY MINERALS

The process by which clay soils adsorb ions of solution when wetted is generally defined as ion adsorption. This phenomenon is the result of charged surfaces on the individual minerals which attract the oppositely charged ions of solution. The electric charge of clay mineral arises from one or more of the following.

A.5.1. ISOMORPHOUS SUBSTITUTIONS

Consist of substitutions within the lattice of Al^{+3} for Si^{+4} in the tetrahedral sheet and of ions of lower valence, particularly Mg^{+2} for Al^{+3}, in the octahedral sheet without any changes in the structural orientation taking place. These substitutions create a negative imbalance of charge of which the major portion occurs in the tetrahedral layers.

A.5.2. LOCAL DISCONTINUITIES

Arise from unsatisfied valence charge at the edges of the particles. These are referred to as broken-bond charges. The clay crystal lattice is continuous in two directions, but at the edges must be broken bonds between oxygen's and silicon, and between oxygen and aluminum. The most probable breaking plane is shown in figure A.5 (Yong and Warkentin 1975) A charge due to broken bonds would also arise if pieces were broken out of flat surfaces.

In figure A.5 the broken bonds are shown to attract hydrogen or hydroxyl ions from pore water. The ease with which hydrogen can be exchanged increases as the pH of the pore water increases, i.e., as the hydrogen ion concentration of the pore water decreases. At low pH, i.e., below pH 4, some of these sites on kaolinite may become positively charged by attracting extra hydrogen ions. In the case of montmorillonite, the source of charge is ion substitution, with a small contribution to broken bonds compared with illite and kaolinite (Yong and Warkentin 1975).

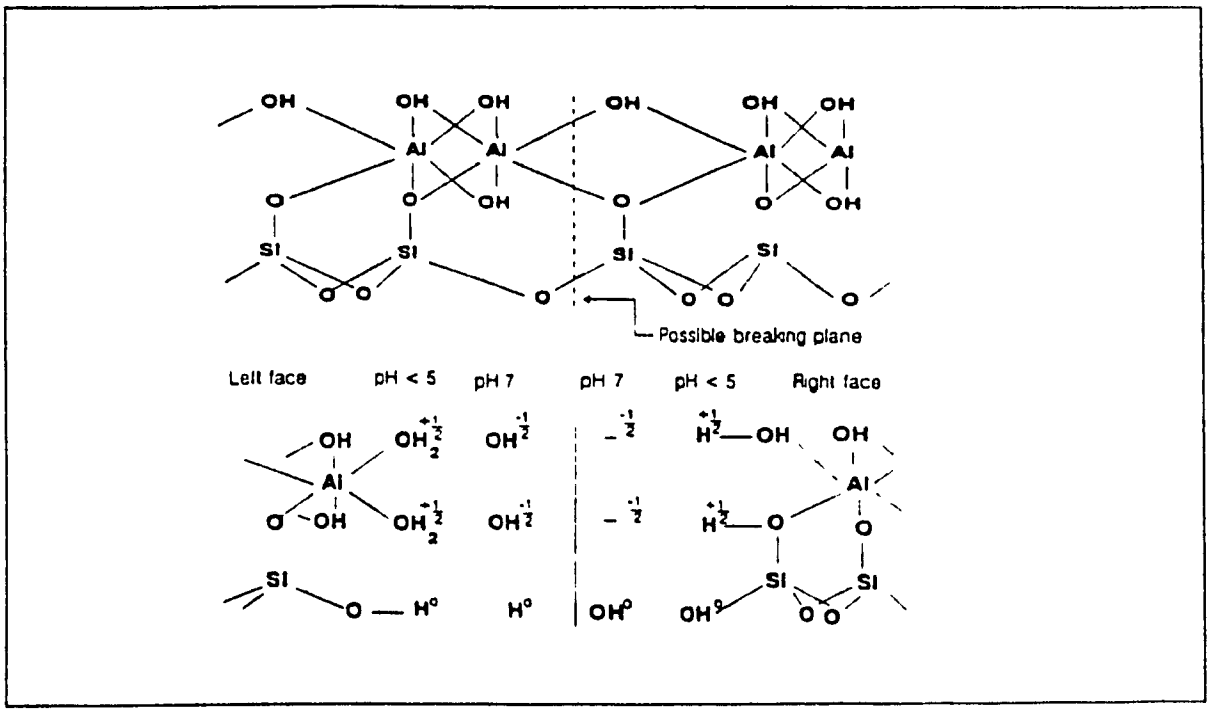

Figure A.5. Kaolinite structure showing probable breaking plane and mechanism for edge charge by picking up hydrogen or hydroxyl from solution give positive charge at low pH and negative charge at higher pH (Yong and Warkentin 1975).

A.6. ENGINEERING PROPERTIES OF THE CLAY MINERALS

The different groups of clay minerals exhibit a wide range of engineering properties within any one group, the range may also be great and is a function of such factors as particle size, degree of crystallinity, type of adsorbed cations and type and amount of free electrolyte in the pore water. In general, the importance of these factors increase in the order kaolin < hydrous mica (illite) < smectite. The chlorites exhibit characteristics in the kaolin-hydrous mica range. Vermiculite's and the relatively uncommon Attapulgite type of mineral behave in the hydrous mica-smectite range.

Because of the influence of the above compositional factors, as well as the effects of environmental influences, only ranges of values for the various engineering properties of the different minerals can be given.

A.6.1. ATTERBERG LIMITS

Several general conclusions can be made concerning the Atterberg limits of the clay minerals.

1 The liquid and plastic limit values of any one clay mineral species may vary over a wide range, even for a given adsorbed cation type.

2. For any given clay mineral, the range in liquid limit values is greater than the range in plastic limit values.

3. The variation in liquid limit among different clay mineral groups is much greater than the variation in plastic limit values.

4. The type of adsorbed cation has a much greater influence on the high plasticity minerals, for example, montmorillonite, than on the low plasticity minerals, for example, kaolinite.

5. Increasing cation valence decreases the liquid limit values of the expansive clays, but tends to increase the liquid limit of the non expansive minerals
6. The greater the plasticity the greater the shrinkage on drying (lower shrinkage limit).

A.6.2. PARTICLE SIZE AND SHAPE

The different clay minerals tend to occur in somewhat different size ranges . Most reported size analyses indicate the amount finer than 2 μm but do not consider the distribution of sizes within this fraction. however, it can be possible that there is some concentration of different clay mineral within different size ranges.

A.6.3. VOLUME CHANGES CHARACTERISTICS

In general, the swelling and shrinking properties of the clay minerals follow the same pattern as their plasticity properties; the more plastic the mineral, the more the potential swell and shrinkage. The actual amount of swell or shrinkage observed as a result of wetting or drying depends on factors in addition to mineralogy, such as particle arrangement, initial water content, and confining pressure. The potential expansion of the different clay minerals follows closely their respective plasticity indexes.

A.6.4. INFLUENCE OF EXCHANGEABLE CATIONS AND pH

In general, the influence of cations on properties increase with the increasing activity of the clay. The most important characteristics of the cations are their valence and size. These factors exhibit a major influence on the interparticle physico-chemical forces of interaction.

In soils containing expansive clay minerals, the type of exchangeable cation exerts a controlling influence over the amount of expansion that takes place in the presence of water. For example, sodium and lithium montmorillonite can exhibit almost unrestricted interlayer swelling provided water is available, the confining pressure is small, and the excess electrolyte concentration is low. Di - and trivalent forms of montmorillonite do not expand beyond a basal spacing of about 18 A° regardless of the environment.

In soils composed mainly of non expansive clay minerals, the type of adsorbed cation is of greatest importance in influencing the behavior of the material in suspension and the nature of the fabric in sediments formed. Therefore, monovalent cations, particularly sodium and lithium, promote deflocculation; whereas, clay suspensions ordinarily flocculate in the presence of di- and trivalent cations. The role of pH in influencing interparticle repulsion and the existence of positive edge charge in low pH environments are considered. These effects are of greatest importance in kaolinite, lesser importance in illite, and relatively unimportant in montmorillonite. In kaolinite the pH may be the single most important factor controlling the fabric of sediments formed from suspension.

APPENDIX B

QUANTITATIVE DESCRIPTION OF DIFFUSE ION LAYER THEORY

TABLE OF CONTENTS

LIST OF FIGURES

LIST OF TABLES

B.1. GOUY-CHAPMAN THEORY

The mathematical description of the electric double layer was first developed by Gouy (1910) and later Chapman (1913), but received little attention, as research during this period was mainly devoted to the first layer of ions at the interface This portion of the double layer was the most uncertain part of the Gouy-Chapman theory, as all deviation from the basic assumptions becomes intensified in the region. A correction of the Gouy-Chapman theory considering the behavior of the ions at the interface was proposed by Stern (1924), but was not given any significance at the time due to its complexity. Recently, efforts to explain the flocculation and the electrokinetic phenomena in colloid systems have resulted in increased interest in the Gouy-Chapman theory. The theory was revised by (Kruyt 1952), and by (Verwey et al. 1948), to account for the deflocculation phenomenon, and by Schofield (1946), to calculate negative absorption and osmotic pressure respectively in clays.

MODEL :

The model used to describe the ion distribution function and the potential of the region near the charged interface was developed independently by Gouy-Chapman by combining the Poisson equation for the second derivative for the electric potential as a function of charge density with the Boltzman equation for the charge density as a function of potential.

The Gouy-Chapman theory considers a negatively charged plate of counterions and co-ions. The basic assumptions of the theory are expressed in the following three equations

The Poisson equation:

$$\frac{d^2\psi}{dX^2} = \frac{4\pi\rho}{e} \qquad [2\ 1]$$

The Boltzman Equation.

$$N_i = N_O \exp\left(\frac{-W_i}{kT}\right) \qquad [2\ 2]$$

with $W_i = Z_i\, e\, \psi_i$ [2 3]

where ε = Dielectric constant

e = electronic charge

k = Boltzman constant

N_i = the concentration of ions of species i at a point where the potential is ψ_i

W_i = Work done in bringing an ion to point where the potential is ψ_i

X = distance from particle surface

Z_i = ionic valence

ρ = surface charge density

ψ = electric potential

Equation [2.3] shows the relationship between the electric potential and the distance from the particle surface. From equation [2.2], the local concentration of ions at a distance X from the particle surface can be written as a function of the electric potential.

According to double layer theory, the swelling of clays is due to the difference in osmotic pressure between the mid-plane of two adjacent particles and the bulk solution. Assuming ideal behavior of the ions and neglecting the

attractive forces between the particles, the osmotic pressure can be quantitatively defined by the Van't Hoff equation (Schofield, 1946) which states:

$$P = RT\,(N_i - N_o) \qquad [2.4]$$

in which P denotes the swelling pressure and R is gas constant. Substituting Equations [2.2] and [2.3] into Equation [2.4] and considering both anions and cations of a symmetrical electrolyte

$$P = 2\,RT\,N_o\,[\cosh \frac{Ze\psi_c}{kT} - 1] \qquad [2\,5]$$

From this equation, the factors influencing the swelling pressure are concentrations of electrolyte solution, valence of ions, electric potential, electric charge and absolute temperature, provided that the Gouy-Chapman theory is valid

The value of electric potential (ψ_c) can be obtained from the integrated Poisson-Boltzman equation (Taylor, 1962 and Yang, 1966). The resulting equation derived by (Verwey et al. 1948), by assuming infinite surface electric potential is:

$$\kappa X_c = 2 \exp\left(\frac{-Y_c}{2}\right) \int_o^{\pi} \frac{d\phi}{\sqrt{1 - \exp(-2Y_c)\sin^2\phi}} \qquad [2.6]$$

Where $\sin^2\phi = \dfrac{\exp(-Y)}{\exp(-Y_c)}$

$$\kappa = \sqrt{\frac{8\pi Z_i^{\,2} e^2 N_o}{\varepsilon\, kT}}$$

X_C = the half distance between two parallel plates (Fig. B 1)

Y_C = ψ_C electric potential in the line midway between parallel interacting particles (Figure B.1)

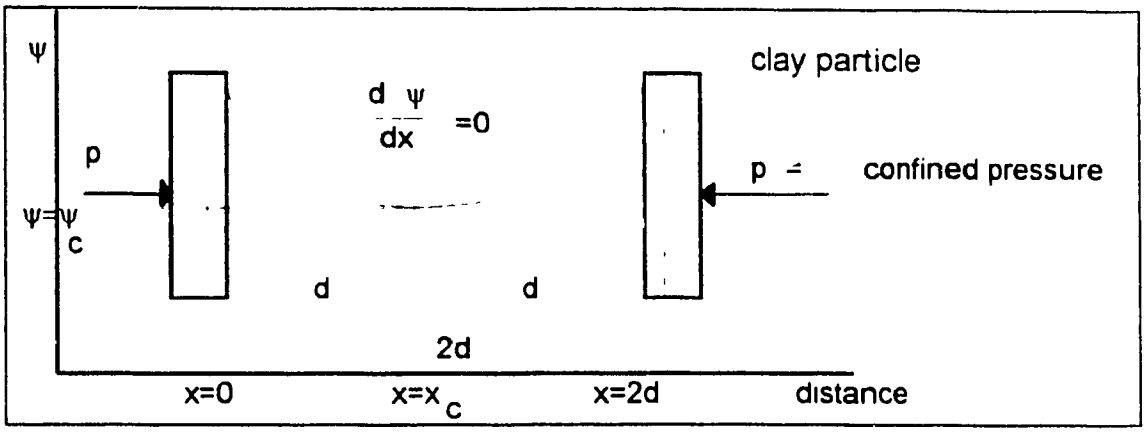

Figure B.1. Variation in electrical Potential ψ between parallel plates (Taylor 1962).

For a small amount of overlap, the resulting electric potential is the algebraic sum of the potentials from single plates. At close spacing of particles, the anions can be neglected.

Therefore, the application of Equation [1.3] in practice can be simplified by the substitution of the Langmuir approximation and by a summation of the potentials due to single layers. Equation [2.6] becomes

$$Y_c = 2 \ln\left(\frac{\pi}{\kappa X_c}\right) \qquad [2.7]$$

and

$$\psi_c = \frac{2\,kT}{Z_i e} \ln\left(\frac{\kappa X_c}{\pi}\right) \qquad [2.8]$$

This solution is valid only when $Y_C > 1$

The accuracy of the approximation methods is shown in Table B.1 from which it is evident that as the Langmuir approximation becomes untrustworthy, the summation of separate potentials may be successfully applied.

Table B.1. Comparison of midpoint potential from Langmuir approximation and summation of separate potentials (after Taylor 1962).

κX_C	Y_C from E [3 6]	Y_C from Langmuir	Y_C from Potentials
4.0	0.15	-	0.15
3 0	0.40	0.10	0.40
2.0	0.98	1.03	1 10
1.5	1.50	1.48	1.70
1.0	2.30	2.38	3.10
0.75	2.85	2.86	4.1
0.50	3.60	3.68	5.6

By substituting Equation [2.8] into Equation [2.5] and then by putting $\beta = \frac{8\pi e^2}{\varepsilon kT}$ yields (Yang, 1966).

$$P = RT\left[\frac{\pi^2}{\beta Z_1^2 X_c^2} - 2N_o\right] \qquad [2.9]$$

There is a small error resulting from the assumption that the plane of infinite charge is at the face of the plate. A correction should, therefore, be made to the half distance between two parallel plates. The swelling pressure can then be easily calculated by

$$P = RT\left[\frac{\pi^2}{\beta Z_1^2 (X_d + X_o)^2} - 2N_o\right] \qquad [2.10]$$

Where $$X_o = \frac{\varepsilon kT}{2\pi Z_i e\sigma}$$

σ is the surface charge density of the clay

X_o is constant depending on the valence of the exchangeable ions and the charge density on the clay particles, and varies from 1 to $4A^o$ for clay. For Na-montmorillonite, X_o is approximately $4A^*$ (Yong and Warkentin, 1959).

The relationship between water content, W, and half distance between particles, X_c in A^o, is given by

$$W = \frac{S X_c}{100} \qquad [2.11]$$

In which W = water content in wt, percentage

S = surface area of clay, m^2/g

These calculations adequately predict measured swelling pressures for the high-swelling Na-montmorillonite at low-salt concentration as shown in figure B.2.

The measured pressures of Na-montmorillonite exceed calculated values at higher salt concentrations. It probably results from the errors in using concentrations rather than activities of the exchangeable cations, and from neglecting the tactoid structure.

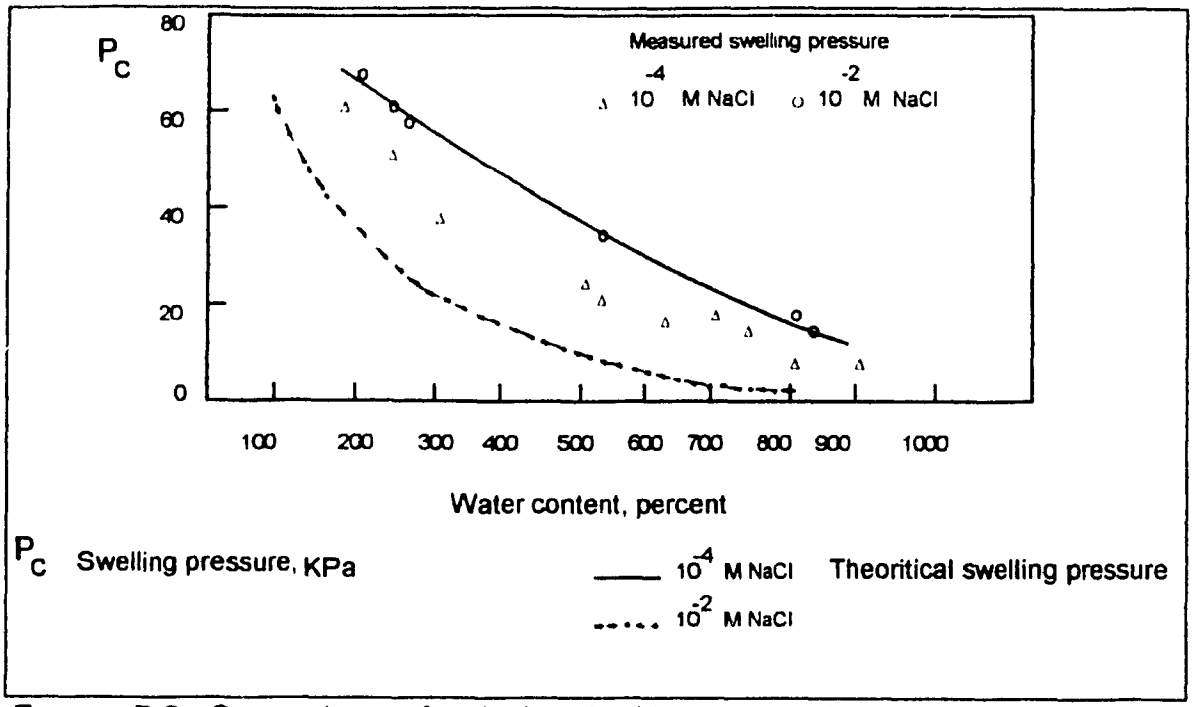

Figure B.2. Comparison of calculated with measured swelling pressure for sodium montmorillonite at two salt concentrations (Warkentin and Schofield 1962).

B.2. STERN DOUBLE-LAYER THEORY

Stern made corrections in the double layer theory by taking into consideration the ionic dimensions. The influence of ionic dimension is greatest near the colloid. In the Stern theory, the first layer is similar to that of the previous theories. However, the second layer has been divided into (1) a sub layer nearest the colloid surface and (2) a diffuse layer:

The first sub layer is tightly packed with cations, and is called the Stern layer. The potential distribution appears to be a combination of the Helmholtz and the Gouy-Chapman diffuse double layer. The decrease in potential is also divided into two parts. In the Stern layer, the potential decreases with distance from the surface according to the Helmholtz theory. From here on (in the diffuse layer), the decrease in potential with distance follows the Gouy-Chapman theory.

B.3. THE DLVO THEORY

The Derjaquin, Landau, Verwey, and Overbeek theory of colloid stability states that the stability of a colloidal suspension is essentially dependent on the relation of two independent interactions between colloid particles. These interactions are (figure B.3):

(a) The Van der Waals attraction and,

(b) The electrostatic repulsion between electrical double layers of identical size.

Consider two parallel charged plates of infinite extent and separated by a distance 2X such that their double layers overlap (figure B.4). If the double layers are assumed to be of the Gouy-Chapman type, the expression for the energy of repulsion between charged plate is:

$$V_R = \frac{64\, N_o\, kT\, \gamma_o}{\kappa} \exp(-2\kappa X) \qquad [3.1]$$

where

$$\gamma_o = \frac{\exp[Z_i e\psi_o / 2\, kT] - 1}{\exp[Z_i e\psi_o / 2\, kT] + 1} \qquad [3.2]$$

N_O = the number of ions of each kind in the bulk solution per unit volume

k = Boltzman constant

T = the absolute temperature

κ = Debye Hückel reciprocal thickness of the diffuse double layer

$$= \left(\frac{8\pi N_o e^2 Z^2}{\varepsilon\, kT}\right)^{1/2}$$

ε = dielectric constant of the solvent

e = electronic charge

ψ_o = surface potential

X = half distance of separation between plates

z = ionic valence

This particular form is limited in applicability to situations in which the separation of the surfaces is large compared to κ^{-1}, and ψ_o is large so that $\gamma_o \cong 1$. Equation [3 1] indicates that the energy of repulsion varies exponentially with the separation (2X).

Van der Waals forces gives rise to an energy of attraction between two parallel plates separated by a distance 2X of approximately

$$V_A = \frac{-A}{48\pi X^2} \qquad [3.3]$$

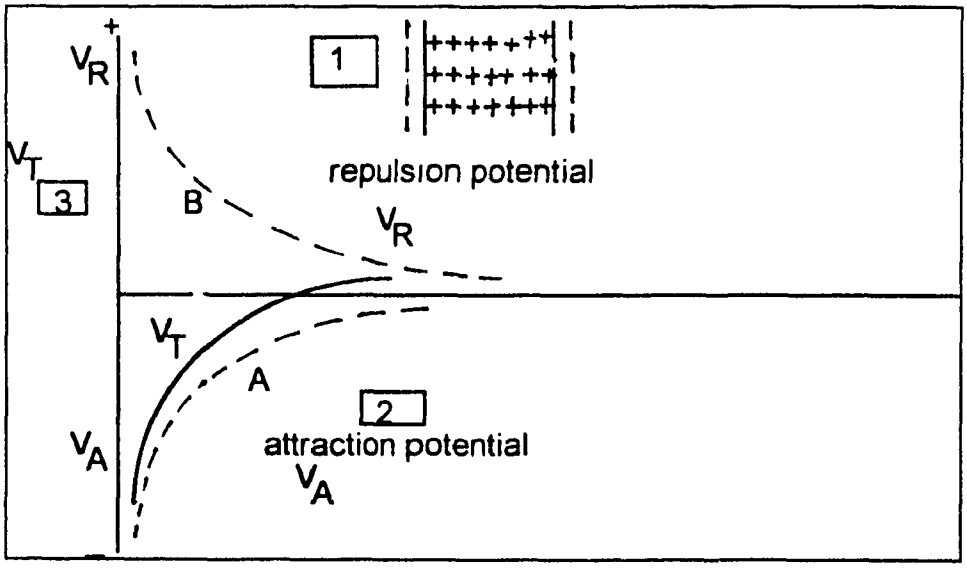

Figure B.3 (Schematic). The DLVO theory refers colloidal stability to the distance of two independent potentials (Friberg 1976).

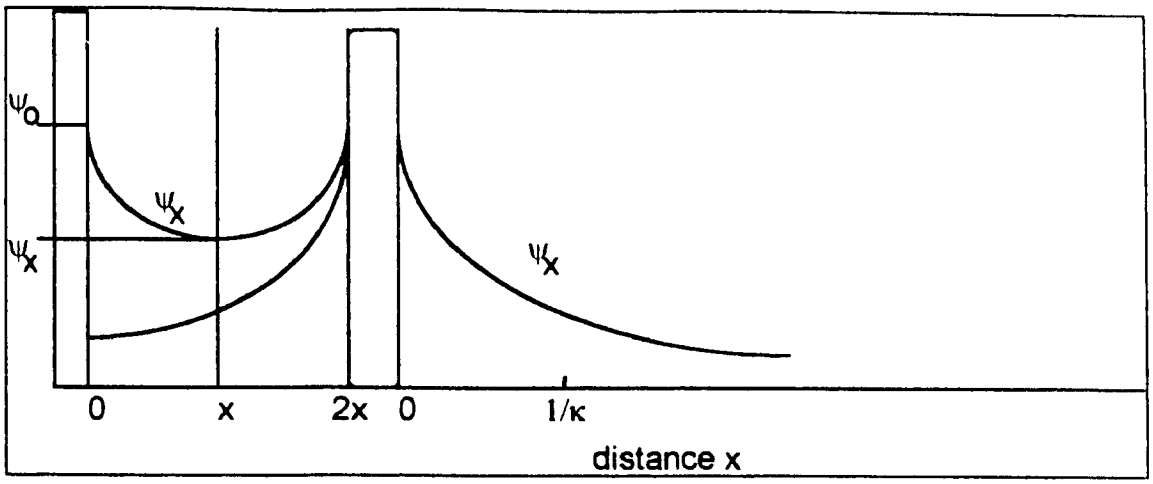

Figure B.4 (Schematic). Comparison of the double layer potential between two plates with that of a single double layer (Shaw 1966).

where A is Hamaker constant (generally between 10^{-13} and 10^{-12} ergs) which depends on the nature of the material

$$A = \left(\frac{\rho N_A \pi}{M}\right)^2 \beta \qquad [3\ 4]$$

in which $\frac{\rho N_A}{M}$ is the number of atoms per cubic centimeter in the material and β is a constant. Equation [3.3] shows that the attraction varies intensely with the square of the separation (2X).

Two observations about theses functions will prove helpful:

(a) As $2X \rightarrow 0$: $V_R \rightarrow$ constant and $V_A \rightarrow \infty$

(b) As $2X \rightarrow \infty$: V_R and $V_A \rightarrow 0$ with V_R decreasing more rapidly.

These indicate that attraction will predominate at very small and very large separations. At intermediate separations the details of the two

contributions must be considered. Figure B.5. is a qualitative sketch of a potential energy curve which is the resultant of a repulsive and an attractive component:

$$V_T = V_R + V_A \qquad [3.5]$$

The curve indicates a maximum and two minima as sketched, even though some of these features may be masked if one contribution greatly exceeds the other. The height of the maximum above $V_T = 0$ is called the height of the energy barrier.

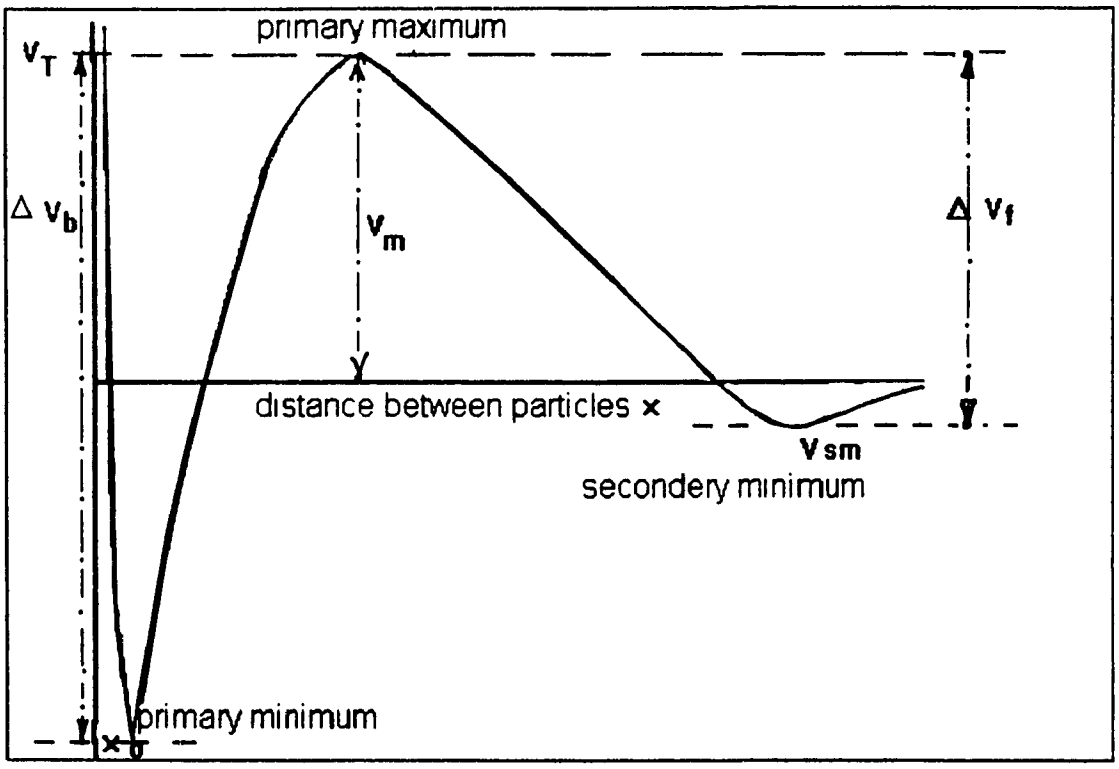

Figure B.5 (Schematic). Curve of net potential energy ($V_T = V_R + V_A$) against the distance of surface separation for the interaction between two particles (Le Bell 1978).

The deeper minimum is termed the primary minimum; and the more shallow one, the secondary minimum. Although attraction predominates at large distances - that is, the secondary minimum is generally present - it may be quite shallow, especially in view of the effects of retardation and the medium on attraction. Eq. [3.1] and Eq. [3.3] can be substituted into Eq. [3.5] to give the net potential energy between two parallel flat charged surfaces as a function of their separation ($2X_c$):

$$V_T = \frac{64N_o\, kT\, \gamma_o^{\,2}}{\kappa} \exp\left(-2\kappa X_c\right) - \frac{A}{48\pi X_c^{\,2}} \qquad [3.6]$$

APPENDIX C

EXPERIMENTAL

TABLE OF CONTENTS

LIST OF FIGURES

LIST OF TABLES

C.1. PROPERTIES OF AVONLEA NA-BENTONITE AND SOLUTIONS

C.1.1. AVONLEA-BENTONITE

The Na-Bentonite was determined to have a water content of 6.85% by weight. The specific gravity of the Avonlea-Bentonite was calculated to be 2.65. Liquid limit and plastic limit were found in the range of 240 and 60. Distilled water and ground water suspensions yielded pH reading of approximately 7 for concentrations of 0.01 to 0.1% bentonite by weight at room temperature.

C.1.2. RESIDUAL SALT CONTENT

A sample of 1 gm Avonlea bentonite clay was diluted into 50 ml of DDW , the solution was injected in the ionchromotography apparatus to detect the components of the solution.The results of the test are shown in table C.1.1

Table C.1 1. Residual salt content in Avonlea-bentonite

component	concentration mg/L
Lithium	0.006
Sodium	31.345
Ammonium	0.000
Potassium	0.546
Magnesium	0.900
Calcium	5.817
Total	38.614

It is clear from the results that the sample contains sodium as major salt in the Avonlea bentonite , the sodium and calcium found in the sample are in the range of the CCC calculated in the 15% wt gel in dispersion tests as will be shown later .

C.1.3. SOLUTIONS

WN-1 ground water was prepared as outlined in the standard procedure. A cation and anion analysis included below. Anion analysis of the SCSSS is also detailed below Ionic strength for WN-1 & SCSSS were calculated in tables.

WN-1 SOLUTION

Recipe for 20 litres

1. Prepare the following stock solution in 1L DDW by adding :

(a) 2.686 g KCl

(b) 9.408 g $NaHCO_3$

(c) 4.505 g $NaNO_3$

2. Pipette 200 ml of this stock solution into a 20 L container and dilute to 20 L with DDW. Then add the following dry chemicals:

(e) 131.112 g $CaCl_2.2H_2O$

(f) 12.324 g $MgSO_4.7H_2O$

(g) 95.204 g NaCl

(h) 12.818 g $Ca(OH)_2$

(i) 1.48 g $SrCl_2.6H_2O$

(j) 0.056 g $FeSO_4.7H_2O$

(k) 4.7 ml conc. H_2SO_4

Stir this solution thoroughly and adjust the pH to 7.0± 0.5, if necessary, with HCl Filter the solution through #40 Whatman filter paper before storage. Refilter through 0.45 μm Millipore filter , submit for analysis before use and determine its density.

Table C.1.2 Composition of WN-1 groundwater.

SAMPLE	WN-1 mg/l
Ca	2210±120
Fe	<0.1
K	11.0±0 4
Mg	58.1±0.7
Na	1720±60
Sr	15.8±0.3
Cl	6410±385
NO_3	40.8±1.3
SO_4	1080±200
HCO3	28±2

Table C.1 3 Composition of SCSSS groundwater

SAMPLE	SCSSS-1 mg/l
Ca	16000±300
Fe	0.74±0.09
K	43.5±0.3
Mg	215±3
Na	4560±200
Si	19±2
Sr	1.94±0.06
Cl	33200±2000
NO_3	99.1±6.5
SO_4	758±23
HCO_3	72±2

Table C.1.4 Calculation of ionic strength for WN-1 groundwater

$I = 1/2 (\Sigma mv^2)$ m = Molecular weight v = valance

SAMPLE WN-1	CALCULATIONS	IONIC STRENGTH
Ca	$(2210 * 2^2) / 40 * 1000$	0.221
Fe	$(11.0 * 3^2) / 56 * 1000$	1.77E-3
Mg	$(58.1 * 2^2) / 24 * 1000$	9.7E-3
K	-------	-------
Na	$(1720 * 1) / 23 * 1000$	7.5E-2
Cl	$(6410 * 1) / 35.5 * 1000$	0.18
NO_3	$(40.8 * 1) / 62 * 1000$	6.6E-4
SO_4	$(1080 * 2^2) / 96 * 1000$	0.045
HCO_3	$(28 * 1) / 61 * 1000$	4.6E-4

IONIC STRENGTH $I = 0.267$

Table C.1.5. Calculation of ionic strength for SCSSS solution

SAMPLE SCSSS-1	CALCULATIONS	IONIC STRENGTH
Ca	(16000 × 2^{2}) / 40 × 1000	1 6
Fe	----------	--------
K	(43.5 × 1) / 39 × 1000	1.11E-3
Na	(4560 × 1) / 23 × 1000	0 198
Si	----------	-------
Sr	----------	--------
NO_3	(99.1 × 1) / 62 × 1000	1.6E-3
SO_4	(758 × 2^{2}) / 96 × 1000	3.16E-2
HCO_3	(72 × 1) / 61 × 1000	1 18E-3

IONIC STRENGTH: I = 0.9167

C.2. SEDIMENTATION TEST DATA

Avonlea Bentonite was dried at 65 C for 24 hours and sieved to a particle size distribution of less than 45 micrometers. Suspensions of 2 wt % bentonite were prepared in the following media table:

Table C.2.1. Clay suspensions 2Wt. % in different electrolytes with different concentrations

ELECTROLYTE	CONCENTRATION, Mole/Litre
DDW	
WN-1 GROUND WATER	
SCSSS GROUND WATER	
CaCl2	0.00001
	0.0001
	0.001
	0.01
	0.1
NaCl	0.00001
	0.0001
	0.001
	0.01
	0.1

The suspensions are in graduated centrefuge tubes to enable direct volume readings. The suspensions were allowed to settle for 18 hours prior to being photographed and observations recorded

The samples were centrifuged for periods of one hour, two hours and three hours. After three hours, the DDW sample remained cloudy. Sediment heights are recorded, observations are recorded and the samples are photographed. This initial experiment indicated that the C.C.C for $CaCl_2$ is in the region of 0.001 to 0.01 M. Visual observations both prior to and following centrifuging was used as the basis for this conclusion. For NaCl, the C.C.C was determined to be around the range 0.1 to 0 01 M

Sediment volume percentages are calculated and plotted =

Final volume after centrifuging × 100 ÷ initial volume (30 ml)

Table C.2.2 .Trial 1 and 2 Initial observations (prior to centrifuging) 18 hours of settling

Electrolyte's Concentration	Observations
DDW	Remains cloudy
WN-1	Clear above surface; surface of sediment distinct
SCSSS	Clear above surface; surface of sediment disinct
0.00001 CaCl2	Cloudy
0.0001 CaCl2	Cloudy
0.001 CaCl2 CCC	*Cloudy*
0.01 CaCl2 CCC	*Clear above surface of sediment; surface distinct*
0.1 CaCl2	*Clear above surface of sediment; surface distinct*
0.00001 NaCl	Cloudy
0.0001 NaCl	Cloudy
0.001 NaCl	Cloudy
0.01 NaCl CCC	*Cloudy*
0.1 NaCl CCC	*Clear above surface of sediment; surface distinct*

From initial observations of table C.2.2, one can conclude the following -

* CCC for NaCl is found within the range of 0.01 to 0.1 M.

* CCC for $CaCl_2$ is found within the range of 0.001 to 0.01 M

For higher accuaracy in determining the CCC, the following additional samples are prepared. The same procedure as outlined above is repeated and the results are as follows:

Table C.2.3: NaCl, CaCl2 salts with different concentrations

Electrolyte	Concentraion (Mol/ L)
NaCl, CaCl2	0.0005
	0.001
	0.003 CCC for Ca
	0.005 CCC for Ca
	0.007
	0.01 CCC for Na
	0.03 CCC for Na
	0.05
	0.07
	0.1
	0.3
	0.5

Results of the above test indicate that the C.C.C for NaCl is within the range of 0.01 to 0.03 M. and CCC values for $CaCl_2$, within the range of 0.003 to 0.005 M.

Table C.2 4. Sedimentation test results for NaCl salt after 18 hrs settling.

Sampl Concentration. Mole/Litre	Sediment Volume (ml)	Percent Sediment Volume (%)
NaCl		
0 5	6 1 clear	17
0 3	7.2 clear	24
0.1	7.5 clear	25
0.07	7.5 clear	25
0.05	12.6 clear	42
0.03 ccc	15.0 clear	50
0 01 ccc	11.4 cloudy	38
0.007	6-9 cloudy	25
0.005	6-9 cloudy	25
0.003	7.5-9 cloudy	27
0.001	9.6 cloudy	32
0.0005		

Table C.2.5. Sedimentation test results for $CaCl_2$ salt 18 hrs.

Sample Conc. Mole\Litre	Sediment Volume (ml)	Percent Sediment Volume (%)
Cacl2		
0.5	4.2 clear	14
0.3	4.5 clear	15
0.1	4.5 clear	15
0.07	4.8 clear	16
0.05	4.8 clear	16
0.03	4.8 clear	16
0.01	5.2 clear	17
0.007	6.9 clear	23
0.005 ccc	6.0 clear	20
0.003 ccc	7.0 cloudy	23
0.001	8.4 cloudy	28
0.0005		

Observations prior to centrifuging (16 hrs of settling)

Electrolyte concentration Mole/litre	Observations
0.5 NaCl	Clear above sediment surface
0.3 NaCl	Clear above sediment surface
0.1 NaCl	Clear above sediment surface
0 07 NaCl	Cloudy above sediment surface
0.05 CaCl2	Clear above sediment surface
0.03 CaCl2	Clear above sediment surface
0.01 CaCl2	Clear above sediment surface
0.007 CaCl2	Clear above sediment surface
0.005 CaCl2	Clear above sediment surface
0.003 CaCl2	Cloudy above deiment surface
0.001 CaCl2	Cloudy above sediment surface

From initial observations, it is concluded :-

* C.C.C for NaCl was found to be in the range of 0 07 to 0 1 M

* C.C.C for CaCl2 was found to be in the range of 0.003 to 0.005 M.

Table C.2.6. Experimental results of sedimentation test (centrifuge) trial1

Elecrolyte Conc. Mole/Litre	Sediment Volume 1hr(ml)	Sediment Volume 2hrs (ml)	Sediment Volume 3hrs (ml)	Percent Sediment Volume (%)
DDW	4.5 cloudy	4.0-4.5 cloudy	4.0-4 5	13.3-15
WN-1	1.4 clear	1.4		4.7
SCSSS	1.3 clear	1.3		4.3
1.0 CaCl2	1.2 clear	1.2		1.0
0.1 CaCl2	1.5 clear	1.45	1 45	4.8
0.01 CaCl2	1.5 clear	1.5		5 0
0.001 CaCL2	3.8 cloudy	3.4-3.6	3.3-3.6	11.0
1.0 NaCl				
0.1 NaCl	2.9 clear	2.9		9.7
0.01 NaCl	5.4 cloudy	4.9		16 3
0.001 NaCl	4 cloudy	3.5-4.1	3 5	11 7

Table C.2 7 Experimental results of sedimentation test (3 hrs centrifuge) Trial 2

Concentration Mole/Liter		Sediment Volume 3hrs (ml)	Percent Sediment Volume (%)
DDW		3.0	10.0
WN-1		1 5	5.0
SCSSS		1.2	4.0
1 0	$CaCl_2$	1.4	4.7
0 1	CaCl2	1 5	5.0
0.01	CaCl2	1.5	5.0
0 001	CaCl2	2.8	9.3
0.0001	CaCl2	3.0	10.0
0 00001	CaCl2	3 0	10.0
1 0	NaCl	1.5	5.0
0 1	NaCl	2 5	8.3
0.01	NaCl	3.6-3 8	12.0-12 7
0.001	NaCl	3 2	10.7
0 0001	NaCl	3.2	10.7
0 00001	NaCl	3.0	10

Table C 2 8. Experimental results of sedimentation test (3 hour centrifuge)
Trial 3 Electrolyte $CaCl_2$

Concentration Mole\Litre	Sediment Volume (ml) 3hrs	Percent Sediment Volume (%)
$CaCl_2$		
0.5	1.4 clear	4.7
0 3	1.5 clear	5.0
0.1	1.5 clear	5.0
0.07	1 6 clear	5.3
0.05	1.6 clear	5.3
0.03	1.6 clear	5.3
0 01	1.7 clear	5.7
0 007	2.3 clear	7.7
0.005 CCC	2.0 clear	6.7-14.7
0 003 CCC	2.5 cloudy	8.3
0.001	2.8 cloudy	9.3
0.0005		

Table C.2.9. Experimental results of sedimentation test (3 hour centrifuge)
Trial 3 Electrolyte NaCl

Concentration Mole/Litre	Sediment Volume (ml) 3hrs	Percent Sediment Volume (%)
NaCl		
0 5	1 7 clear	5 7
0.3	2.4 clear	8 0
0.1	2.5 clear	8 3
0.07	2.5 clear	8.3
0.05	4.5 clear	15.0
0.03 CCC	6.0 clear	20.0
0.01 CCC	3 8 cloudy	12 7
0.007	2.0-3.0 cloudy	6.7-10.0
0.005	2.0-3.0 cloudy	6.7-10.0
0.003	2.5-3.0 cloudy	8 3-10 3
0.001	3.2 cloudy	10.7

Table C.2.10. Sedimentation values for different ionic strength solutions

Sample	**vol1 0hr**	**vol2 2hr**	**%SED.**	**vol3 2hr**	**%SED.**	
	ml	**1hr ml**		**ml 2hr**		
Ionic strength I						
I=0.267	4.4	2.37	7.9	1.5	5	**WN-1**
I=0.917	3.5	1.95	6.5	1.25	4.2	**SCSSS**
I= 0	8.75	5.5	18.3	4.25	13.3	**DDW**
CaCl2						
I=0.003	9.5	5.15	17.2	3.1	10.3	
I= 0.03	8.25	3.15	10.5	2	6.7	
I= 0.3	3.4	2.3	7.72	1.4	4.7	
I= 3	3.8	4.2	14	1.35	4.5	
NaCl						
I=0.001	12.3	5.4	18	4	11.7	
I= 0.01	21	7		4.6	15.3	
I= 0.1	10.5	4.5	15	2.8	9.3	
I= 1	3.75			1.5	5	

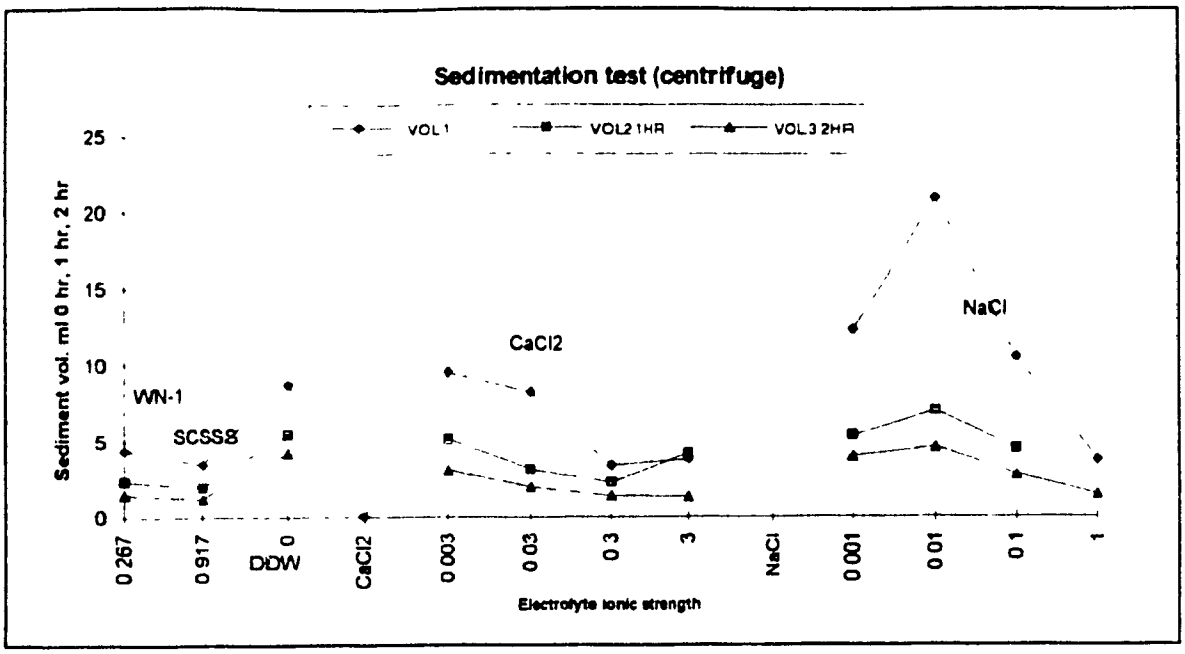

Figure C.2.1. Sedimentation values for different ionic strength solutions from table C.2.10

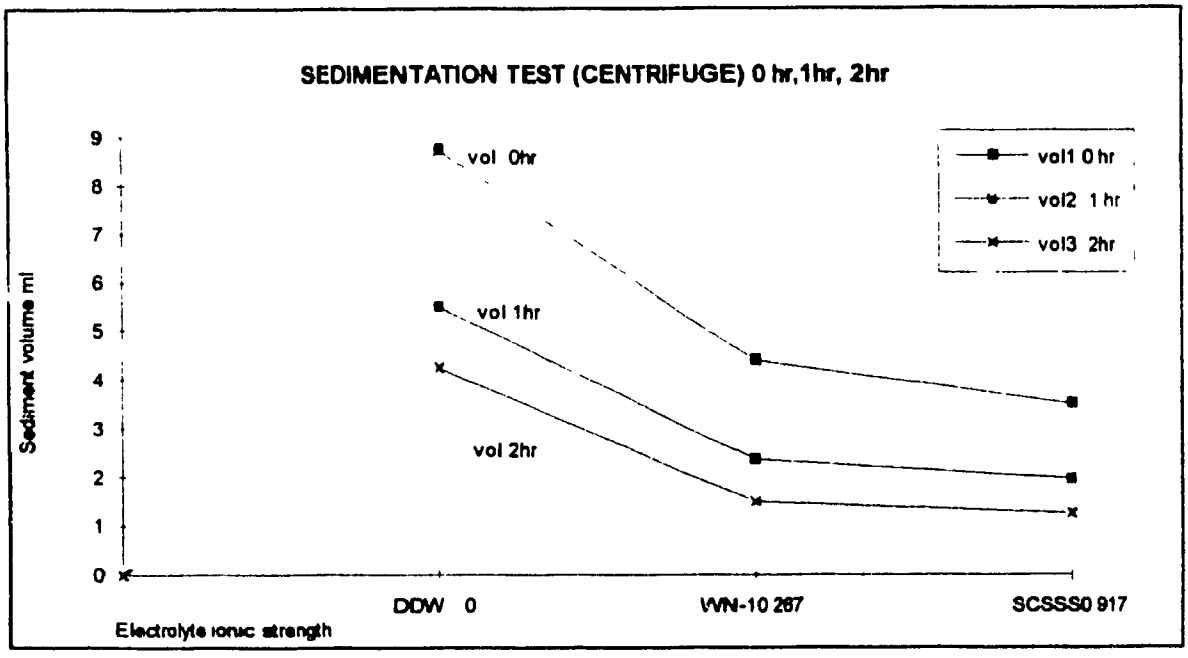

Figure C.2.2 Sedimentation volumes of WN-1,SCSSS and DDW (data as in table C.2.10)

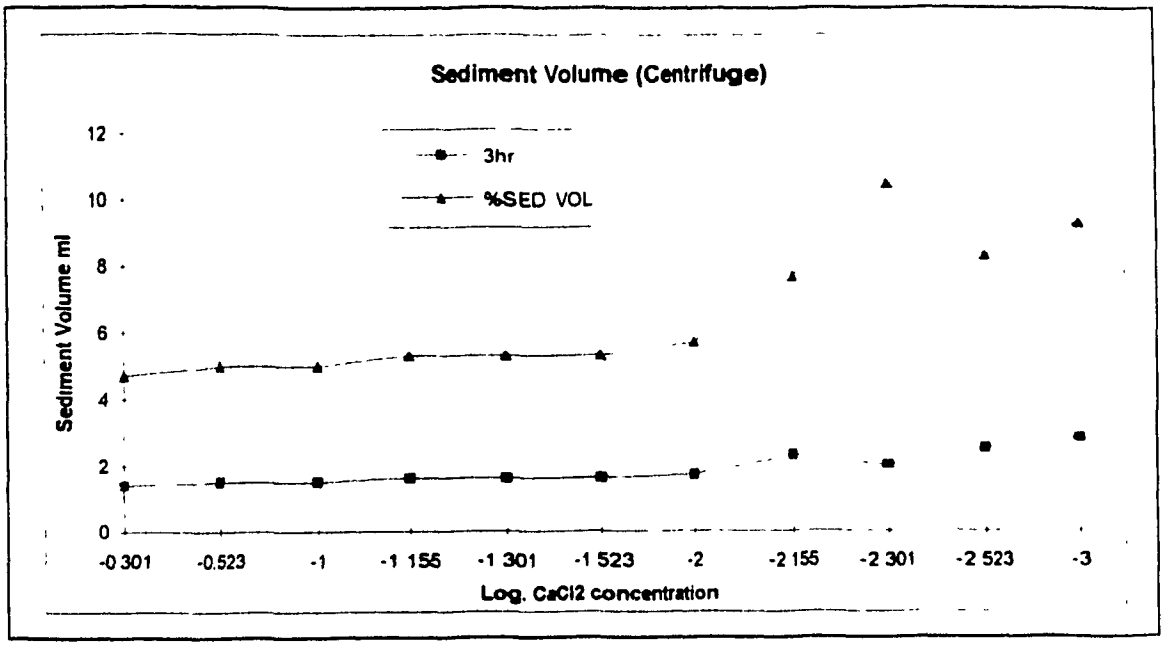

Figure C.2.3. Sedimentation values of bentonite suspension in $CaCl_2$ solution

APPENDIX D

DIFFUSION TESTS and DATA

TABLE OF CONTENTS

LIST OF FIGURES

LIST OF TABLES Page

D.1. APPARATUS CALIBRATION

1. To minimize the drift on the electrometer and yet provide a signal of reasonable magnitude, a setting of 10^{-7} amperes full scale was selected. The electrometer does significantly contribute to the noise levels.

2. The photomultiplier tube should not receive in excess of 1500 V from the high voltage power supply. Saturation of the photomultiplier tube may result in an irreparable damage.

3. To achieve a differentiated signal which remains on-scale and centered on the strip chart recorder, the 10 mV scale was found to be appropriate.

4. The voltage output form the power supply was checked using a high voltage probe.

5. The electrometer performance was checked using a known current supplied from a picoammeter source.

6. The calibration of the strip chart recorder was adjusted using a multimeter

7. The position of the lens relative to the photomultiplier tube was adjusted to 1 focal length.

8. Weight percent bentonite in DDW standards were prepared at 0.02% and below (refer to section on standards).

9. The lens and photomultiplier tube were aligned at various distances from the sample cell at angles of 90°, 45°, 35° and 20°. To gather the maximum amount of scattered light, the lens should be as close as possible to the sample cell. The angular distribution of scattered light is influenced by the size of the particles. In general, for particles 1μm in dia. and less, most of the scattered intensity is found within 10° of the incident beam For particles of 10μm in dia., the scattered light intensity is concentrated within 1° of the incident beam (Treatise on Analytical Chemistry, Part I, Vol. 5, pg. 3317). Due to the configuration of the apparatus, an angle of less than 25° was found to be inappropriate. At an angle of 45°, the optimum differentiation for the standards was achieved. A prepared graph illustrates that an angle of 90° gathered a smaller fraction of the available light than an angle of 45°.

10 Calibration of the apparatus was difficult due to the number of parameters involved. It would undoubtedly be possible to improve upon the calibration curve obtained, however, time limitations are in effect. The distilled water signal is reproducible with time. Readings for the prepared standards vary with time due to differences in agitation of each standard prior to measurement. The calibration curve does however provide an indication of the level of dispersion present in a sample.

The apparatus is extremely sensitive to position and the conditions present for each measurement. A rigid frame on an optical bench is highly recommended. A spatial filter would improve results, however alignment was extremely difficult with the present arrangement. The electrometer drift introduces an error. A dust free environment with temperature control would be very advantageous. Sample cells of extremely similar optical properties would improve results.

Table D.1: Determination of the Reproducibility of Measurements With Time Calibration Curve.

Angle 45°
120V
10^{-7} amps. Standards: wt% Bentonite in DDW
10mV
4cm/min

Standard %		Reading (mV)			
		Trial 1	Trial 2	Trial 1	Trial 2
DDW	2.6	3.8/3.9	4.0	3.8	4.0
0.02	7.1	10 8	10.7	9.0	9 5
0.0175	5.4	7.7	7.9	6.8	7.1
0.015	4.6	7.1	7.3	6.5	6.7
0.0135	3.7	5.6	5.9	5.3	5 7
0.01	3.8	5.8	6.0	5.1	5.4
0.0075	3.6	5.0	5.1	4.6	5.1
0.005	3.9	6.1	6.2	5.4	5.7
0.004	3.6	5.5	5.3	4.7	5.1
0.003	3.1	5.2	4.8	4.6	4.7
0.002	3.1	5.3	4.9	4.8	4.7
0.001	2.7	4.4	3.8	4.3	3.9
0.0005	2.8	4.4	-	-	-
Black Current	0.2	0.2/0.2	0.2	0.2	0.2

Note: As maximum dispersion does not exceed 0.015 wt% standard, all standards above this previously used shall be discarded. This permits the scale to be increased as shown below.

Table D 2: Calibration Data

980V 10^{-7} amps ●45° Black Current: 0.20mV
10mV 4 cm/min

Standard (%)	Reading (mV)
DDW	4.1
0.0001	4.3
0.0005	4.2
0.001	4.4
0.002	5.5
0.003	5.5
0.004	6.0
0.005	7.0
0.0075	6.2
0.01	7.1
0.0135	7.0
0.015	9.6

Dispersion Trials

DDW/Bent/DDW ~ 3mm above surface 5.25mV
~ 20mm above surface 6.7mV

Bent/SCSSS/SCSSS ~ 3mm above surface 4.05mV
~ 20mm above surface 5.3mV

The bentonite ir DDW suspensions provided the basis for a calibration between bentonite particle concentration and scattered light intensity.

Particle concentrations of the standards are approximate, however, sufficient information was obtained from the calibration to provide bounds on the level of particle concentration. The standards were subsequently used to normalize dispersion data. Normalization of the dispersion data was required to minimize

the effect of minute positional changes of the optical components of the apparatus.

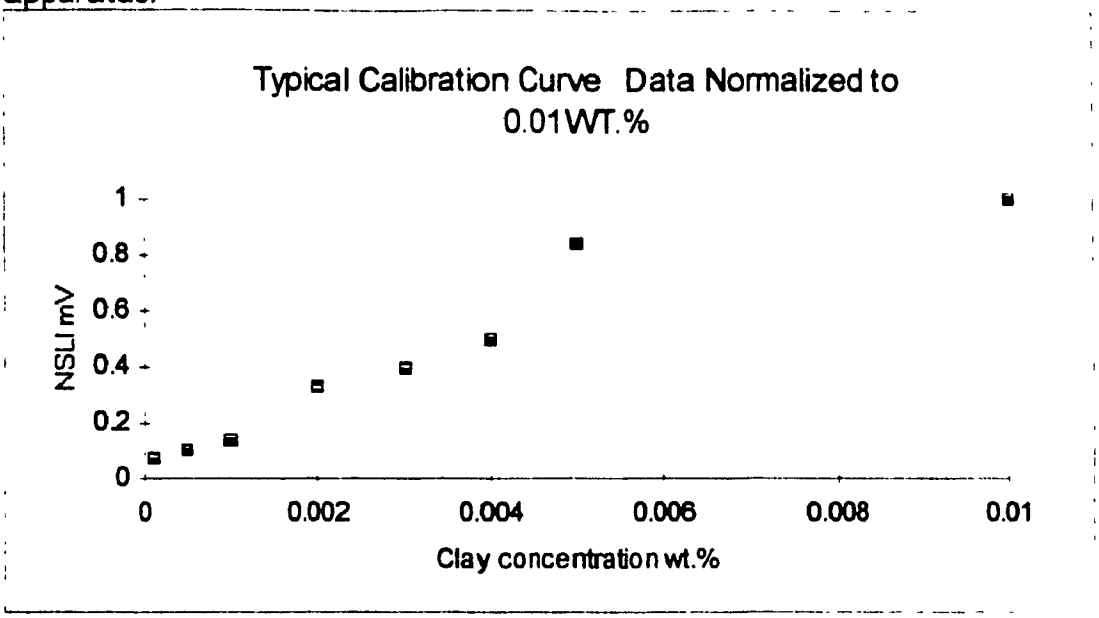

Figure D.1. Typical Calibration Curve.

As an example on calibration of NSLI readings in mV to mg/l is the concentration profiles illustrated in figure 5.5 shown below and also illustrated in chapter 5.

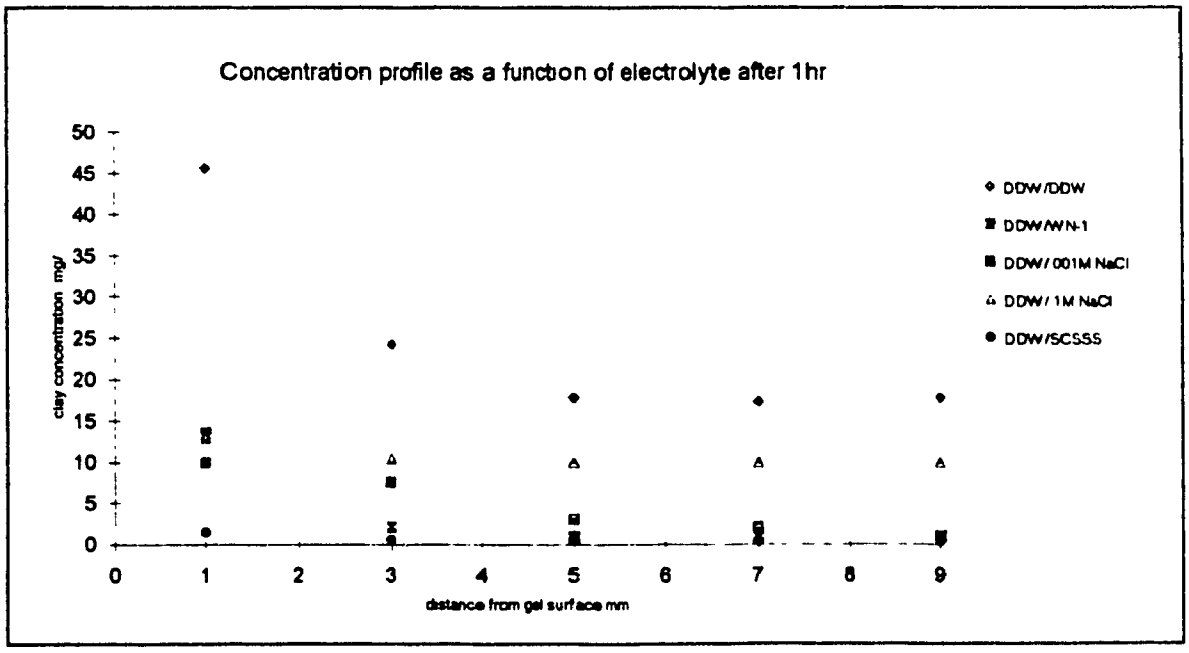

D.2. PROCEDURE FOR OBTAINING DATA IN DIFFUSION TESTS:

1. The electrometer, power supply and laser remain on stand-by at all times to ensure reproducible output. The laser produces a cyclic output if not given sufficient warm-up time and electrometer drift is excessive.

2. A sample is buffed to remove particles from the exterior surface. After agitation of the sample, it is mounted in the support stand. The alignment of the sample cell with the laser beam is checked and adjustments made if necessary.

3. The strip chart recorder is zeroed to the electrometer scale to enable monitoring of the drift. The zero is checked before and after each sample reading.

4. The room light is removed as much as possible prior to sending a voltage to the photomultiplier tube. A black current is then measured.

5. The laser aperture is opened and the light scattered by the sample is collected, amplified and recorded as a signal on the strip chart recorder.

6. To determine the effect of the position of the tube, the laser aperture is closed, the test tube position altered, and the aperture re-opened for a second reading. This is usually repeated several times to obtain an average reading.

D.3 CLAY SUSPENSION CONCENTRATION PROFILES

Figure D.2: Dispersion rate as a function of time and distance DDW/DDW(Disper1)

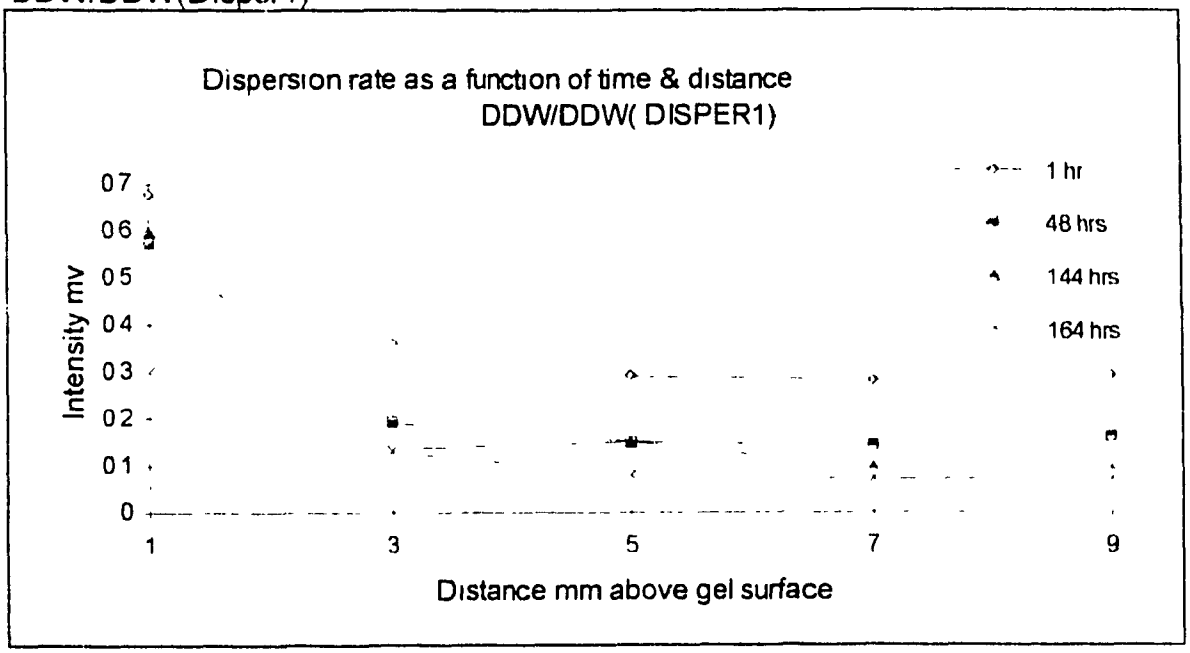

Figure D.3: Dispersion rate as a function of time and distance

DDW/WN-1(Disper2)

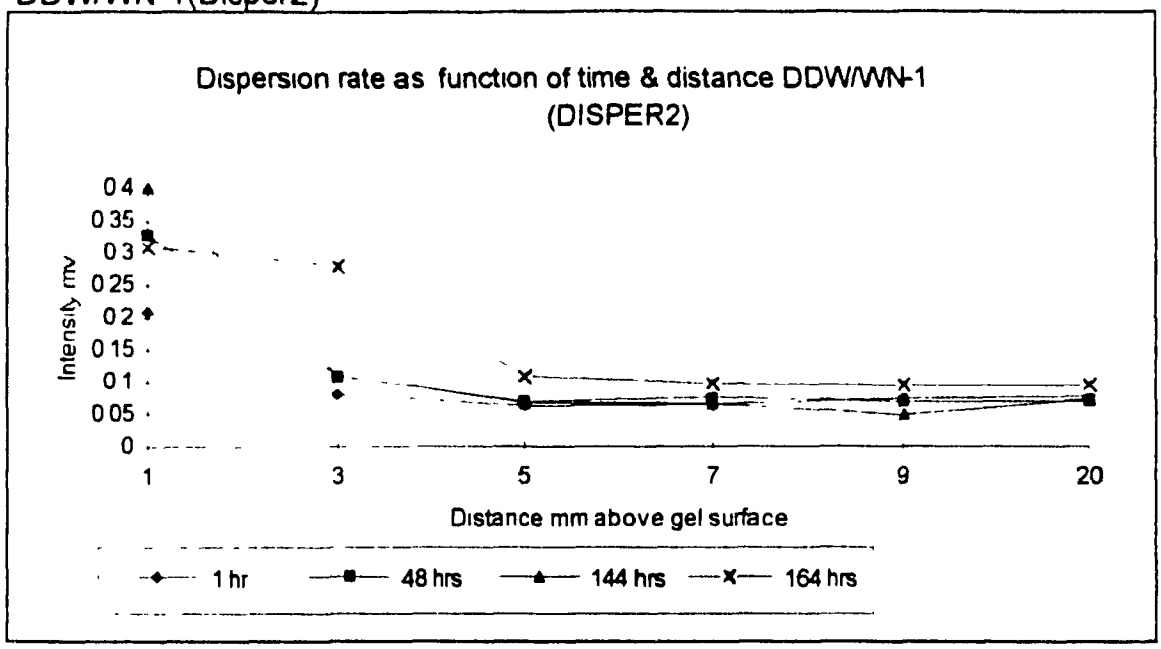

Figure D.4: Dispersion rate as a function of time and distance

DDW/10 E -1 M NaCl (Disper3)

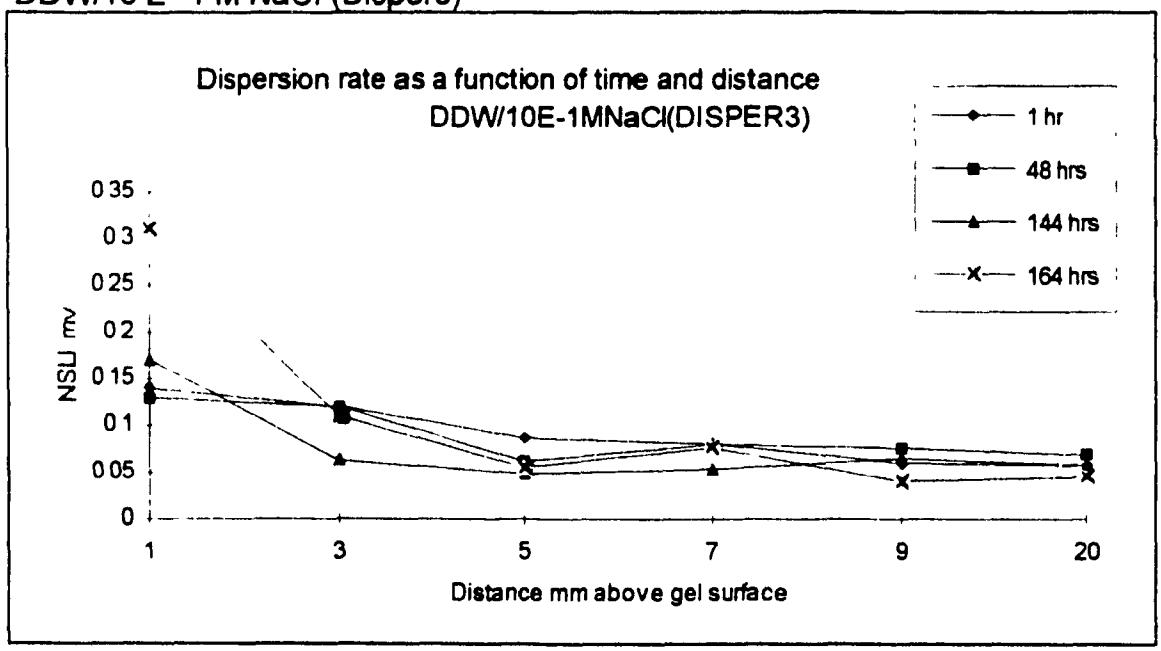

Figure D.5: Dispersion rate as a function of time and distance

DDW/10 E -1 M NaCl (Disper 4)

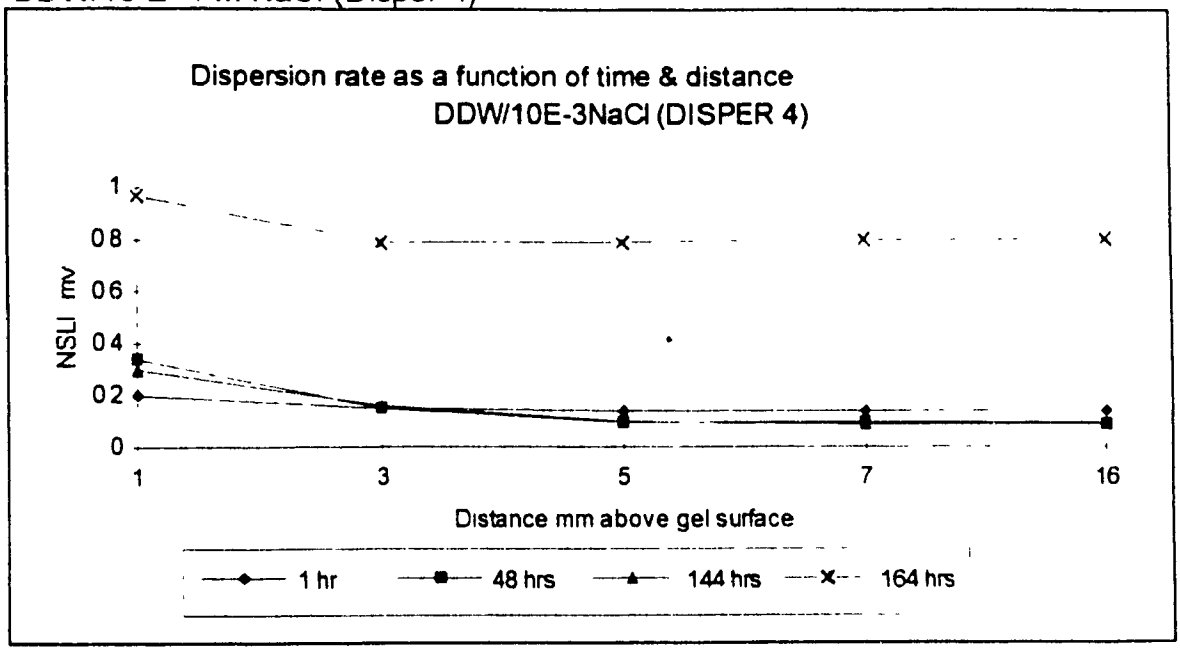

Figure D.6: Dispersion rate as a function of timeand distance

DDW/SCSSS(Disper5)

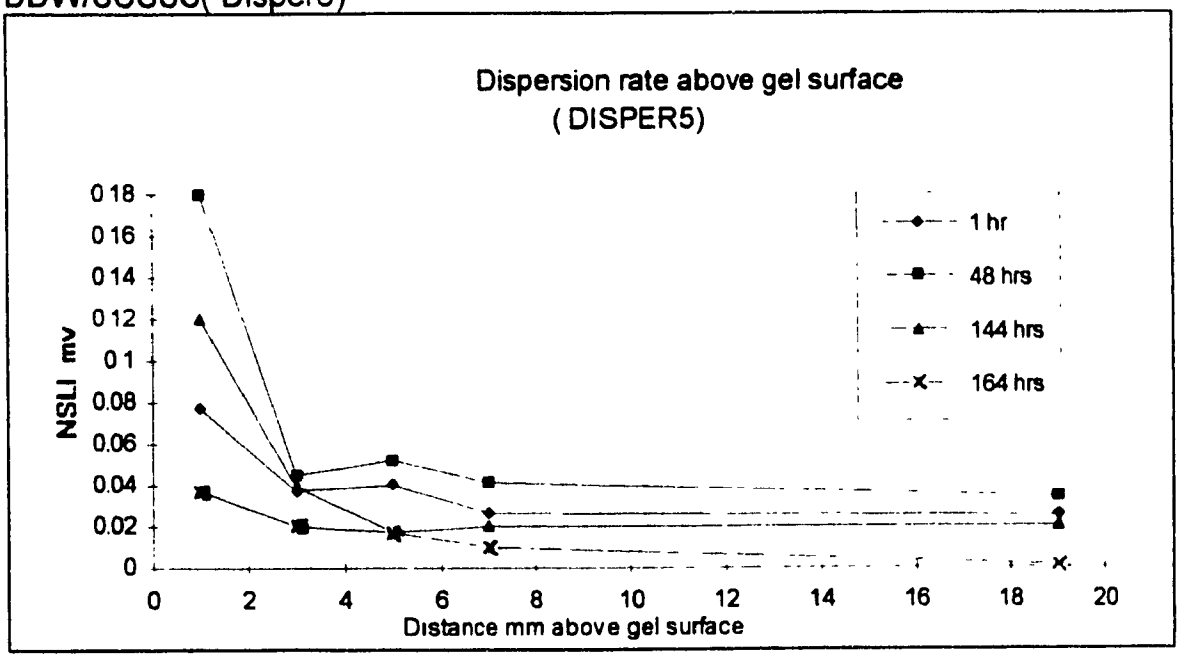

Figure D 7: Dispersion rate as a function of time and distance

DDW/10 E -2 M CaCl2 (Disper6)

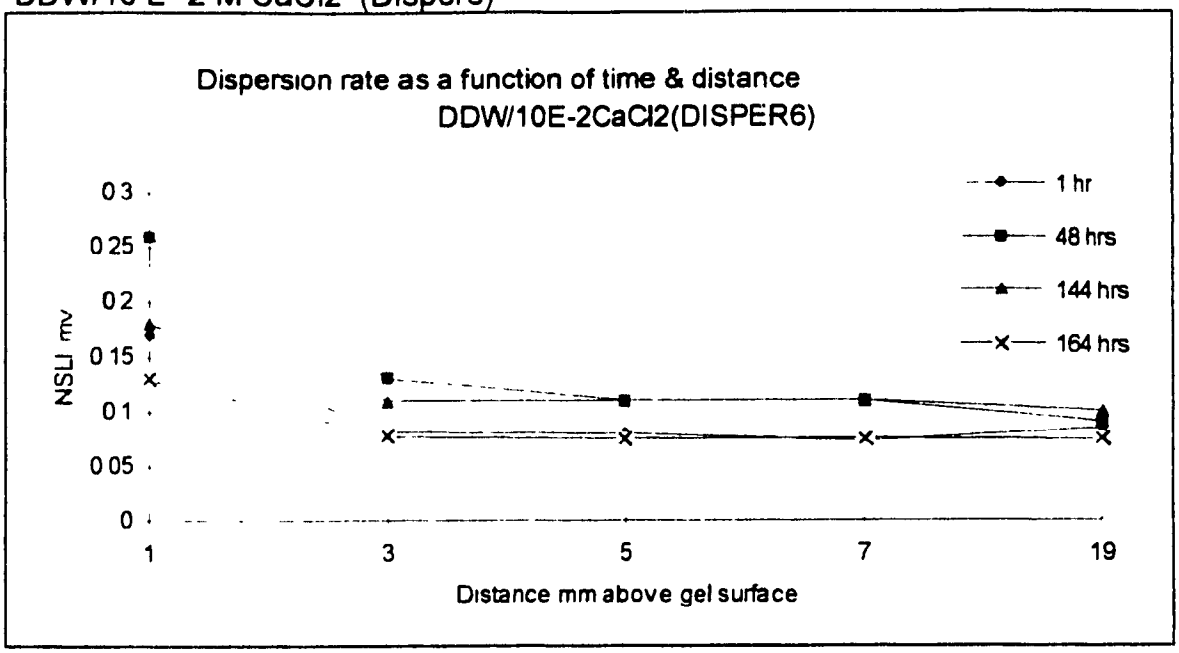

Figure D.8: Dispersion rate as a function of time and distance

SCSSS/SCSSS (Disper7)

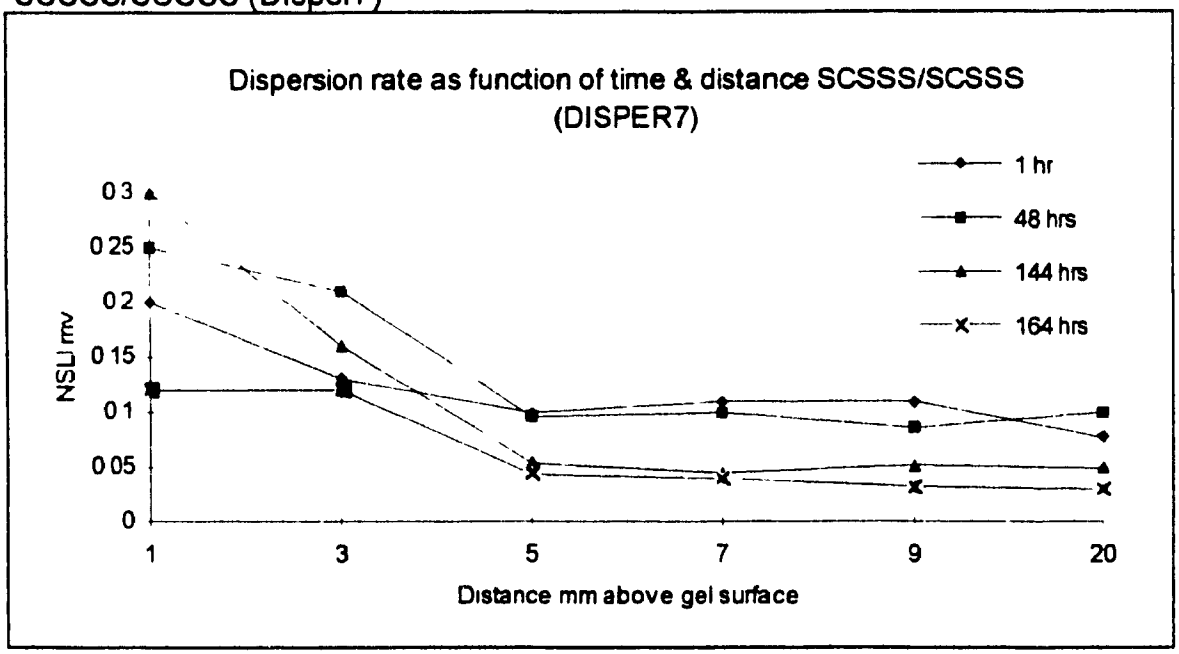

Figure D.9: Dispersion rate as a function of time and distance

SCSSS/DDW (Disper8)

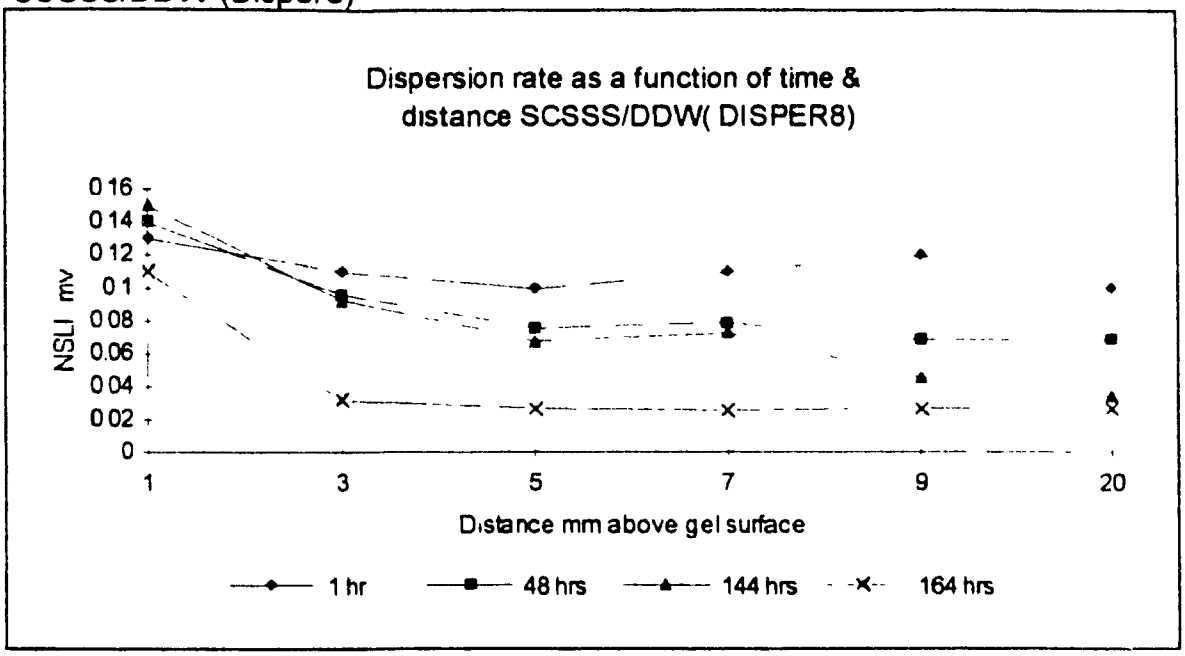

Figure D.10: Dispersion rate as a function of time and distance

WN-1/WN-1(Disper9)

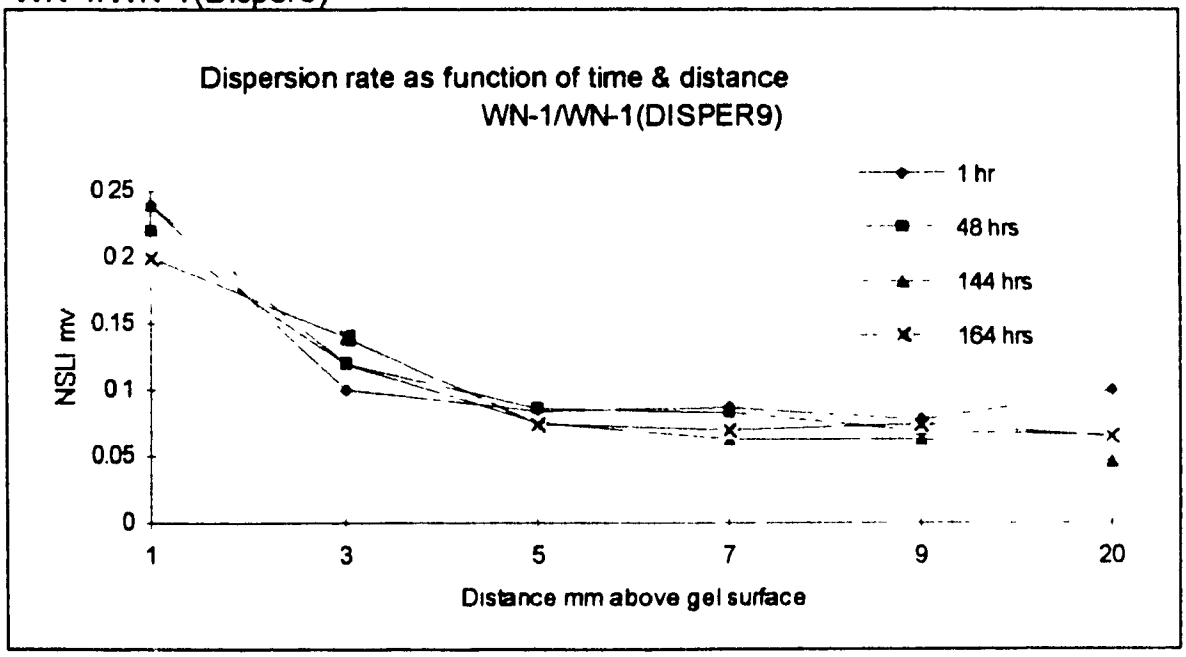

Figure D 11 Dispersion rate as a function of time and distance

WN-1/DDW (Disper10)

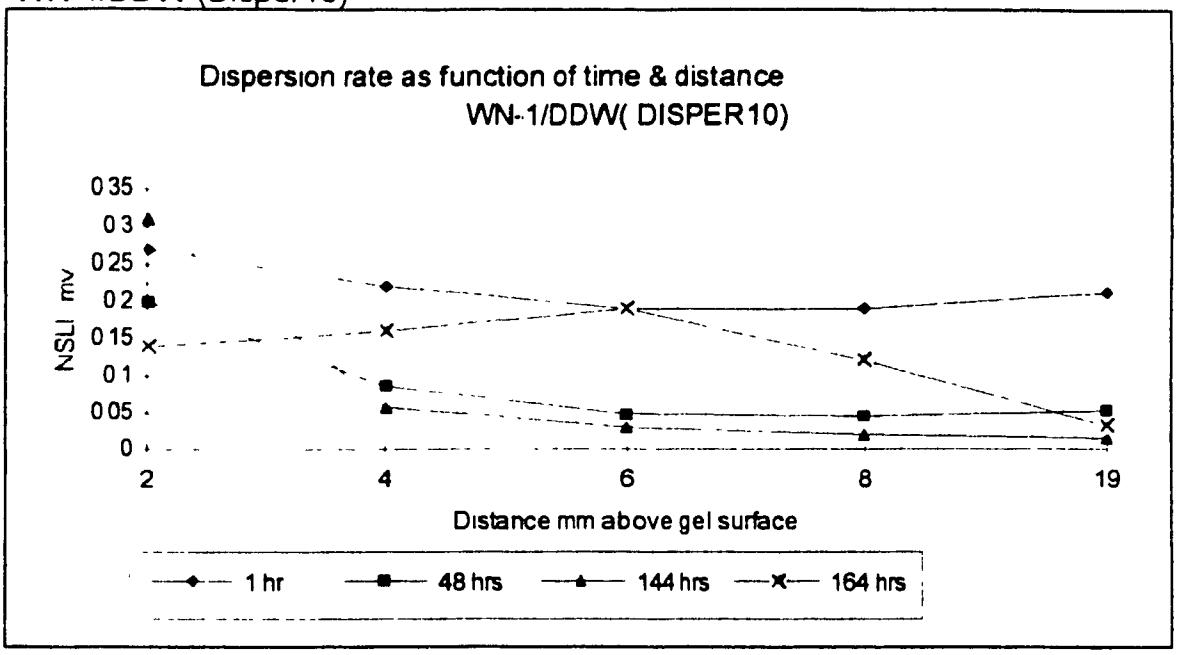

Figure D.12: Dispersion as a function of time and distance DDW/DDW

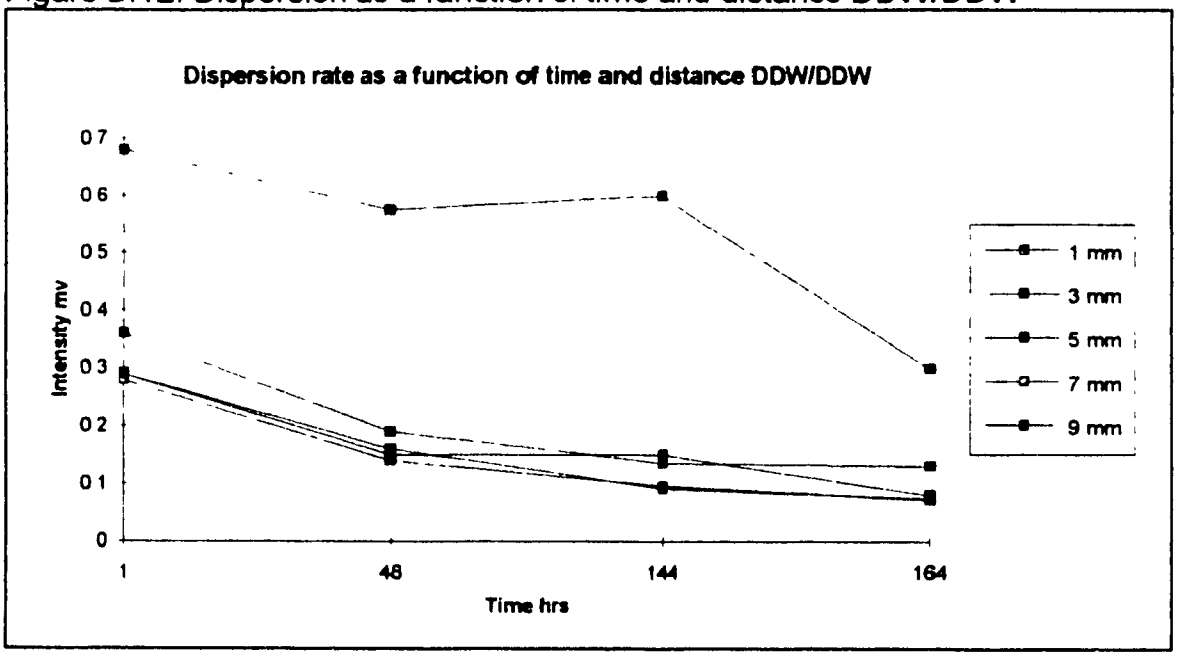

Figure D.13: Dispersion as a function of time and distance DWW-WN-1

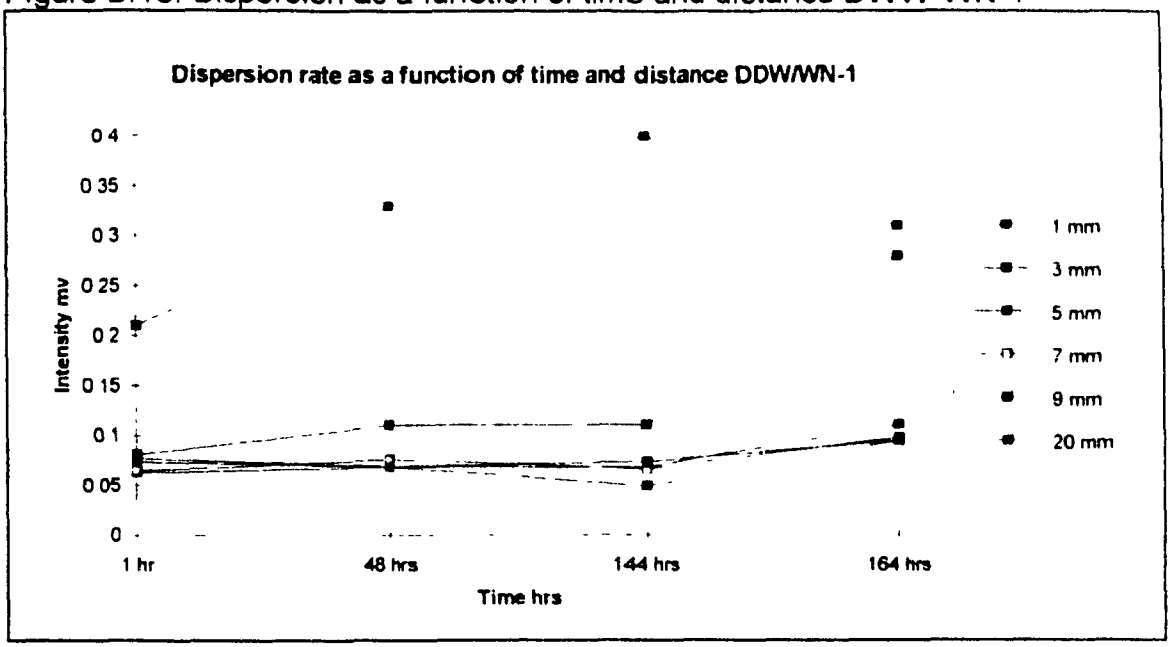

Figure D.14: Dispersion as a function of time and distance DDW/10 E -1 NaCl

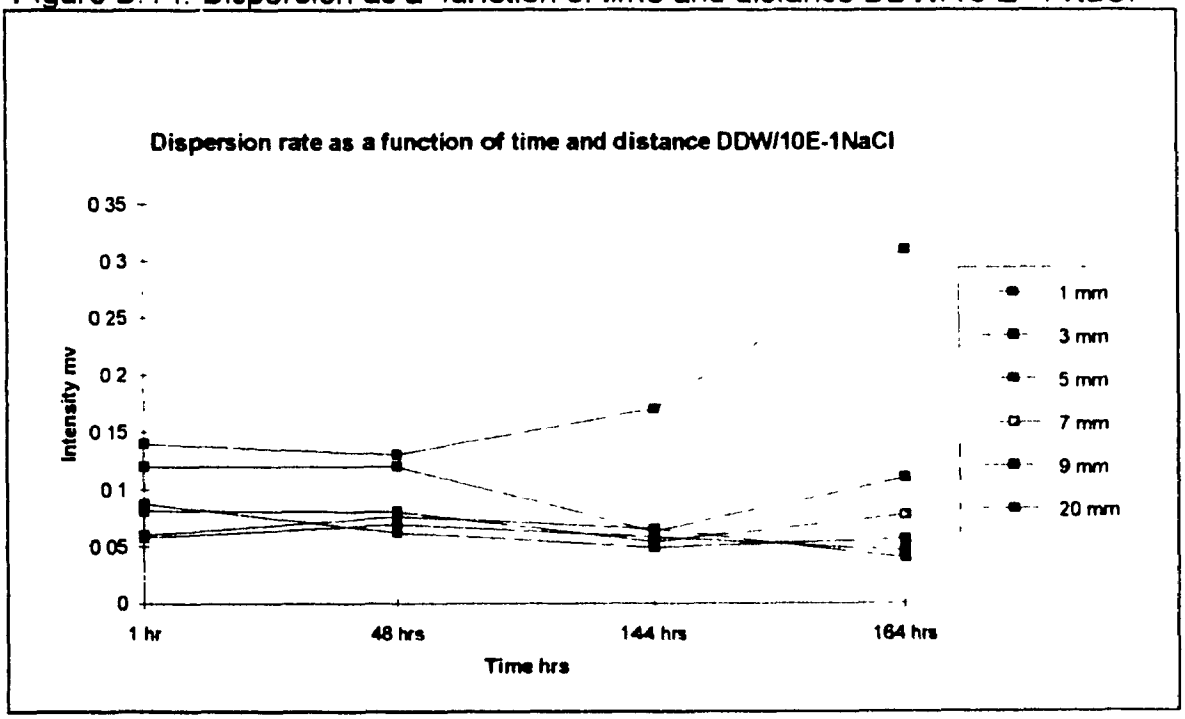

Figure D.15: Dispersion as a function of time and distance DDW/SCSSS

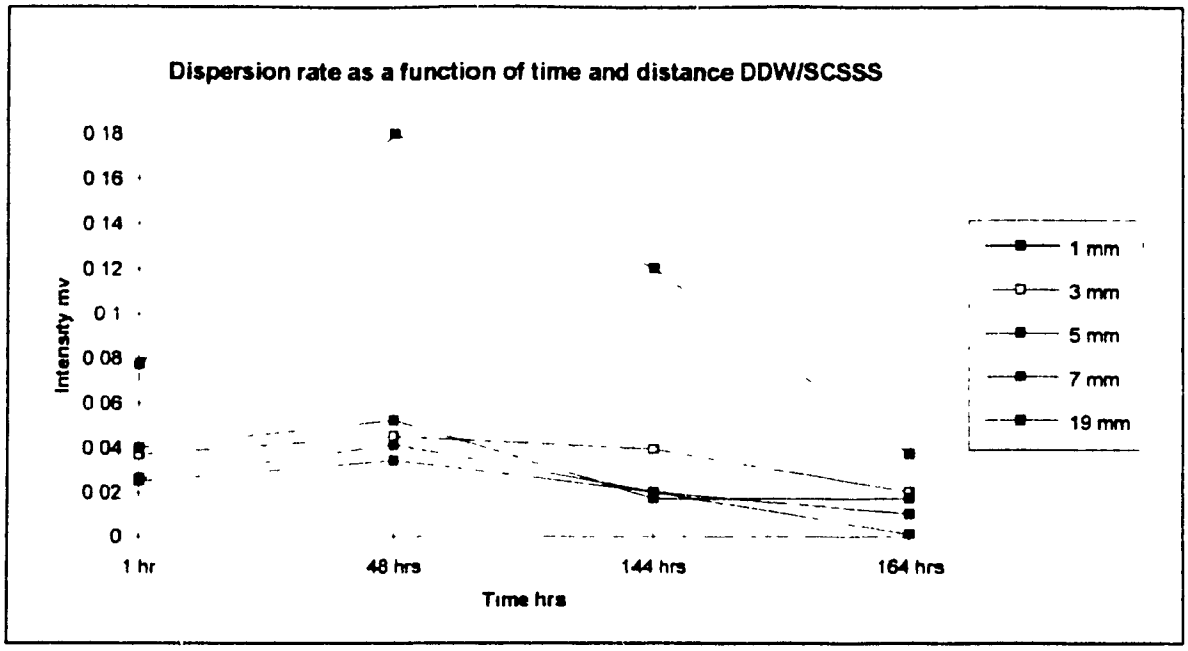

Figure D.16: Dispersion as a function of time and distance DDW/10E-2 M CaCl2

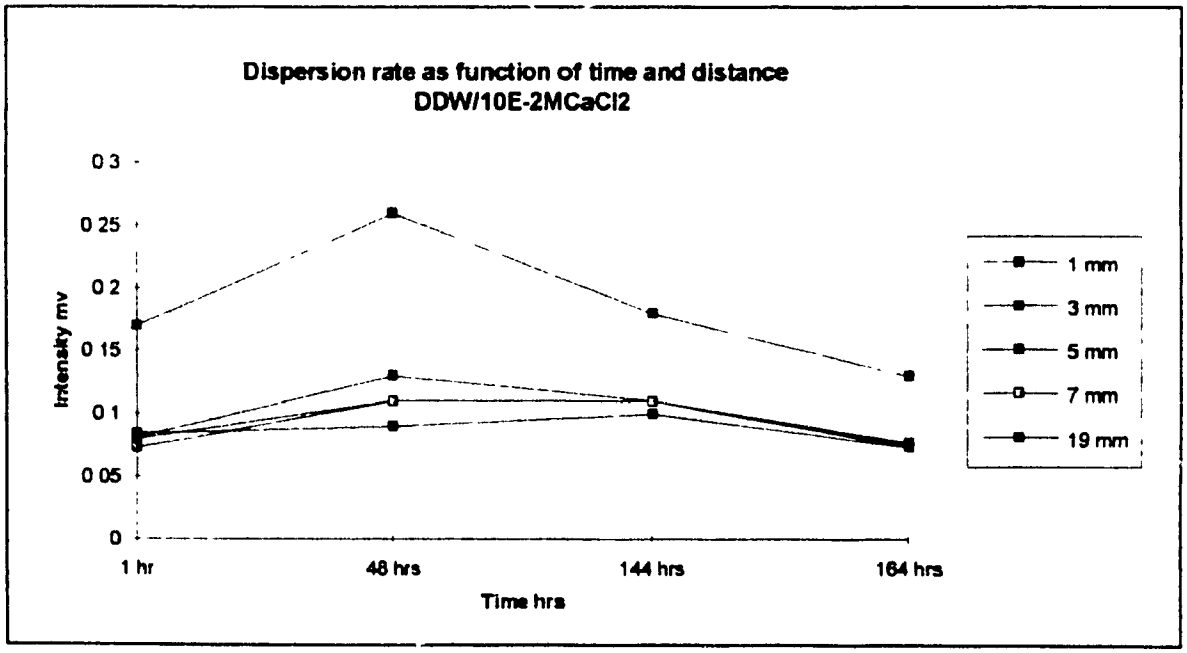

Figure D.17: Dispersion as a function of time and distance SCSSS/SCSSS

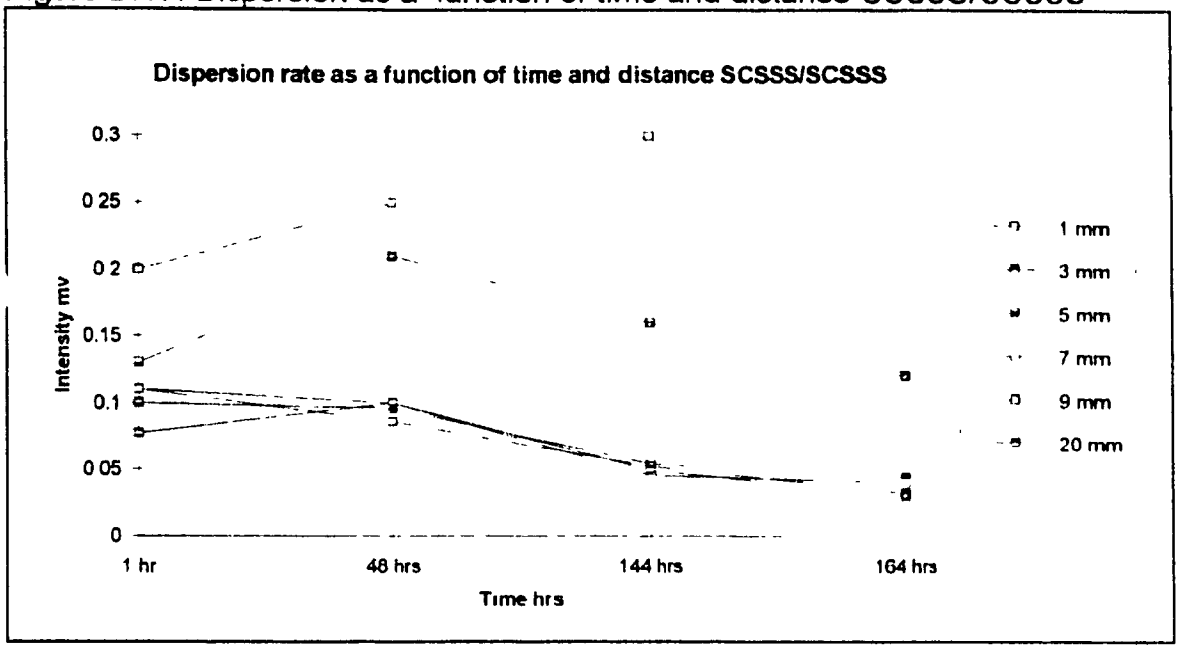

Figure D.18: Dispersion as a function of time and distance SCSSS/DDW

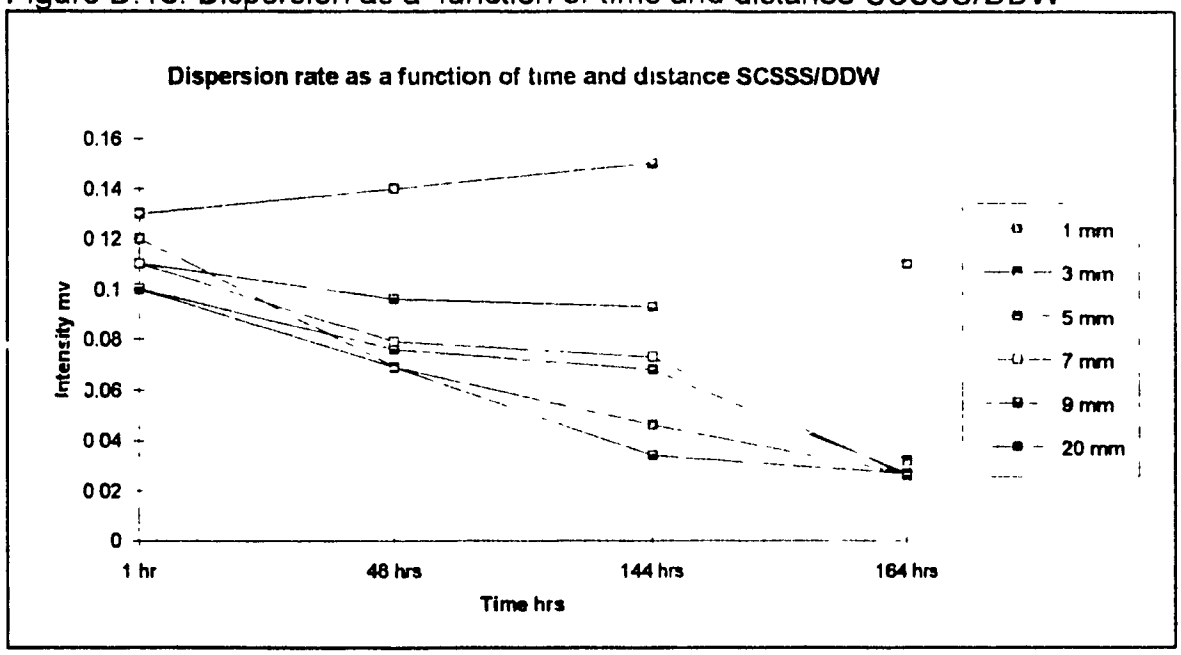

Figure D 19 dispersion as a function of time and distance WN-1/WN-1

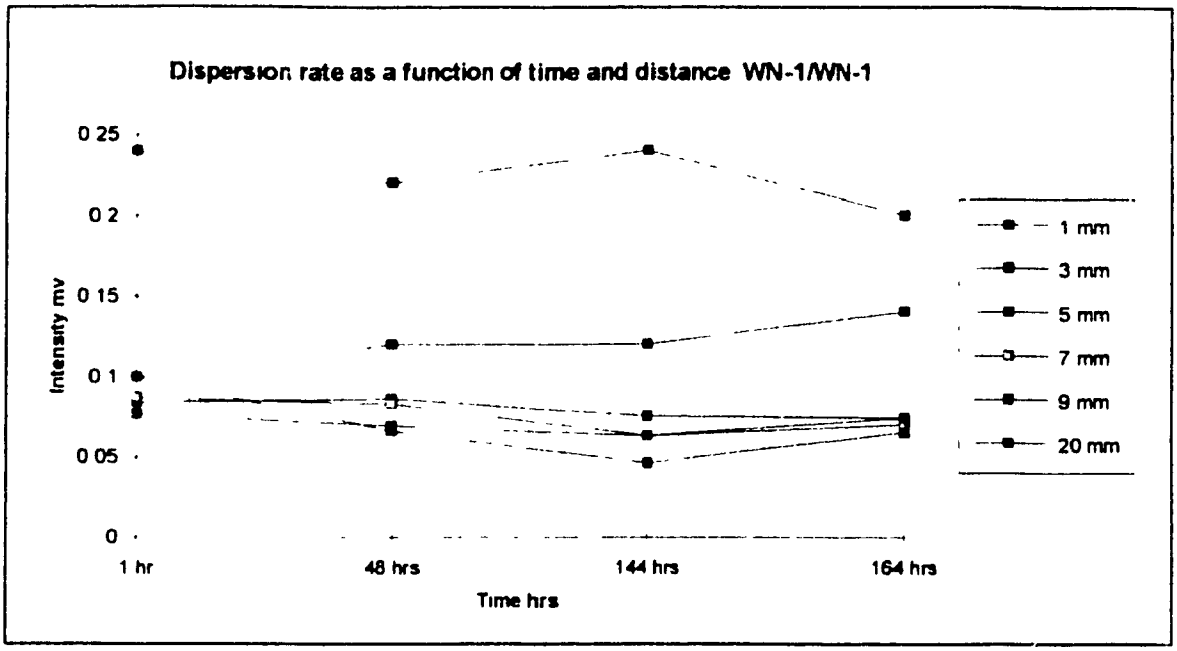

Figure D.20: Dispersion as a function of time and distance WN-1/DDW

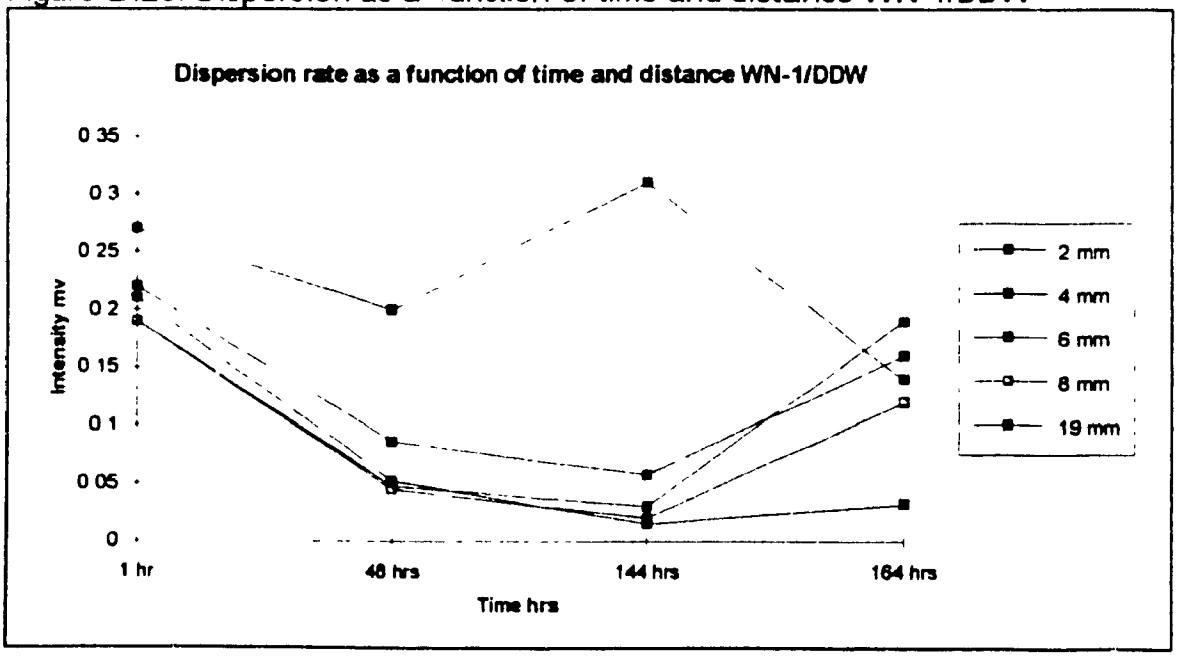

Figure D.21: Dispersion as a function of time and distance DDW/10E-3 M NaCl

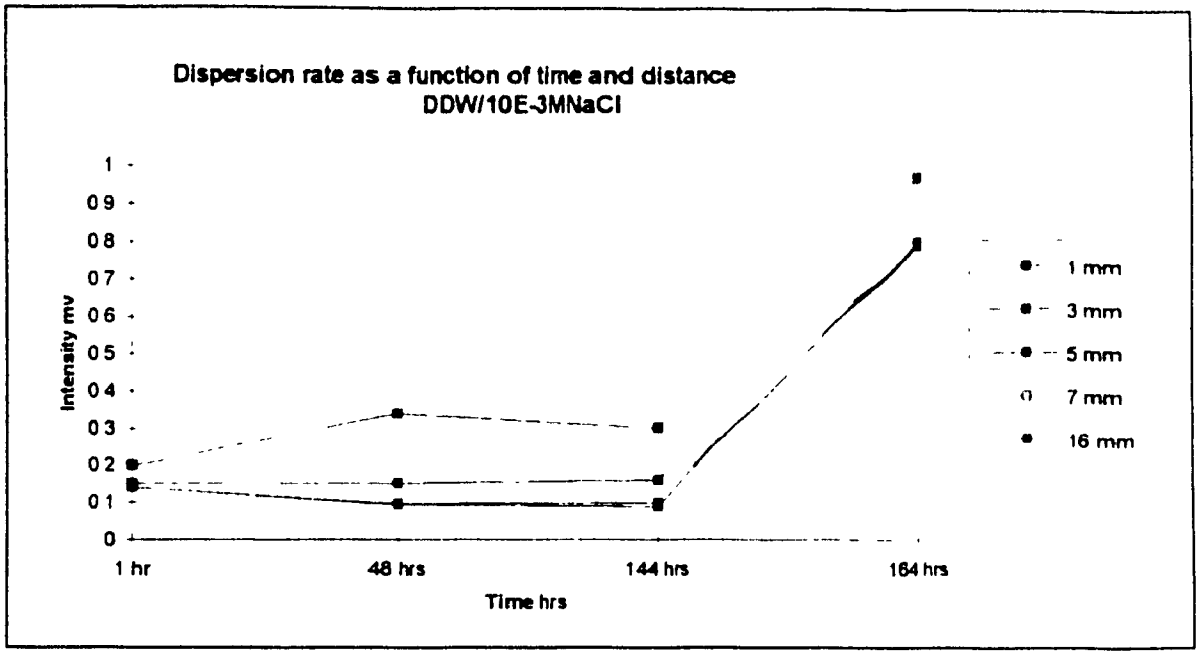

D.4 SUMMARY OF DISPERSION DATA

Dispersion Data as a function of time → and distance ↓

Table D 3 Normalized Scattered Light Intensity (NSLI)

Referenced to swelling surface

1 mm ≡ 1 mm above swollen surfac

DDW/DDW				
Disper1.XLS	1 hr	48 hr	144 hr	164 hr
1 mm.	0.6	0.575	0.60	0.3
3 mm.	0.36	0.19	0.135	0.13 ←
5 mm	0 29	0 15	0.15	0.08
7 mm	0.28	0.14	0.096	0.072
9 mm.	0.29	0.16	0.091	0.074
DDW/WN-1	1 hr	48 hr	144 hr	164 hr
Disper2.XLS 1 mm.	0.21	0.33	0.40	0.31
3 mm.	0.081	0.11	0.11	0.28
5 mm.	0.063	0.069	0.068	0.11
7 mm.	0.065	0.076	0.066	0.097
9 mm	0.074	0.069	0.049	0.094
20 mm	0.077	0.069	0.073	0.094
DDW/10^{-1}MNaCl	1 hr	48 hr	144 h	164 hr
Disper3.XLS 1mm.	0.14	0.13	0.17	0.31
3 mm	0.12	0.12	0.063	0.11
5 mm.	0.087	0.062	0.049	0.056
7 mm.	0.081	0.08	0.054	0.077
9 mm.	0.06	0.076		0.04
20 mm.	0.058	0.069	0 58	0.046

DDW/10^{-3}MNaCl	1 hr	48 hr	144 hr	164 hr
Disper4 XLS				
1 mm.	0.20	0 34	0 30	0 97
3 mm.	0.15 (0 12-0.19)	0.15	0.16 (0.11-0.20)	0 79
5 mm.	0.14 (0 11-0 17)	0 096	0.098 (0.078-0 12)	0.79
7 mm.	0.14 (0.12-0 17)	0.096	0.088 (0.079-0.098)	0.80
16 mm.	0.14 (0.11-0 18)	0.093	0.088 (0.079-0 098)	0 799(18 mn)
DDW/SCSSS	1 hr	48 hr	144 hr	164 hr
Disper5.XLS				
1 mm.	0 077	0.18	0.12	0 037
3 mm.	0 037 (0 02-0 06)	0.045 (0 027-0 048)	0 039 (0 029-0 049)	0 02
5 mm.	0.04 (0.03-0 06)	0.052 (0.044-0.060)	0.017 (0 0097-0 025)	0 017
7 mm.	0.026 (0.0170.037)	0.041 (0.027-0.070)		
19 mm.	0.025 0.016-0.036)	0.034 (0.017-0.053)	0.02 (0.0097-0.029)	0.001
DDW/10^{-2}M$CaCl_2$	1 hr	48 hr	144 hr	164 hr
Disper6.XLS				
1 mm.	0.17	0.26	0.18	0.13
3 mm.	0.081 (0.06-0 11)	0.13 (0.11-0.15)	0.11 (0.097-0.12)	0 077
5 mm.	0.08 (0 05-0 10)	0.11 (0.10-0 13)	0.11 (0 10-0 12)	0 075
7 mm.	0.073 (0.049-0.10)	0.11 (0.10-0.12)		
19 mm.	0.084 (0.063-011)	0.090 (0.081-0.098)	0.10 (0.095-0.11)	0 074 (16 mm)
SCSSS/SCSSS	1 hr	48 hr	144 hr	164 hr
Disper7.XLS				
1 mm.	0.20		0.30	0 12
3 mm.	0.13 (0.095-0.19)	0.21		0.12
5 mm.	0.10 (0.074-0.14)	0.096	0.054 (0.046-0.061)	0.044
7 mm.	0.11 (0.083-0.15)	0.10	0.045 (0.029-0 064)	
9 mm.	0.11 (0.06-0.17)	0.086	0.052 (0.032-0.093	0.032
20 mm.	0.077 (0.057-0.10	0.10	0.049 (0.022-0.076	0.030

SCSSS/DDW	1 hr	48 hr	144 hr	164 hr
Disper8 XLS				
1 mm.	0.13	0.14	0 15	0.11
3 mm.	0 11 (0.08-0 14)	0 096 (0.078-0 12)	0.093 (0.066-0.12)	0.032
5 mm	0.10 (0.086-0 12)	0 076 (0.057-0.095)	0.068 (0.47-0 090)	0.027
7 mm.	0.11 (0.088-0.13)	0.079 0.068-0.092)	0.073 (0.032-0.12)	0.026
9 mm.	0 12 (0.097-0.14)	0.069 (0.037-0.10)	0.046 (0.032-0.054)	0.027
20 mm	0.10 (0 086-0.12)	0.069 (0.054-0.084)	0.034 (0.017-0.051)	0.027
WN-1/WN-1	1 hr	48 hr	144 hr	164 hr
Disper9.XLS				
1 mm	0.24	0.22	0.24	0.20
3 mm.	0.10 (0.071-0.13)	0.12 (0.088-0.15)	0.12 (0.11-0.13)	0.14
5 mm.	0.084 (0.062-0.11)	0.086 (0.064-0.11)	0.075 (0.053-0.096)	0.074
7 mm.	0.087 (0.068-0.11)	0.083 (0.068--0.093)	0.063 (0.053-0.073)	0.070
9 mm.	0.077 (0.06-0 1)	0.069 (0.057-0.081)	0.063 (0.044-0.083)	0.074
20 mm	0.10 (0.076-0.14)	0.066 0.051-0.081	0.046 0.036-0.056)	0.065
WN-1/DDW	1 hr	48 hr	144 hr	164 hr
Disper10.XLS				
2 mm	0.27	0.20	0.31	1.14
4 mm.	0.22 (0.17-0.27)	0.086 (0.078-0.095)	0.058 (0.041-0.076)	0.55
6 mm.	0.19 (0.15-0.24)	0.048 (0.04-0.056)	0.03 (0.015-0.039)	0.19
8 mm.	0.19 (0.15-0.24)	0.045 (0.037-0.053	0.02 (0.01-0.03)	0.12
10 mm.				
19 mm.	0.21 (0.17-0.25)	0.052 (0.044-0.060)	0.015 (0.01-0.02)	0.032

TABLES D.4 Scattered light intinsity readings normalized to 0.01 wt.%
Normalized Data **Normalized to 0.01 wt. %** 15.5 ± 2 1/2
Time – 1 hrs. 10^{-8} amps. 1330V 13.5-17.5

Sample						
DDW/DDW	1 mm	3 mm.	5 mm.	7 mm.	9 mm.	20 mm
50 mV	0 61					
	0.50-0.74					
20 mV	0.76	0.36	0.30			
	0.54-1.0	0.26-0.50	0 25-0.38			
10 mV			0.28	0.28	0.29	0.29
			0.23-0.34	0.22-0.36	0.24-0.35	0.24-0.35
	Avg 0.68		Avg 0.29			
	0.50-1.0		0.23-0.38			
DDW-WN-1	1 mm.	3 mm.	5 mm.	7 mm.	9 mm.	20 mm.
10 mV	0.21	0.081	0.063	0.065	0.074	0.077
10 mV	0.16-0.27	0.057-0.11	0.051-0.096	0.046-0.089	0.048-0.11	0.057-0.10
DDW/SCSSS	2 mm.	4 mm.	6 mm.	8 mm.	10 mm.	21 mm.
10 mV	0.077					
	0.057-0.10					
5 mV		0.037	0.04	0.026	0.025	
		0.02-0.06	0.03-0.06	0.017-0.037	0.016-0.036	
DDW/10^{-2}M$CaCl_2$	1 mm.	3 mm.	5 mm.	7 mm.	9 mm.	20 mm.
10 mV	0.17	0.081	0.074			
	0.14-0.20	0.06-0.11	0.057-0.096			
5 mV			0.077	0.073	0.084	
			0.057-0.10	0.049-0.10	0.063-0.11	
			Avg 0.0755			
			0.057-0.10			

Normalized Data (Normalized to 0.01 wt. % Standard) cont. 2/2

Time 1hr 15.5±2 13.5-12.5

$DDW/10^{-3}MCaCl_2$	1 mm.	3 mm.	5 mm.	7 mm.	9 mm.	15 mm.
10 mV		0.27	0.12	0.13		0.13
$DDW/10^{-1}MNaCl$	1 mm.	3 mm	5 mm.	7 mm.	9 mm.	20 mm.
10 mV	0.14	0.12	0.087	0.081	0.06	0.058
	(0.11-0.18)	(0.083-0.16)	(0.05-0.14)	(0.051-0.12)	(0.043-0.085)	(0.043-0.078)
$DDW/10^{-3}MNaCl$	2 mm.	4 mm.	6 mm.	8 mm.	10 mm.	21 mm.
10 mV	0.2	0.15	0.14	0.14	0.14	0.14
	(0.16-0.25)	(0.12-0.19)	(0.11-0.17)	(0.12-0.17)	(0.11-0.18)	(0.11-0.18)
SCSSS/SCSSS	1 mm.	3 mm.	5 mm.	7 mm.	9 mm.	20 mm.
10 mV	0.20	0.13	0.10	0.11	0.11	0.077
	(0.15-0.25)	(0.095-0.19)	(0.074-0.14)	(0.083-0.15)	(0.06-0.17)	(0.057-0.10)
SCSSS/DDW	1 mm.	3 mm.	5 mm.	7 mm.	9 mm.	20 mm.
10 mV	0.13	0.11	0.10	0.11	0.12	0.10
	(0.10-0.17)	(0.08-0.14)	(0.086-0.12)	(0.088-0.13)	(0.097-0.14)	(0.086-0.12)
WN-1/WN-1	1 mm.	3 mm.	5 mm.	7 mm.	9 mm.	20 mm.
10 mV	0.24	0.10	0.084	0.087	0.077	0.10
	(0.21-0.29)	(0.071-0.13)	(0.062-0.11)	(0.068-0.11)	(0.06-0.1)	(0.076-0 14)
WN-1/DDW	2 mm.	4 mm.	6 mm.	8 mm.	10 mm.	19 mm.
10 mV	0.27	0.22	0.19	0.19		0.21
	(0.21-0.36)	(0.17-0.27)	(0.15-0.24)	(0.15-0.24)		(0.17-0.25)

Dispersion Data
Time ~ 1 hr.
1330V, 10^{-8} amp. unless otherwise indicated

Sample						
DDW/DDW	1 mm.	3 mm.	5 mm.	7 mm.	9 mm.	20 mm.
50 mV	9.4±0.55					
20 mV	11.82±2.4	5.6±1.1	4.7±0.4			
10 mV			4.3±0.25	4.35±0.55	4.5±0.30	4.5±0.30
DDW/WN-1	1 mm.	3 mm.	5 mm.	7 mm.	9 mm.	20 mm.
10 mV	3.2±0.40	1.25±0.25	1.1±0.20	1.0±0.20	1.15±0.30	1.2±0.20
DDW/SCSSS	2 mm.	4 mm.	6 mm.	8 mm.	10 mm.	21 mm.
10 mV	1.2±0.20					
5 mV		0.575±0.23	0.675±0.125	0.4±0.1	0.39±0.1	
DDW/10^{-2}MCaCl$_2$	1 mm.	3 mm.	5 mm.	7 mm.	9 mm.	20 mm.
10 mV	2.6±0.15	1.25±0.2	1.15±0.15			
5 mV			1.2±0.2	1.13± 0.275	1.3±0.2	
DDW/10^{-3}MCaCl$_2$	1 mm.	3 mm.	5 mm.	7 mm.	9 mm.	15 mm.
10 mV		4.15±0.25	1.9±0.2	2.0±0.2		2.0±0.2

Dispersion Data cont.2/2

Time 1 hr

DDW/10^{-1}MNaCl	1 mm.	3 mm.	5 mm.	7 mm.	9 mm.	20 mm.
10 mV	2.2±0.25	1.8±0.35	1.35±0.50	1.25±0.35	0.95±0.2	0.9±0.15
DDW/10^{-3}MNaCl	2 mm.	4 mm.	6 mm.	8 mm.	10 mm.	21 mm.
10 mV	3.1±0.25	2.35±0.5	2.15±0.2	2.15±0.1	2.2±0.2	2.2±0.2
SCSSS/SCSSS	1 mm.	3 mm.	5 mm.	7 mm.	9 mm.	20 mm.
10 mV	3.05±0.35	2.0±0.50	1.6±0.3	1.75±0.3	1.65±0.6	1.2±0.20
SCSSS/DDW	1 mm.	3 mm.	5 mm.	7 mm.	9 mm.	20 mm.
10 mV	2.05±0.25	1.65±0.25	1.6±0.1	1.6±0.1	1.8±0.1	1.6±0.1
*						
WN-1/DDW	2 mm.	4 mm.	6 mm.	8 mm.	10 mm.	21 mm.
10 mV	4.25±0.57	3.35±0.35	2.95±0.25	3.0±0.3		3.2±0.2
*						
WN-1/WN-1	1 mm.	3 mm.	5 mm.	7 mm.	9 mm.	20 mm.
10 mV	3.8±0.17	1.5±0.25	1.3±0.22	1.35±1.5	1.2±1.5	1.6±0.27

Normalized data to DDW 0 25±0.1 0.15±0.35 **TIME 1 hr**

DDW/DDW	1 mm	3 mm	5 mm	7 mm.	9 mm.	20 mm.
50 mV	37.6					
	25.3-66.3					
20 mV	47 28	22.4	18.8			
	26.9-94.8	12.8-44.7	12.3-34			
10 mV			17.2	17.4	18.0	18.0
			11.6-30.3	10 9-32.7	12.0-32.0	12.0-32
DDW/WN-1	1 mm.	3 mm.	5 mm.	7 mm.	9 mm.	20 mm.
10 mV	12.8	5 0	4.4	4 0	4.6	4.8
	8.0-24.0	2.9-10	2.6-8.7	2.3-8.0	2.4-9.7	2.9-9.3
DDW/SCSSS	2 mm.	4 mm	6 mm.	8 mm.	10 mm.	21 mm.
10 mV	4.8					
	2.9-9.3					
5 mV		2.3	2.5	1.6	1.56	
		0.99-5.4	1.4-5.0	0.86-3.3	0.83-3.3	
DDW/10^{-2}MCaCl$_2$	1 mm.	3 mm.	5 mm.	7 mm.	9 mm.	20 mm.
10 mV	10.4	5.0	4.6			
	7.0-18.3	3.0-9.7	2.9-8.7			
5 mV			4.8	4.52	5.2	
			2.9-9.3	2.4-9.4	3.1-1.00	

Normalized data to DDW (2) **TIME 1 hr** cont. 2/2

DDW/10^{-3}MCaCl$_2$	1 mm.	3 mm.	5 mm.	7 mm.	9 mm.	20 mm.
10 mV		16.6	7.6	8.0		8.0
		15.6-29.3	4.9-14.0	5.1-14.7		5.1-14.7
DDW/10^{-1}MNaCl	1 mm.	3 mm.	5 mm.	7 mm.	9 mm.	20 mm.
10 mV	8.8	7.2	5.4	5.0	3.8	3.6
	5.6-16.3	4.1-14.3	2.4-12.3	2.6-10.7	2.1-14.0	2.1-7.0
DDW/10^{-3}MNaCl	2 mm.	4 mm.	6 mm.	8 mm.	10 mm.	21 mm.
10 mV	12.4	9.4	8.6	8.6	8.8	8.8
	8.1-22.3	6.1-10.2	5.6-15.7	5.9-15.0	3.1-16.0	3.1-16.0
SCSSS/SCSSS	1 mm.	3 mm.	5 mm.	7 mm.	9 mm.	20 mm.
10 mV	12.2	8.0	6.4	7.0	6.6	4.0
	7.7-22.7	4.3-16.7	3.7-12.7	4.1-13.7	3.0-15.0	2.9-9.3
SCSSS/DDW	1 mm.	3 mm.	5 mm.	7 mm.	9 mm	20 mm.
10 mV	8.2	6.6	6.4	6.6	7.2	6.4
	5.1-15.3	4.1-12.7	4.3-11.3	4.4-11.7	4.9-12.7	4.3-11.3
WN-1/DDW	2 mm.	4 mm	6 mm.	8 mm.	10 mm.	21 mm.
10 mV	14.2	11.2	9.8	10.0		10.7
	9.2-24.1	7.5-18.5	6.75-16.0	6 8-16.5		7.5-17.0
WN-1/WN-1	1 mm.	3 mm	5 mm.	7 mm.	9 mm.	20 mm.
10 mV	12.7	5.0	4.3	4.5	4.0	5.3
	9.1-19.8	3.1-8.8	2 7-7.6	3.0-7.5	2.6-6.75	3.3-9.35

Dispersion Data

Time – 48 hrs. **Normalized to 0.01 wt. %** 14.2-14.8

i e , 14.5±0 3

Sample						
DDW/DDW	1 mm.	3 mm.	5 mm.	7 mm.	9 mm.	20 mm
50 mV		0.54	0 16			
		0.52-0.57	0.13-0.19			
20 mV		0.61	0.21	0 15	0.14	0.16
		0.57-0.65	0.19-0 24	0.14-0.16	0.11-0.16	0.14-0.17
		Avg 0.57	Avg 0.19			
		0.52-0.65	0.13-0.24			
DDW/WN-1	1 mm.	3 mm.	5 mm.	7 mm.	9 mm.	20 mm.
20 mV		0.10				
		0.081-0.13				
10 mV	0.33	0.12	0.069	0.076	0.069	0.069
	0.32-0.36	0.11-0.13	0.061-0.077	0.068-0.084	0.057-0.081	0.051-0.088
DDN/SCSSS	2 mm.	4 mm.	6 mm.	8 mm.	10 mm.	21 mm.
10 mV		0.18	0.045	0.052	0.041	0.034
		0.15-0.20	0.027-0.048	0.044-0.060	0.027-0.070	0.017-0.053
DDW/10^{-2}M $CaCl_2$	1 mm.	3 mm.	5 mm.	7 mm.	9 mm.	20 mm.
10 mV		0.26	0.13	0.11	0.11	0.090
		0.25-0.28	0.11-0.15	0.10-0.13	0.10-0.12	0.081-0.098

Normalized to 0.01 wt.% CONT. 2/2
Time 48 hr.

Sample						
DDW/10^{-3}MCaCl$_2$	1 mm.	3 mm.	5 mm.	7 mm.	9 mm.	20 mm.
10 mV						
5 mV						
DDW/10^{-1}MNaCl	1 mm.	3 mm.	5 mm.	7 mm.	9 mm.	20 mm.
10 mV	0.13	0.12	0.062	0.080	0.076	0.069
	0.11-0.15	0.10-0.13	0.047-0.077	0.047-0.11	0.068-0.084	0.057-0.081
DDW/10^{-3}MNaCl	2 mm.	4 mm.	6 mm.	8 mm.	10 mm.	20 mm.
10 mV			0.34	0.15	0.096	0.093
SCSSS/SCSSS	1 mm.	3 mm.	5 mm.	7 mm.	9 mm.	20 mm.
10 mV		0.21	0.096	0.10	0.086	0.10
SCSSS/DDW	1 mm.	3 mm.	5 mm.	7 mm	9 mm.	20 mm.
10 mV	0.14	0.096	0.076	0.079	0 069	0.069
	0.10-0.18	0.078-0.12	0.051-0.095	0.068-0.092	0.037-0.10	0.054-0.084
mm. mm../DDW	2 mm.	4 mm.	6 mm.	8 mm	10 mm.	19 mm.
10 mV	0.20	0.086	0.048	0.045		0.052
	0 13-0.26	0.078-0.095	0.040-0 056	0.037-0.053		0.044-0.060
WN-1/WN-1	1 mm.	3 mm.	5 mm	7 mm	9 mm.	20 mm.
10 mV	0.22	0.12	0.086	0.083	0.069	0.066
	0.19-0.26	0.088-0.15	0.064-0.11	0.68-0.098	0.057-0.081	0.051-0.081

Dispersion Data

Time – 48 hrs. 1330V; 10^{-8} amp. unless otherwise indicated

Sample						
DDW/DDW	1 mm.	3 mm.	5 mm.	7 mm.	9 mm.	20 mm.
50 mV	*	7.9±0.2	2.4±0.35			
20 mV		8.9±0.4	+4	2.2±0.12	2.01±0 31	2.29±0.18
10 mV						
5 mV						
DDW/WN-1	1 mm.	3 mm.	5 mm.	7 mm.	9 mm.	20 mm.
50 mV						
20 mV	4.9±0.2	1.75±0.15				
10 mV		1.5±0.3	1 0±0.1	1.1±0.1	1.0±0.15	1.0±0.25
5 mV						
DDW/SCSSS	2 mm.	4 mm.	6 mm.	8 mm.	10 mm.	21 mm.
50 mV						
20 mV						
10 mV		2.55±0.3	0.65±0.25	0.75±0.1	0.6±0.2	0.5±0.25
5 mV						
DDW/10^{-2}MCaCl$_2$	1 mm.	3 mm.	5 mm.	7 mm.	9 mm.	20 mm.
50 mV						
20 mV						
10 mV		3.8±0.15	1.9±0.2	1.65±0.15	1.65±0.1	1.3±0.10
5 mV						

*Swollen – 2 mm. above surface

Dispersion Data CONT. 2/2

Time ~ 48 hrs.

Sample						
DDW/10^{-3}MCaCl$_2$	1 mm.	3 mm.	5 mm	7 mm.	9 mm.	20 mm.
50 mV						
20 mV						
10 mV						
5 mV						
DDW/10^{-3}MNaCl	1 mm.	3 mm.	5 mm.	7 mm.	9 mm.	20 mm.
10 mV	1.9±0.25	1.7±0.15	0.9±0 2	1.15±0 45	1 1±0.1	1 0±0.15
DDW/10^{-3}MNaCl	2 mm.	4 mm.	6 mm.	8 mm	10 mm.	20 mm.
10 mV			4.95±0.10	2.15±0 1	1.4±0 15	1.35±0 15
SCSSS/SCSSS	1 mm.	3 mm.	5 mm.	7 mm	9 mm	20 mm.
10 mV		3.0±0.7	1 4±0 55	1.5±0.15	1 25±0 15	1.5±0.5
SCSSS/DDW	1 mm	3 mm.	5 mm	7 mm	9 mm.	20 mm
10 mV	2.0±0.5	1 4±0.25	1 1±0 25	1.15±0 15	1.0±0 45	1.0±0.2
.... ./DDW	2 mm	4 mm.	6 mm	8 mm	10 mm	19 mm.
10 mV	2 85±0 90	1.25±0 10	0 7±0 1	0 65±0 1		0.75±0 1
WN-1/WN-1	1 mm.	3 mm	5 mm.	7 mm	9 mm	20 mm
10 mV	3 2±0.45	1.7±0 40	1 25±0.30	1 2±0 2	1 0±0 15	0 95±0.20

Normalized dispersion data to DDW 0 2±0 1

TIME 48 hr 1/3

Sample						
DDW/DDW	1 mm	3 mm.	5 mm	7 mm	9 mm	20 mm
50 mV		39 5	16 2			
		25.7-81 0	7.5-42 5			
20 mV		44.5	15 5	11 0	10 05	11.45
		28.3-93.0	9 3-34 0	6 9-23.2	6 0-23.2	7 0-24 7
10 mV						
		Avg 42.0	15 8			
5 mV		25.7-93.0	7.5-42.5			
DDW/WN-1	1 mm	3 mm	5 mm.	7 mm	9 mm	20 mm
50 mV						
20 mV		8.75				
		3.1-19.0				
10 mV	7.5	4.0	5 0	5 5	5 0	5 0
	4.0-18.0	2.0-10.0	3 0-11.0	3.3-12.0	3 5-13.5	2.5-12.5
5 mV						
DDW/SCSSS	2 mm.	4 mm	6 mm.	8 mm	10 mm.	21 mm
mm. mm. mV		12.75	3.25	3.75	3.0	2 5
		7.5-28.5	1.3-9.0	2.2-8.5	1 3-8.0	0.83-7.5

Normalized data to DDW time 48hr 2/3

Sample						
DDW/10^{-2}MCaCl$_2$	1 mm.	3 mm	5 mm.	7 mm.	9 mm.	20 mm.
10 mV		19.0	9.5	8.25	8.25	6 5
		12.2-39.5	5 7-21.0	5.0-18.0	5.2-17 5	4.0-14.0
DDW/10^{-3}MCaCl$_2$						
50 mV						
20 mV						
10 mV						
5 mV						
DDW/10^{-1}MNaCl	1 mm.	3 mm	5 mm	7 mm.	9 mm.	20 mm.
10 mV	9 5	8.5	4 5	5.75	5.5	5
	5.5-21.5	5.2-18.5	2 3-11 0	2.3-16.0	3 3-12 0	2.8-11.5
DDW/10^{-3}MNaCl	2 mm	4 mm	6 mm.	8 mm.	10 mm	20 mm
10 mV			24 75	10 75	7 0	6.75
			16 2-50.5	1 8-22.5	4 2-15 5	4 0-15 0
SCSSS/SCSSS	1 mm	3 mm	5 mm	7 mm	9 mm	20 mm
10 mV		15.0	7 0	5 75	6 25	7.5
		7 7-37 0	2 8-19.5	4.5-16.5	3 7-14 0	5.0-20.0

Normalized data to DDW TIME 48 hr

SCSSS/DDW	1 mm.	3 mm.	5 mm	7 mm	9 mm	20 mm
10 mV	10.0	7 0	5.5	5 75	5 0	5 0
	5.0-25.0	3 8-16.5	2 8-13 5	3 3-13.0	1.8-14 5	2 7-12.0
WN-1/DDW	2 mm	4 mm.	6 mm	8 mm.	10 mm	19 mm
10 mV	14.25	6.25	3.5	3.25		3 75
	6.5-3.75	3.8-13.5	2.0-8.0	1.8-7 5		2 2-8.5
WN-1/WN-1	1 mm.	3 mm.	5 mm	7 mm.	9 mm.	20 mm.
10 mV	16.0	8.5	6.25	6.0	5.0	4.75
	9.2-36.5	4 3-21.0	3.2-15.5	5.0-14.0	2.8-11.5	2 5-11.5

Normalization of Dispersion Data 1/3

Time ~ 144 hrs.

Normalized to 0.01 wt. % (20.5 ± 0.1) mV

(20.4 - 20.6) mV

Sample						
DDW/DDW	9 mm.	11 mm.	13 mm.	15 mm.	17 mm.	20 mm.
50 mV	0.66	0.134				
	0.62-0.70	0.13-0.14				
20 mV	0.54	0.136	0.15	0.096	0.071	0.089
	0.48-0.60	0.13-0.144	0.14-0.15	0.099-0.10	0.086-0.095	0.084-0.093
	Avg 0.60	0.135				
	0.48-0.70	0.13-0.14				
DDW/WN-1	1 mm.	3 mm.	5 mm.	7 mm.	9 mm.	20 mm.
20 mV	0.40	0.11	0.068			
	0.33-0.46	0.11-0.12	0.056-0.080			
10 mV		0.11	0.068	0.066	0.049	0.073
		0.10-0.12	0.058-0.078	0.053-0.078	0.039-0.059	0.063-0.083
	Avg 0.11	Avg 0.068				
	0.10-0.12	0.56-0.080				
DDW/SCSSS	4 mm.	6 mm.	8 mm.	19 mm.		
10 mV	0.12	0.039	0.017	0.02		
	0.056-0.19	0.029-0.049	0.0097-0.025	0.0097-0.029		
... ... $CaCl_2$	5 mm	7 mm.	9 mm.	20 mm.		
10 mV	0.18	0.11	0.11	0.10		
	0.17-0.19	0.097-0.12	0.10-0.12	0.095-0.11		

Normalized to 0.01 wt. % TIME 14.1 hrs

CONT. 2/3

DDW/10^{-3}MCaCl$_2$	9 mm.	11 mm.	13 mm	15 mm.	19 mm	
20 mV	0.26	0.091	0 064			
	0.24-0.28	0.071-0.11	0.054-0.074			
			0 071	0 063	0.054	
			0 063-0.078	0 048-0.078	0.046-0.061	
			Avg 0.0675			
			0.054-0.078			
DDW/10^{-1}MNaCl	3 mm.	5 mm.	7 mm.	9 mm.	20 mm	
10 mV	0.17	0.063	0.049	0.054	0.058	
	0.14-0.20	0.044-0.083	0.032-0.066	0.037-0.070	0.046-0.071	
DDW/10^{-3}MNaCl	10 mm.	12 mm.	14 mm.	16 mm.	20 mm.	
20 mV	0.30	0.16	0.098	0 088	0.088	
	0.22-0 37	0.11-0.20	0.078-0.12	0.079-0.098	0.079-0.098	
SCSSS/SCSSS	1 mm.	3 mm.	5 mm.	7 mm.	9 mm.	20 mm
20 mV	0.30	0.11				
	0.27-0.34	0.10-0.12				
10 mV			0.054	0.037	0 041	0.049
			0.046-0.061	0.029-0.044	0.032-0.051	0.022-0.076
				0.053	0.063	
				0.044-0.064	0.034-0.093	
				Avg 0.045	0.052	
				0.029-0.064	0.032-0.093	

Normalized to 0.01 wt. % **TIME~ 144 hrs.** 3/3

SCSS/DDW	1 mm.	3 mm.	5 mm.	7 mm.	9 mm.	20 mm.
10 mV	0.15	0.093	0.068	0.073	0.046	0.034
	0.13-0.17	0.066-0.12	0.47-0.090	0.032-0.12	0.039-0.054	0.017-0.051
WN-1/WN-1	1 mm.	3 mm.	5 mm.	7 mm.	9 mm.	20 mm.
10 mV	0.24	0.12	0.075	0.063	0.063	0.046
	0.23-0.25	0.11-0.13	0.053-0.096	0.053-0.073	0.044-0.083	0.036-0.056
WN-1/DDW	2 mm.	4 mm.	6 mm.	8 mm.	19 mm.	
10 mV	0.31	0.058	0 027	0.02	0.015	
	0.28-0.33	0.041-0.076	0.015-0.039	0.0097-0.029	0.0073-0.022	
			0.032			
			0.023-0.039			
			0.0295			
			0.015-0.039			

Dispersion Data
Time – 144 hrs.
1330 V, 10^{-8} amp unless otherwise indicated

Sample						
DDW/DDW	9 mm.	11 mm.	13 mm	15 mm.	17 mm.	20 mm.
50 mV	13.5±0.75	2 75±0.05				
20 mV	11.1±1.2	2.8±0.14	3 0±0.08	1.96±0.12	1.86+0 8	1.82±0.8
DDW/WN-1	1 mm.	3 mm.	5 mm.	7 mm.	9 mm.	20 mm.
20 mV	8.1±1.3	2.34±0.08	1.4±0 24			
10 mV		2.25±0.2	1.4±0.2	1.35±0.25	1.0±0.2	1.5±0.2
DDW/SCSSS	4 mm.	6 mm.	8 mm.	19 mm.		
10 mV	2.5±1.35	0.8±0.2	0.35±0.15	0.4±0.2		
DDW/10^{-2}MCaCl$_2$	5 mm.	7 mm.	9 mm.	20 mm.		
10 mV	3.67±0.13	2.25±0 25	2 3±0.2	2.1±0.15		
DDW/10^{-3}MCaCl$_2$	9 mm.	11 mm.	13 mm.	15 mm.	19 mm.	
20 mV	5.3±0.42	1.86+0.4	1.31±0.2			
10 mV			1.45±0.15	1.3±0.3	1.1±0.15	
DDW/10^{-1}MNaCl	3 mm.	5 mm.	7 mm.	9 mm.	20 mm.	
10 mV	3.45±0.65	1.3±0.4	1.0±0.35	1.1±0.325	1.2±0.25	

Dispersion Data
Time – 144 hrs.

Sample						
DDW/10^{-3}MNaCl	10 mm.	12 mm.	14 mm.	16 mm.	20 mm.	
20 mV	6.1±1.5	3.2±0.96	2.0±0.4	1.81±0.19	1.81+0.19	
SCSSS/SCSSS	1 mm.	3 mm.	5 mm.	7 mm.	9 mm.	20 mm.
20 mV	6.2±0.7	2.3±0.2	1.1±1.5	0.75±0.15	0.85±0.2	1.0±0.55
				1.1±0.2	1.3±0.6	
SCSSS/DDW	1 mm.	3 mm.	5 mm.	7 mm.	9 mm.	21 mm.
10 mV	3.1±0.4	1.9±0.55	1.4±0.43	1.5±0.85	0.95±0.15	0.7±0.35
WN-1/WN-1	1 mm.	3 mm.	5 mm.	7 mm.	9 mm.	20 mm.
10 mV	4.95±0.25	2 5±0.2	1.53±0.43	1.3±0.2	13±0.4	0.95±0.2
*WN-1/DDW	2 mm.	4 mm.	6 mm.	8 mm.	19 mm.	
10 mV	6.35±0.48	1.2±0.35	0.55±0.25	0.4±0.2	0.3±0.15	
			0.65±0.15			

*DDW 0.35±0.08
0.27–0.43

Normalized Dispersion Data

Time – 144 hrs. **DDW** 0 5 ± 0 1 (0 4 - 0.6)

DDW/DDW	9 mm	11 mm.	13 mm	15 mm	17 mm.	20 mm.
50 mV	27.0	5.5				
	21 25-35 6	4 5-7.0				
20 mV	22.2	5.6	6 0	3 92	3 72	3.64
	16.5-30.75	4.4-7.35	4 9-7 7	3 1-5.2	3 0-4 85	2.9-4.75
DDW/WN-1	1 mm.	3 mm.	5 mm.	7 mm.	9 mm.	20 mm
20 mV	16.2	4.68	2.8			
	11.3-23.5	3.8-6.05	1.9-4.1			
10 mV			2.8	2 7	2 0	3 0
			2.0-4.0	1 8-4.0	1.3-3.0	2.2-4 25
DDW/SCSSS	4 mm.	6 mm.	8 mm.	19 mm.		
10 mV	5.0	1.6	0.7	0.8		
	1.9-9.6	1.0-2.5	0.3-1.25	0.3-1 5		
DDW/10^{-2}MCaCl$_2$	5 mm.	7 mm.	9 mm.	20 mm.		
10 mV	7.3	4.5	4.6	4.2		
	5.9-9.5	3.3-6.25	3.5-6.25	3.25-5.6		
DDW/10^{-3}MCaCl$_2$	9 mm.	11 mm.	13 mm.	15 mm.	19 mm.	
20 mV	10.6	3.72	2.62			
	8.1-14.3	2.4-3.8	1.85-3.8			
10 mV			2.9	2.6	2 2	
			2.2-4.0	1.7-4.0	1.6-3.1	

Normalized Dispersion
Time – 144 hrs.

Sample						
DDW/10^{-1}MNaCl	3 mm.	5 mm.	7 mm.	9 mm.	20 mm.	
10 mV	6.9	2.6	2.0	2.2	2.4	
	4.7-10.25	1.5-4.25	1.1-3.4	1.3-3.6	1.6-3.6	
DDW/10^{-3}MNaCl	10 mm.	12 mm.	14 mm.	16 mm.	20 mm.	
20 mV	12.2	6.4	4.0	3.62	3.62	
	7.7-19.0	3.7-10.4	2.7-6.0	2.7-5.0	2.7-5.0	
SCSSS/SCSSS	1 mm.	3 mm.	5 mm.	7 mm.	9 mm.	20 mm.
20 mV	12.4	4.6				
	9.2-17.2	3.5-6.2				
10 mV			2.2	1.5	1.7	2.0
			1.6-3.1	1.0-2.2	1.1-2.6	0.75-3.9
				2.2	2.6	
				1.5-3.2	1.2-4.8	
SCSSS/DDW	1 mm.	3 mm.	5 mm.	7 mm.	9 mm.	20 mm.
10 mV	6.2	3.8	2.8	3.0	1.8	1.4
	4.5-8.8	2.2-6.1	1.6-4.6	1.1-5.9	1.3-2.8	0.58-2.6

Normalized Dispersion

Time – 144 hrs.

Sample						
WN-1/WN-1	1 mm.	3 mm.	5 mm.	7 mm.	9 mm.	20 mm.
10 mV	9.3	5.0	3.1	2.6	2.6	1.3
	7.8-13.0	3.8-6.8	1.8-4.9	1.8-3.8	1.5-4.2	1.2-2.9
WN-1/DDW	2 mm.	4 mm.	6 mm.	8 mm.	19 mm.	
10 mV	18.1	3.4	1.6	1.1	0.85	
			0.7-3.0	0.5-2.2	0.35-1.7	
			1.8			
			1.2-3.0			

Normalized Dispersion Data **Normalized to 0.01 wt. %** 14.9±0.175 1/2
TIME 164 hrs. 14.7-15.1

Sample						
DDW/DDW	11 mm.	13 mm.	15 mm.	17 mm.	19 mm.	20 mm.
20 mV	0.32	0.13	0.08	0.072	0.074	0.064
DDW/WN-1	1 mm.	3 mm.	5 mm.	7 mm.	9 mm.	18 mm.
10 mV	0.31	0.28	0.11	0.097	0.094	0.094
DDW/SCSSS	4 mm.	6 mm.	8 mm.	19 mm.		
10 mV	0.037	0.02	0.017	0.001		
DDW/10^{-2}MCaCl$_2$	5 mm.	7 mm.	9 mm.	20 mm.		
10 mV	0.13	0.077	0.075	0.074		
DDW/10^{-3}MCaCl$_2$ 10^{-7} amp.	10 mm.	12 mm.	14 mm.	16 mm.		
10 mV						
DDW/10^{-1}MNaCl	3 mm.	5 mm.	7 mm.	9 mm.	11 mm.	22 mm.
10 mV	0.31	0.11	0.056	0.077	0.04	0.046
DDW/10^{-3}MNaCl	10 mm	12 mm.	14 mm.	16 mm.	18 mm.	
10 mV	0.97	0.79	0.79	0.795	0.799	

Normalized Dispersion Data
TIME 164 hrs

CONT 1/2

SCSSS/SCSSS	1 mm.	3 mm.	5 mm.	7 mm.	9 mm.	20 mm.
10 mV	0.12	0.12	0.044		0.038	0.030
SCSSS/DDW	1 mm.	3 mm.	5 mm.	7 mm.	9 mm.	20 mm.
10 mV	0.11	0.032	0.027	0.026	0.027	0.027
WN-1/DDW	2 mm.	4 mm.	6 mm.	8 mm.	10 mm.	19 mm.
10 mV	1.14	0.55	0.19	0.12		0.032
WN-1/WN-1	1 mm.	3 mm.	5 mm.	7 mm.	9 mm.	20 mm.
10 mV	0.20	0.14	0.074	0.07	0.074	0.065

Dispersion Data TIME 164 hrs. ....CONT. 1/2

DDW/DDW	11 mm.	13 mm.	15 mm.	17 mm.	19 mm	20 mm.
20 mV	4.7±0.2	1.83±0.15	1.14±0 1	1.07±0.13	1.1±0.15	0.95±0.15
DDW/WN-1	1 mm.	3 mm	5 mm.	7 mm.	9 mm.	18 mm.
10 mV	4.6±0.12	4.1±0.15	1.65±0.1	1.45±0.1	1.4±0.1	1.4±0.1
DDW/SCSSS	4 mm.	6 mm.	8 mm.	19 mm.		
10 mV	0.55±0.2	0.3±0.15	0.25±0.15	0.15±0.075		
DDW/10^{-2}MCaCl$_2$	5 mm.	7 mm.	9 mm.	20 mm.		
10 mV	1.78±0.18	1.15±0.2	1.125±0.145	1.1±0.2		
DDW/10^{-3}MCaCl$_2$ 10^{-7} amp.	10 mm.	12 mm.	14 mm.	16 mm.		
10 mV	1.35±0.22					
DDW/10^{-1}MNaCl	3 mm.	5 mm.	7 mm.	9 mm.	11 mm.	22 mm.
10 mV	4.68±0.3	1.65±0.25	0.835±0.2	0.7±0.15	0.6±0.1	0.63±0.2
DDW/10^{-3}MNaCl	11 mm.	13 mm.	15 mm.	17 mm.	19 mm.	
10 mV	14.45±0.65	11.8±0.04	11.75±	11.85±0.35	11.9± 0.22	
SCSSS/SCSSS	1 mm.	3 mm.	5 mm.	7 mm.	9 mm.	20 mm.
10 mV	1.8±0.15	1.75±0.55	0.65±0.75		0.575± 0.225	0.45±0.2

Dispersion data
TIME 164 hr

CONT 2/2

Sample						
SCSSS/DDW	1 mm.	3 mm.	5 mm.	7 mm.	9 mm.	20 mm.
10 mV	1.68±0.33	0.475±0.125	0.4±0.2	0.39±0.14	0.4± 0.175	0.4±0.25
WN-1/DDW	2 mm.	4 mm.	6 mm.	8 mm.	10 mm.	19 mm.
10 mV	17±1.5	8.15±0.85	2.9±0.35	1.75±0.23		0.475±0.3
WN-1/WN-1	1 mm.	3 mm.	5 mm.	7 mm.	9 mm.	20 mm.
10 mV	3±0.04	2.1±0.04	1.1±0.26	1.05±0.15	1.1±0.3	0.975±0.2